CATALYTIC HYDROGENATION OF BIO-OIL: A PROCEDURE FOR JP8 HYDROCARBON PRODUCTION FROM MISCANE

A Dissertation

by

APRIL LOVELADY

Submitted to the Office of Graduate Studies of
Texas A&M University
in partial fulfillment of the requirements for the degree of

DOCTOR OF PHILOSOPHY

May 2012

Major Subject: Biological and Agricultural Engineering

Catalytic Hydrogenation of Bio-oil: A Procedure For JP8 Hydrocarbon Production From Miscane

CATALYTIC PRODUCTION OF BIO-OIL: A PROCEDURE FOR JP8 HYDROCARBON PRODUCTION FROM MISCANE

A Dissertation

by

APRIL LOVELADY

Submitted to the Office of Graduate Studies of
Texas A&M University
in partial fulfillment of the requirements for the degree of

DOCTOR OF PHILOSOPHY

Approved by:

Chair of Committee,	Sergio Capareda
Committee Members,	Ronald Lacey
	John A. Gladysz
	R. Karthikeyan
	Zivko Nikolov
Head of Department,	Steve Searcy

May 2012

Major Subject: Biological and Agricultural Engineering

ABSTRACT

Catalytic Hydrogenation of Bio-oil: A Procedure for JP8 Hydrocarbon Production From Miscane. (May 2012)

April Lovelady, BS, Texas A&M University;

MS, Texas A&M University

Chair of Advisory Committee: Dr. Sergio Capareda

The purpose of this research was to develop a process to produce JP8 hydrocarbons from miscane, a hybrid plant of sugarcane and *Miscanthus*. Bio-oil was produced from the pyrolysis of miscane at 400ºC, 500ºC and 600ºC. It was then fractionated via vacuum distillation. The distillates each contained substantial amounts of hydrocarbon compounds identical to those found in the JP8 standard without further upgrading. Distilling the bio-oil significantly reduced the MC and the TAN, but rendered small distillate fractions.

After characterization tests were performed, there was not enough of the individual distillate fractions to hydrogenate any remaining oxygenates. Therefore, a model mixture composed of the oxygenated distillate components (i.e. phenolics and alcoholic compounds) was catalytically hydrogenated instead of the distillates themselves. Three catalysts were tested: fluorous Pd, Pd/C and Shvo's catalyst. The data showed that on average, the fluorous Pd, Pd/C and Shvo's catalyst each converted 94.25%, 94.78%, and 94.34% respectively of the oxygenated compounds in the model mixture the hydrocarbons. The statistical analysis concluded that there was no

significant difference at the 5% alpha level ($p = 0.895$ and $F_0 < 4.46$) in the deoxygenation ability of the catalysts.

DEDICATION

I would like to dedicate my research to the Creator who continues to create through us with each new idea we have. Daniel and Lauren continue to be my motivation, with smiles that fuel my determination. I love and adore you both fervently. To my parents who instilled in me initiative and an unyielding fortitude, both of which have preserved me through difficult times. And to the people who became my family as we encouraged each other throughout our graduate school journeys: Thomas Abia, Seaborn Carter, and Charles Rogers, I dedicate this dissertation to each of you.

ACKNOWLEDGEMENTS

I would like to acknowledge the USDA National Needs Fellowship Program and the Alfred P. Sloan Foundation for funding my research and making it possible for me to obtain a PhD. I would also like to acknowledge the efforts of my advisor and committee members, Dr. Sergio Capareda, Dr. Ronald Lacey, Dr. John Gladysz, Dr. R. Karthikeyan and Dr. Zivko Nikolov for providing insight and encouragement when they were most needed. Finally, I must acknowledge Jewel Capunitan, Monet Maguyon, Bjorn Santos and Amado Maglinao for supporting me every step of the way. Thank you all very much.

NOMENCLATURE

GCMS	Gas Chromatograph Mass Spectrometer
TAN	Total Acid Number
MC	Moisture Content
HHV	High Heating Value
UA	Ultimate Analysis
PA	Proximate Analysis
JP8	Jet Propellant 8
GC	Gas Chromatograph
MS	Mass Spectrometer
PIANO	Paraffins, Isoparaffins, Aromatics, Naphthenics, Olefins

TABLE OF CONTENTS

LIST OF FIGURES

LIST OF TABLES

CHAPTER I

INTRODUCTION

The major source of modern society's energy supply is met by fossil fuels. The increased demand for limited fossil fuels has led to a rise in world petroleum prices and rekindled interests in renewable energy sources. According to a recent International Energy Agency (IEA) report, the global demand for oil is approaching 88 million barrels per day with a demand that has been forecasted to increase by 40% from 2007-2030 (Boas 2010). Beginning with the Arab Oil Embargo of the 1970's and continuing with the Energy Development Act of 2005, biomass resources have been considered to be an alternative method of fuel production suitable for helping to meet global energy demand. Renewable energy technologies are needed in order to reduce dependency on fossil fuels. Traditionally, biomass such as corn cobs and stover (Mullen 2010), southern pine sawdust and bark (Sheu 1988) or numerous other feedstocks (Elliott 2007) have been used for the production of biofuels. This research will focus on the production of aviation transport biofuels from a novel feedstock known as "miscane."

Miscane is a hybrid plant resulting from the crossbreeding of sugarcane and miscanthus. In order to address the qualities of miscane bio-oil that make it less than desirable for use as an aviation biofuel, the crude bio-oil must first be characterized, which includes determining its chemical composition. Then, the bio-oil was catalytically hydrogenated under mild conditions. Bio-oil can be produced by the pyrolysis of

---

This dissertation follows the style of the *American Society of Agricultural and Biological Engine*ers.

miscane and catalytically upgraded into jet propellant 8 (JP8). Pyrolysis is a thermochemical conversion process in which organic materials are decomposed at elevated temperatures in the absence of oxygen. The co-products of pyrolysis include syngas, bio-oil, and char. Their proportions can be influenced by controlling the temperature (Bridgwater 1996) and the composition of the bio-oil itself can be influenced by pyrolysis temperature, reaction rate, and residence time (Bridgwater 1994; Elliott 2007). However, batch pyrolysis was used to produce the miscane bio-oil. In comparison to raw biomass, the crude bio-oil produced from pyrolysis has a higher energy density but is generally composed of a complicated mixture of oxygenated hydrocarbons.

The complexity of the raw bio-oil decreases its suitability for use as a drop-in biofuel, where the term "drop-in" refers to fuels that are compatible with existing infrastructure. Crude bio-oil typically has a high total acid number (TAN) as well as elevated O_2 and moisture contents (MC) making them inferior to traditional crude oil. Therefore, if the pyrolysis bio-oil is to be useful as an aviation transport biofuel, it must first be catalytically upgraded to decrease the volatility and viscosity while increasing the thermal stability. Specifically, the aim of this research is to produce refinery ready hydrocarbons found within JP8 that have a reduced TAN, with MC and oxygenate concentration near zero under mild hydrogenation conditions.

Biofuel production processes need to be developed that address the on-going global energy crisis which can be characterized by increasing consumption of petroleum based products and a corresponding increase in crude oil prices. This increased demand

is in part driven by the transportation sector because it consumes the largest proportion of energy. This demand will mostly be met by fossil fuels with renewables making a significantly increasing contribution as a supplement to the current fuel supply. The use of bioresources like miscane, will aid the production of cost effective biofuels with the added expectation of decreasing present day fuel costs.

CHAPTER II

OBJECTIVES

The overarching goal of this research project was to address the on-going global energy crisis by producing JP8 hydrocarbons that can be used as bio-fuel or rather a supplement to the present fuel supply. JP8 is an aviation transport fuel used by military planes and jets.

- Objective 1.0 Characterize the Miscane Feedstock and Pyrolysis Co-products: The miscane feedstock will be characterized prior to pyrolysis. Then, the miscane will be pyrolyzed at various temperatures and the pyrolysis co-products will be characterized.
- Objective 2.0 Determine and Evaluate the Deoxygenation Efficiency of the Catalysts and the catalyst Best Suited for Bio-oil Hydrogenations: While the catalysts selected are primarily used to catalyze hydrogenations, they may also be effective deoxygenation catalysts. As such, the percent of oxygenates present in the distillates will be compared to the percent of oxygenates remaining in the biofuel product after hydrogenation.The bio-oil distillates will be catalytically hydrogenated using three different catalysts and the results statistically analyzed to determine the catalyst best suited for JP8 production.
- Objective 3.0 Evaluate the JP8 Product Quality: The quality of the JP8 produced will be based on achieving a reduction in the TAN, with MC and oxygenate percentages near zero.

CHAPTER III

LITERATURE REVIEW

3.1 Miscane

Cellulosic biofuel feedstocks, like C_4 grasses, are a promising component in a future mix of alternative renewable energy solutions (Jakob, Zhou et al. 2009). Biomass feedstocks must provide an economical and sustainable basis for the industries they serve (Mascia 2010). Feedstocks should be resilient to biotic and abiotic stresses, require few inputs to produce high quantities of biomass, and be adaptable to areas close to the locations of the industries they supply (Vermerris 2008; Carroll and Somerville 2009). Mascia (2010) described a list of traits that are essential for a successful variety to sustain the bioproducts industry. These traits are listed in Table 1.

Table 1. Valuable Traits for Improvement

Value	Trait for Enhancement
Increase biomass, increase yield potential, lower production and transport costs, increase carbon sequestration	Architecture, canopy structure, photosynthesis, flowering time
Protect yield in stresses and on marginal land	Drought tolerance, heat tolerance, cold tolerance, salt tolerance, disease resistance, heavy metal tolerance, pH tolerance, root structure
Reduce cost of inputs	Nitrogen use efficiency, water use efficiency, reduced greenhouse gas emissions, seed propagation
Increase yield in industrial processes, reduce capital and operational costs of refineries	Composition, conversion to sugars, higher heating values, reduced Cl, K and other metals
Enhance overall economics	Addition of co-products

Enhancing specific biomass traits could result in value added bioproducts. This table shows the relationship between a few of those traits and their industrial value (Mascia 2010).

In light of the requirements for a successful biomass variety, sugarcane is likely to be a major contributor as feedstock for biofuel production. Sugarcane is a C4 plant that has a favorable total energy output (Heichel 1973) and due to recent public and private investments, has been brought to the forefront as the most productive first generation energy crop (Lam, Shine et al. 2009). There are numerous advantages for the use of sugarcane as an energy crop including: it can be harvested annually for a number of years without replanting, rapid growth, high biomass density per unit area and low nutrient and water needs (Rubin 2008). However, in the United States, one of the biggest challenges for energy production from sugarcane is the expansion of its adaptability to include drought and cold tolerance (Lam, Shine et al. 2009). To aid the improvement of sugarcane as a feedstock, it was crossbred with another C4 grass known as *Miscanthus* that has more tolerance to cold and drought. The resulting hybrid is called "miscane" and is the subject of this research effort.

For large-scale biofuel production facilities, biomass feedstocks like miscane are important. The miscane hybrid could potentially combine the high productivity of both species with the adaptation o*f Miscanthus* to colder climates (Jakob, Zhou et al. 2009). Particularly in more temperate climates, crop adaptation for sustainable production is needed.

Evidence suggests that transportation fuels based on lignocellulosic biomass represents the most scalable alternative fuel source (Jason, Nelson et al. 2006). However, the successful implementation of cellulosic feedstocks will depend on the improvement of critical crop characteristics (Jakob, Zhou et al. 2009). Existing challenges related to

the use of cellulosic biomass as feedstocks may be addressed by developing new breeds of plants.

3.2 Pyrolysis of Biomass

Pyrolysis is a thermal degradation process that involves heating organic materials either in the absence of O_2 or in a limited O_2 environment (Tahir 2009). The process occurs between 400°C and 800°C. Pyrolysis produces three different co-products: char, syngas and pyrolysis liquids. The relative proportion of these pyrolysis co-products depends on the pyrolysis conditions and the organic material being decomposed. The pyrolysis temperature, reaction rate, and residence time all effect the bio-oil composition (Bridgwater 1994; Elliott 2007). There are different kinds of pyrolysis processes including ablative, vacuum, fluidized bed, and fast pyrolysis which has been shown to maximize the yield of bio-oil (Sheu, Anthony et al. 1988). However, this researched focused on the use of batch pyrolysis for the production of biofuels.

3.2.1 Batch Pyrolysis

Batch pyrolysis has been used to study the production of hydrocarbons for fuel gas production (Williams and Horne 1994; Chen, Andries et al. 2003; Chen, Andries et al. 2003), the impact of biomass blends on pyrolysis co-products (Jones, Kubacki et al. 2005), and fuel properties of biofuel blends (Garcia-Perez, Adams et al. 2007). In cases where the focus was on the production of gas, the liquid product yields were reported but no analyses were performed to characterize the liquid products. Specifically, Chen and Andries (2003) obtained tar yields ranging from 15.5% to 26%. This is significant because it is an order of magnitude more than the bio-oil yields resulting from this

research effort and tar can still be distilled to capture liquid hydrocarbon fractions. The biomass feedstock studied was Whatman Filter Paper No. 1 that had been impregnated with catalysts. However, the implication is that the addition of catalysts such as CuO or Cr_2O_3 may improve bio-oil (tar) yields making pyrolysis a more efficient process for the production of liquid hydrocarbons for biofuels.

While it is known that fast pyrolysis maximizes the production of bio-oil (Sheu, Anthony et al. 1988; Bridgwater, Meier et al. 1999), the heating rates and liquid yields of batch pyrolysis experiments were recorded for the experiments below in Table 2.

Table 2. Summary of Slow Batch Pyrolysis Experiments

Feedstock	Heating Rate (°C/min)	Pyrolysis Temperature (°C)	Liquid Product Yield	Reference
palm kernel cake cassava pulp residue	5-20	300-800	varied with feedstock and heating rate	(Weerachanchai, Tangsathitkulchai et al.)
pine wood	5-80	200-750	oil yield directly proportional to heating rate	(Williams and Besler 1996)
Rapeseed	30	700	maximum oil yield occurred at 550°C	(Ozlem and Mete Koçkar 2004)
Miscanthus pine wood	10-100	900	oil yield for pine wood was almost twice that of *Miscanthus*	(de Jong, Pirone et al. 2003)
Euphorbia macroclada	7-40	400-700	maximum oil yield occurred at 550°C and 7°C/min	(Feride and Hasan Ferdi 2004)
municipal solid waste	5-80	300-800	maximum oil yield occurred at 720°C	(Williams 1992)

This table summarizes some of the literature results of slow pyrolysis experiments. The reported results show the effect of slow pyrolysis on the liquid product yield.

Of the experiments listed in table 2 above, none of the researchers reported the pressure at the time of pyrolysis. Also, some of the papers reported the total liquid

product yield and did not note the yield of only the bio-oil. The total liquid product yield is comprised of a bio-oil and aqueous phase. In some cases, no distinction was made between tar and bio-oil. The yield of the bio-oil, tar and aqueous phase depends not only on the feedstock, but also on the moisture content of the feedstock at the time of pyrolysis. For this reason, many of the researchers dried the feedstock prior to pyrolysis but in some cases, the final MC was not reported.

Garcia-Perez and Adams (2007) used a batch pyrolyzer to produce bio-oil that was then blended with a standard biodiesel to extract from the bio-oil those compounds that were chemically and physically similar to the biodiesel. They describe a system where 1.4kg of pine chips were pyrolyzed and maintained at a reaction temperature of 500°C. Five cooling traps were connected in series to collect the pyrolysis vapors that were evacuated using N_2 as the carrier gas. Once the condensed liquids were collected, they were separated into an aqueous phase and a bio-oil phase. The bio-oil phase was blended with a standard biodiesel and the biodiesel rich phase was extracted and analyzed via differential thermogravimetric methods to obtain a global view of the bio-oil composition. The compounds contained within the bio-oil were grouped into five categories: (1) water and organic compounds, (2) monolignols and furans, (3) sugars and dimers, (4) oligomers with molecular weights ranging between 500g mol^{-1} and 1000g mol^{-1} and (5) oligomers with molecular weights greater than 1000g mol^{-1}.

3.3 Catalytic Hydrogenation

3.3.1 General Catalysis

Catalysis is a process by which the addition of a compound, a "catalyst" increases the rate of a chemical reaction by lowering the activation energy of the reaction. The catalysts itself remains unchanged at the end of the process. Catalytic processes can be classified as either heterogeneous or homogeneous. Heterogeneous catalysts exist in a form different from that of the reactants while homogeneous catalysts reside in the same state as the reactants. Catalysis is linked to energy with respect to the large amount of fuel consumed by the transportation industry (Council 2009). The use of biofuels with existing energy technologies requires the catalytic modification of raw bio-oil. In order for the crude bio-oil to be useful as transportation fuels, it must be catalytically upgraded to decrease volatility, increase thermal stability, reduce the viscosity, and remove any oxygenated compounds. Accomplishing the upgrade will require that the compounds found in the crude bio-oil to be hydrogenated, deoxygenated and dehydrated.

3.3.2 Heterogeneous Catalysis

Heterogeneous catalytic processes are more commonly used in the production of fuels than homogeneous catalysis even though their chemistry is more challenging to understand (Matar 1989). The results of heterogeneous catalytic studies can be inconclusive because the reactions can be difficult to reproduce. However, heterogeneous catalysts have been preferred to their homogeneous analogues because they allow for continuous operations and simple separation of reaction products.

The bio-oil optimization work done at Pacific Northwest National Laboratory (PNNL) has focused on the use of heterogeneous catalytic hydroprocessing. Experiments were carried out at temperatures between 300°C and 400°C using commercial catalysts such as CoMo, NiMo and NiW among others. The results are summarized in table 3.

Table 3. Commercial Hydrogenation Catalysts and Their Product Yields

Catalyst	Product	Amount of Product (%)
Sulfided CoMo @ 400°C	Benzene	33.8
	Cyclohexane	3.6
Ni	Benzene	16.9
	Cyclohexane	7.6
Sulfided Ni	Benzene	0.4
	Cyclohexane	8.0
Pd @ 400°C	Benzene	7.8
	Cyclohexane	2.7
	Cyclohexanone	5.5
Pd @ 300°C	Benzene	2.0
	Cyclohexane	2.5
	Cyclohexanone	8.1

The product yields of these hydrogenation experiments were derived from the use of model phenolic compounds (Elliott 1983).

3.3.3 Homogeneous Catalysis

The most predominant limitation for the use of heterogeneous catalysts is their lack of specificity (Matar 1989). This creates an opportunity for homogeneous to expand

its role in the conversion of biomass feedstocks to biofuels. Homogeneous catalysts are highly selective, have good yields, create less waste and exhibit excellent efficiency in the production of biofuels. It is plausible that only one functional group can react at a given time because of the small size of the catalytic entity. Also, homogeneous catalysts react under milder conditions than heterogeneous catalysts thereby reducing the input energy costs (Matar 1989). This is important because traditionally, the more expensive metals such as Pt, Pd, and Rh are among the most effective catalysts.

However, homogeneous catalysts can be difficult to separate from the reaction medium. It is here that catalyst immobilization techniques can be used to overcome this undesirable characteristic of homogeneous catalysis. The term "catalyst immobilization" can be defined as the transformation of a homogeneous catalyst into a heterogeneous catalyst which is able to be separated from the reaction mixture and possibly recycled (Wang). One such method for immobilizing and recycling catalysts that was further explored by this research was fluorous catalysis.

3.3.4 Fluorous Catalysis

First proposed by Horvàth and Ràbai (1994), the idea was to develop catalysts that would exhibit biased partition coefficients with respect to fluorous and organic solvents (Gladysz 2008). These solvents are normally immiscible at room temperature, but by attaching ligands, the catalysis is affected at elevated temperatures where the two phases become miscible. The separation of product and catalyst then occurs at the low temperature, two phase limit. By making use of the temperature dependent solubility of a solid in a liquid phase, the solubility of fluorous molecules can be exploited as

recyclable catalysts. Catalyst recovery would then be affected by a solid-liquid phase separation. This process is illustrated in figure 1.

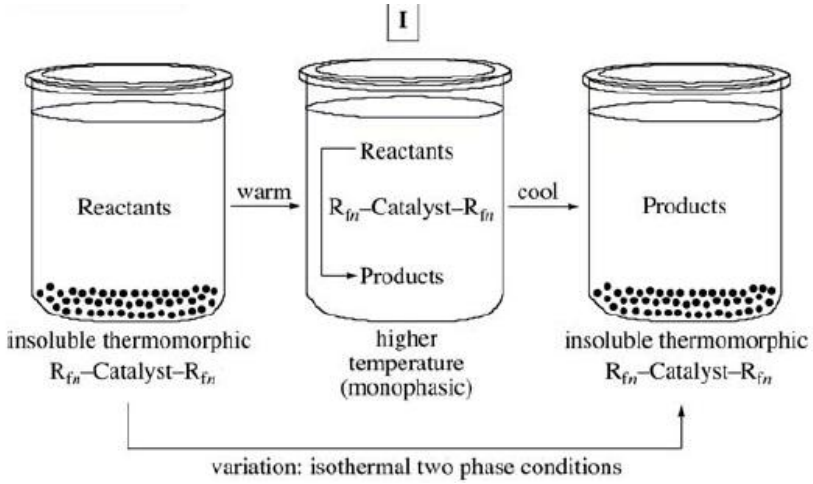

Figure 1. Fluorous Catalyst Recovery Technique. This figure illustrates the strategy for catalyst recovery via phase separation (Gladysz 2008).

Alkenes have been successfully hydrogenated using catalysts developed as a part of a fluorous regenerative system (Richter 2000; Sinou, Maillard et al. 2003; Gladysz 2006). This would be extended to determine the viability of fluorous biphasic catalysis for the hydrogenation and deoxygenation of other compounds found in bio-oil. For example, Garcia-Perez and Adams (2007) analyzed bio-oil from the pyrolysis of soft and hardwood bark. The analyses identified hundreds of compounds that can be classified into the following major chemical families: alkanes, alkenes, ketones, phenols, alcohols, aldehydes, carboxylic acids, and esters. Bio-oil produced from the pyrolysis of A. donax is expected to be of a similar complexity although the compounds may be present in different amounts than those reported by Garcia-Perez and Adams (2007) for bark. Fluorous biphasic catalytic systems have also been used to catalyze syntheses oxidations

(Rocaboy 2002), and metatheses reactions using analogues of Grubbs' second catalyst (da Costa and Gladysz 2007). Previous studies reported the use of fluorous catalysis to hydrogenate alkenes such as 2-cyclohexene-1-one, 1-dodecene, and 1-octene respectively resulting in the production of cyclohexanone, dodecane, and octane (Rutherford, Juliette et al. 1998; Richter, Spek et al. 2000). The turnover numbers (TONs) ranged from 87 to 3117 with yield percentages ranging from 85 to 99.8.

Fluorous catalytic systems are not without their limitations. Some of these limitations are discussed in (de Wolf and Deelman 2008) such as the electron withdrawing effects of the fluorous ligands on the metal centers or the individual preparation of the fluorous ligand analogues. Gladysz and Tesevic (2006) point out that insoluble byproducts are possible and that this method is suited for reactions conducted at elevated temperatures. However, there are some reactions which proceed before the miscibility temperature is reached (Dinh 2005). Additionally, the fluorous ligands are not biodegradable and although biodegradable ligands are available, they are expensive (Gladysz 2011). Finally, the TON will be limited by catalyst death, the mechanism of which may be difficult to identify.

In order to decrease input costs, it is important to capitalize on extending the catalyst life cycle by employing a catalyst recycling technique such as fluorous biphasic separation. Several reviews have reported on this topic (Horváth 1998; de Wolf, van Koten et al. 1999; Hope and Stuart 1999) and fluorous biphasic separation has several advantages over other separation techniques including the fact that during homogeneous single phase reaction conditions, the catalyst activity is not decreased due to mass

transport limitations, the fluorocarbon components are usually inert towards the catalyst, and the fluorous tagging of the catalyst which has an affinity for the fluorous phase can be a mild immobilization technique (de Wolf and Deelman 2008). The successful demonstration of this technique has been carried out using Lewis base, metallacycle, and rhodium catalysts (Gladysz 2008), Grubbs' second generation catalyst (da Costa and Gladysz 2007), and Pd complexes for Suzuki coupling (Rocaboy 2002).

3.3.5 Hydrogenation and Deoxygenation Catalysts

Whether the catalytic method is heterogeneous, homogeneous, or regenerative, the production of biofuels produced from biomass derived bio-oils requires the removal of oxygen and molecular weight reduction (Elliott 2007). The hydroprocessing (Jakob, Zhou et al. 2009) of bio-oils differs from that of petroleum oils because the focus is no longer on the removal of nitrogen or sulfur, but is instead on hydrogenation and deoxygenation. While there are numerous hydrogenation and deoxygenation catalysts utilized for the production of biofuels, this research effort was focused on Pd and Ru complexes.

CHAPTER IV

EXPERIMENTAL METHODOLOGY

4.1 Feedstock and Pyrolysis Co-Product Characterization

The miscane feedstock and pyrolysis co-products will be characterized. Several analyses will be done on the feedstock prior to pyrolysis.

The miscane biomass arrived at the BETA Lab having already been field dried. In preparation for pyrolysis, the miscane biomass was ground to a particle diameter of 1mm. The miscane was characterized by performing UA, PA, and determining the energy content of the raw biomass. Figure 2 shows miscane growing in the field and at the Texas Agricultural Extensions Service (TAEX) greenhouse in Weslaco, TX. Table 4 lists the various parameters of miscane and the test methods used to determine them.

Figure 2. Miscane Field Trials. The left image shows miscane growing in the field and the right image shows miscane growing in a TAEX greenhouse.

Table 4. Test Methods and Parameter Measurements for Miscane Feedstock Analysis

	Parameter	Standard Test Method	Equipment Manufacturer	Model
Proximate Analysis (%)				
	MC	ASTM D3173	Yamato	DX602
	VCM	ASTM D3175	Thermo Scientific	F21135
	Ash	ASTM E1755	Thermo Scientific	3FA1850
	FC*	ASTM D3173		
Ultimate Analysis (%)				
	C	ASTM D5291	Elementar	Vario Microcube
	H			
	O*			
	N			
	S			
Energy Content (Btu lb^{-1})	HHV	ASTM D240	Parr Instruments	6200

This table lists the standard methods used to determine various biomass parameters. Both the percent oxygen and FC were determined by difference.

4.1.1 Batch Pyrolysis of Miscane Biomass

The miscane was pyrolyzed at 400°C, 500°C, and 600°C. Preliminary pyrolysis experiments were conducted to determine how much biomass the reactor bin could accommodate. Trials showed that using more than 1200g resulted in incomplete pyrolysis. Therefore, 1200g of dried miscane was used for all pyrolysis experiments.

A complete pyrolysis experiment included the pyrolysis process itself, cooling the equipment, and cleaning the equipment in preparation for the next experimental run. The pyrolysis process had an average temperature ramp rate of 2°C min^{-1}. Each experiment began at room temperature and terminated at either 400°C, 500°C or 600°C. During experiments, the pressure was monitored and recorded. 400°C experiments ran

for approximately three to four hours, 500°C experiments ran for four to five hours, and 600°C experiments ran for five to six hours. Cooling the equipment between experiments required eight to ten hours and cleaning took about an hour. Considering the time it took to complete each task, only one experiment could be run each day.

The pyrolyzer used was a high temperature, high pressure reactor (model#: 4580) equipped with a PID controller (model# 4848) manufactured by Parr Instruments Company. The cylindrical reactor bin was loaded with 1200g of miscane and purged with N_2 gas for ten minutes. This ensured that all of the air had been evacuated from the reactor bin. Then, the temperature set point was entered into the controller and the stirrer turned on. The PID algorithm did not allow for automatic pressure control and so the pressure was manually controlled by adjusting a valve. The reactor used is pictured in figure 3.

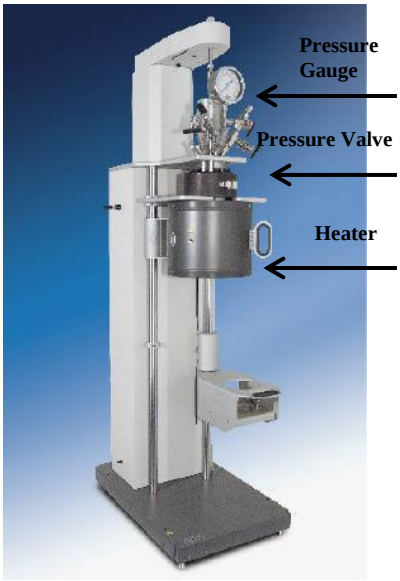

Figure 3. Batch Pyrolysis Equipment. This figure illustrates the pressurized, high temperature batch pyrolysis setup used for all pyrolysis experiments. (http://www.parinstruments.com)

Peripheral components to the reactor included a gas meter (model# 250, Manufacturer: Metris), a bath circulator (model# RF-10, Manufacturer: New Brunswick Scientific), and a stainless steel collection bottle used for collecting the pyrolysis liquid products. The bath circulator was set to 5°C and cold water flowed counter current through the condenser. Hot pyrolysis gases flowed up through the gas lines. The condensable gases were cooled and collected as the liquid product, while noncondensable gases (syngas) were measured by the gas meter. The pyrolysis liquid product was biphasic consisting of an aqueous phase and a bio-oil phase. The two phases were separated and the aqueous phase was stored while the bio-oil phase was further analyzed. The mass percentages of the co-products were calculated.

4.1.2 Experimental Plan and Procedures for Syngas Analysis

The syngas, was analyzed using a GC (model: 8610C, Manufacturer: SRI Instruments) and the following gases were measured:

H_2	C_2H_2
O_2	C_2H_4
N_2	C_2H_6
CO	C_3H_6
CH_4	C_3H_8
CO_2	

The GC utilized two different columns. First, the gas passed through molecular sieve 13X column (Manufacturer: Restek) and then through a ShinCarbon ST column (Manufacturer: Restek). The molecular sieve 13X column was 6 m long with an outer diameter of 3.175 mm. The ShinCarbon ST column was 2 m long with an outer diameter of 1 mm and an inner diameter of 1.588 mm. The GC program began at a column oven temperature of 60°C which was held for 10 minutes. Then, the temperature was ramped to 250°C at a ramp rate of 16°C min^{-1} and was held at 250°C for 10 minutes. The column flow rate was 10 mL min^{-1}. The total GC sample runtime was about 37 minutes, not including the time taken to cool the column between runs. A total of 27 syngas analyses were completed. For statistical purposes, three trials per pyrolysis experiment were carried out. The density of the syngas was determined by weighing a 3 mL, gas tight syringe before and after filling it with a gas sample. The weight differential was divided by the volume resulting in the density. The density along with the volume of gas measured during pyrolysis experiments was used to calculate the mass of the syngas.

The first objective of this research involved the characterization of the miscane pyrolysis co-products. Syngas was produced and analyzed using a GC to determine its composition. A total of 11 gases were quantified namely H_2, O_2, N_2, CO, CH_4, CO_2, C_2H_2, C_2H_4, C_2H_6, C_3H_6 and C_3H_8. For statistical purposes, three GC analyses were performed for each pyrolysis experiment. Three pyrolysis experiments were run at each specified temperature (400°C, 500°C, and 600°C). This produced nine gas analyses for each temperature and a total of 27 analyses for the entire research effort. Because syngas is primarily composed of H_2, CO, CH_4 and CO_2, these gases were further analyzed statistically to identify any existing correlation between production yields (represented as percentages) and pyrolysis temperature. The hypotheses tested were:

H_0: $\mu H_{2\ \text{at}\ 400°C} = \mu H_{2\ \text{at}\ 500°C} = \mu H_{2\ \text{at}\ 600°C}$ (i.e. the percent of H_2 produced does not change with pyrolysis temperature).

H_A: $\mu H_{2\ \text{at}\ 400°C} \neq \mu H_{2\ 500°C} \neq \mu H_{2\ \text{at}\ 600°C}$ (i.e. the percent of H_2 produced changes with the pyrolysis temperature).

A similar set of hypotheses were tested for CO, CH_4, and CO_2. An ANOVA was used to analyze the data. The F-statistic used to test the equality of the means was distributed as $F_{2,24}$. The rejection criteria for H_0 was $F_0 > F_{0.05,\ 2,24}$. All tests were performed at the 5% level of α.

4.1.3 Experimental Plan and Procedures for Char Analysis

After each pyrolysis experiment, the char was collected and weighed. The char was further analyzed by the test methods in table 5 for the parameters listed in table 5.

Table 5. Standard Test Methods Used for Char Characterization

	Parameter	Standard Test Method	Equipment Manufacturer	Model
Proximate Analysis (%)				
	MC	ASTM D3173		
	VCM	ASTM D3175	Thermo Scientific	
	Ash	ASTM E1755		
	FC*	ASTM D3173		
Ultimate Analysis (%)				
	C	ASTM D5291	Elementar	Vario Microcube
	H			
	O*			
	N			
	S			
Energy Content (Btu lb^{-1})	HHV	ASTM D240	Parr Instruments	6200

As with the syngas, the char produced was also statistically analyzed to reveal any relationship between pyrolysis temperature and the mass of char produced, the UA results, PA results and the energy content results.

4.1.4 Analysis of the Char Yields

The amount of char produced from each pyrolysis experiment was weighed and recorded. A total of nine statistical data points were collected resulting from three trials being run for each of the three pyrolysis temperatures. The data was analyzed statistically to test for a relationship between the amount of char produced and the pyrolysis temperature. The hypotheses tested were:

H_0: $\mu Mass_{400°C} = \mu Mass_{500°C} = \mu Mass_{600°C}$ (i.e. the amount of char produced does not vary with pyrolysis temperature).

H_A: $\mu Mass_{400°C} \neq \mu Mass_{500°C} \neq \mu Mass_{600°C}$ (i.e. the amount of char produced varies with pyrolysis temperature).

The F-statistic used to test the equality of the means was distributed as $F_{2,6}$. The rejection criteria was $F_0 > F_{0.05,2,6}$. All tests were performed at the 5% level of α.

4.1.5 Ultimate Analysis of the Char

The ultimate analysis of the char produced the determination of C, H, N, S and O by difference. These elements were regarded as the five response factors that were statistically evaluated. For each pyrolysis experiment, three ultimate analysis trials were run, resulting in a total of 27 statistical data points for each element and 135 total data points. The data was analyzed statistically to test for a relationship between the percentage of the individual elements produced and the pyrolysis temperature. The hypotheses tested were:

H_0: $\mu C_{400°C} = \mu C_{500°C} = \mu C_{600°C}$ (i.e. the percentage of elemental C in the char does not vary with pyrolysis temperature).

H_A: $\mu C_{400°C} \neq \mu C_{500°C} \neq \mu C_{600°C}$ (i.e. the percentage of elemental C varies with pyrolysis temperature).

A similar set of hypotheses can be tested for H, N, S and O. An ANOVA was used to analyze the data. The F-statistic used to test the equality of the means was distributed as $F_{2,132}$. The rejection criteria was $F_0 > F_{0.05,2,132}$. All tests were performed at the 5% level of α.

4.1.6 Proximate Analysis of the Char

As with the UA, the PA for the char produced multiple response factors including the MC, VCM, ash and FC. These parameters were regarded as the four response factors that were statistically evaluated. For each pyrolysis experiment, three ultimate analysis trials were run, resulting in a total of 27 statistical data points for each element and 108 total data points. The data was analyzed statistically to test for a relationship between the percentage of the individual elements produced and the pyrolysis temperature. The hypotheses tested were:

H_0: $\mu MC_{400°C} = \mu MC_{500°C} = \mu MC_{600°C}$ (i.e. the percent MC for char is not effected by pyrolysis temperature).

H_A: $\mu MC_{400°C} \neq \mu MC_{500°C} \neq \mu MC_{600°C}$ (i.e. the percent MC for char is effected by pyrolysis temperature).

A similar set of hypotheses can be tested for VCM, ash and FC. An ANOVA was used to analyze the data. The F-statistic used to test the equality of the means which was distributed as $F_{2,105}$. The rejection criteria for H_0 was $F_0 > F_{0.05,\ 2,105}$. All tests were performed at the 5% level of α.

4.1.7 Analysis of the Char Energy Content

Finally, the char was analyzed to determine its energy content. Pyrolysis temperature was an input factor represented at three levels, and the HHV was the only response factor. For statistical purposes, three heating values were determined for each

pyrolysis experiment and at each pyrolysis temperature for a total of 27 data points. The hypotheses tested were:

H_0: $\mu HHV_{400°C} = \mu HHV_{500°C} = \mu HHV_{600°C}$ (i.e. the HHV of the char is not affected by the pyrolysis temperature).

H_A: $\mu HHV_{400°C} = \mu HHV_{500°C} = \mu HHV_{600°C}$ (i.e. the HHV of the char is affected by the pyrolysis temperature).

A one-way Analysis of Variance (ANOVA) was used to analyze the data. The F-statistic was used to test the equality of the means which was distributed as $F_{2,24}$. The rejection criteria for H_0 was $F_0 > F_{0.05, 2,24}$. All tests were performed at the 5% level of α.

4.1.8 Development of the JP8 Standard Curve

Prior to performing the GCMS analysis on the bio-oil distillates and model mixture, a JP8 standard calibration curve was developed. Serial dilutions were prepared from a standard stock solution of 50,000 ppm JP8 in $MeCl_2$ (Manufacturer: NSI Solutions, Item# UST-215-01). Tetracosane in $MeCl_2$ and androstane (Manufacturer: AccuStandard, Item# GRH-IS) were used as internal standards. Two sets of JP8 standards were prepared according to serial dilution outlined in table 6.

Table 6. Preparation of JP8 Standards for GCMS Analysis

Concentration (ppm)	Volume of JP8 (µL)	Volume of α-androstane (µL)	Volume of Tetracosane (µL)
100	2	5	1
500	10	5	2
750	14	5	3
1000	20	5	4
1500	30	5	5
2000	40	5	6
2500	50	5	7
3000	60	5	8
4000	80	5	9
5000	100	5	10

This table show the compositional volumes of the JP8 standards.

4.1.9 GCMS Method Development

A method is a compilation of the parameters used to control the GCMS for data acquisition and processing. The GC column used was a DB5-MS (Manufacturer: Restek) and is a nonpolar column suited for the analysis of hydrocarbons. The column was 25 m long with a diameter of 0.25 mm and a film thickness of 0.25 µm. The GC program began with in initial column temperature of 35°C and was ramped to 320°C at a ramp rate of 2°C min^{-1}. The injection temperature was 295°C and the column flow rate was 0.61 mL min^{-1}. After two minutes, the split flow ratio was reduced from 50 to 2 to prevent excessive use of carrier gas. The ion source and interface temperatures for the MS were 300°C and 320°C respectively.

4.1.10 GCMS Qualitative Analysis

After a sample was analyzed using the method described in section 3.2.1.3.1, the data was qualitatively analyzed. The GC peaks had to be integrated before the spectra could be chosen for similarity searches. Peak integration was performed based the peak area and a minimum area of 30,000 was selected as an exclusion criterion. Peaks with an area less than 30,000 were not recognized as peaks and were not processed. The peak width was set to 3 seconds and is the width at half-height of the narrowest peak detected. The peak width is a standard used to distinguish between noise and peaks. After the peaks were integrated, the similarity search compared the mass spectrum of an unknown compound to the spectra in a library file. Candidates with varying degrees of similarity are displayed for each spectrum. The most similar spectra from the library file was selected as the compound match.

4.1.11 GCMS Quantitative Analysis

Quantitation refers to the process of determining the concentration of a compound in a sample. After a sample was qualitatively analyzed, a compound table was created. A compound table displays the results of the compound identification and the concentration calculations. A grouping table was included which displayed parameters for the creation of a calibration curve and concentration calculations of the group. A compound table was created from the GCMS analysis of the JP8 standards. These compounds were grouped according to their chemical functionality. The compounds were categorized as paraffins, isoparaffins, aromatics, naphthenics, olefins, (PIANO) oxygenates, or halogenates. Table 7 defines and describes the categories (groups).

Table 7. Description of Chemical Categories

Category	Description
Paraffins	Alkane with the general formula C_nH_{2n+2}
Isoparaffins	A branched version of a straight chain alkane
Aromatics	A hydrocarbon with alternating double and single bonds between carbon atoms
Naphthenics	Cycloalkanes with one or more rings of carbon atoms in their structure
Olefins	Unsaturated chemical compound that contains at least one double bonded carbon with the general formula C_nH_{2n}
Oxygenates	Chemical compounds containing oxygen as a part of their structure
Halogenates	Chemical compound that contains either fluorine, bromine, chlorine or iodine as a part of its chemical structure

This table lists the different chemical groups used resulting from the GCMS analysis and their descriptions.

A calibration curve was created for each compound. Each compound was quantitated by application of an absolute calibration method known as external calibration. This method determined the concentration of target compounds by creating a calibration curve from the relationship between the absolute mass of a compound in a standard and its area. Compounds with similar characteristics were grouped and their concentrations summed to create the PIANO analysis. Additionally, oxygenates and halogenates were also included.

The compound table and calibration curve were saved to the GCMS method file used to analyze the JP8 standards. Then, the same method file was used analyze the bio-oil distillates and hydrogenation products. The analytical conditions for the standard, the bio-oil distillate and the hydrogenation product were exactly the same. The volume of

the sample injected remained constant since the method accuracy is dependent on the sample volume. For each unknown sample, 200 µL of bio-oil distillate or hydrogenated product was added to 1 mL of $MeCl_2$ along with the internal standards. For each unknown sample, a compound table was created that displayed the compositional analysis of the sample. Figure 4 illustrates the qualification and quantification of the samples.

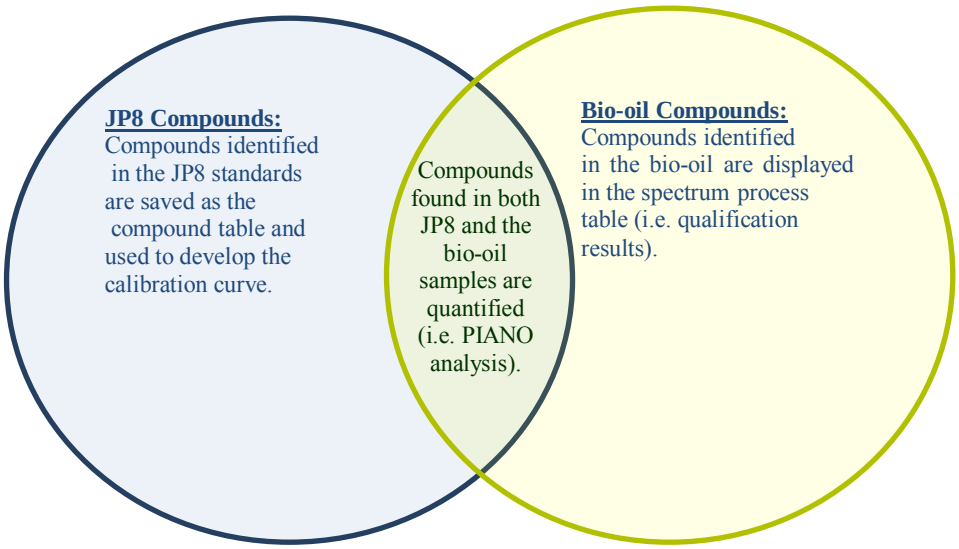

Figure 4. Qualification and Quantification of Sample Compounds. This ven diagram illustrates the qualification and quantification of bio-oil compounds. Compounds not identified in JP8 were not quantified.

4.1.12 Experimental Plan and Procedures for Raw Bio-oil and Distillate Analysis

A portion of the raw bio-oil was set aside for analysis. Table 8 describes the test methods used to characterize the raw bio-oil. The remaining bio-oil was fractionated via vacuum distillation.

Table 8. Test Methods Used for Bio-oil Characterization

	Parameter	Standard Test Method	Equipment Type	Equipment Manufacturer	Model
Ultimate Analysis (%)	C H O* N S	ASTM D5291	Elemental Analyzer	Elementar	Vario Microcube
GCMS	Chemical Composition		Gas Chromatograph Mass Spectrometer	Shimadzu	QP2010S
Moisture Content (%)	MC	ASTM D3173	Karl Fisher Titrator	Metrohm	701 Titrino
Energy Content (Btu lb^{-1})	HHV	ASTM D240	Bomb Calorimeter	Parr Instruments	6200
Density	ρ		Digital Scale	Mettler Toledo	AB304-S
TAN (mg KOH g bio-oil^{-1})	TAN	ASTM D664	pH Meter	Accumet	25
Mass (g)	Mass		Digital Scale	Mettler Toledo	ML4002E

This table lists the standard procedures used for characterizing the bio-oil produced from pyrolysis. The percent oxygen was determined by difference.

4.1.13 Moisture Content (MC) Analysis of Raw Bio-oil

The MCs of the raw bio-oil fractions were determined according to ASTM D3173 using a Karl Fisher titrator (Manufacturer: Metrohm Model: 701 Titrino). The MC values were determined in triplicate resulting in a total of 27 statistical data points. The data was statistically analyzed to determine if the pyrolysis temperature affected the MC of the raw bio-oil. The hypotheses tested were:

H_0: $\mu MC_{400°C} = \mu MC_{500°C} = \mu MC_{600°C}$ (i.e. the MC for each raw bio-oil fraction was not effected by pyrolysis temperature).

H_A: $\mu MC_{400°C} \neq \mu MC_{500°C} \neq \mu MC_{600°C}$ (i.e. the MC for each raw bio-oil fraction was effected by pyrolysis temperature).

An ANOVA was used to analyze the data. The F-statistic used to test the equality of the means was distributed as $F_{2,24}$. The rejection criteria for H_0 was $F_0 > F_{0.05,\ 2,24}$. All tests were performed at the 5% level of α.

4.1.14 Ultimate Analysis of Raw Bio-oil

An ultimate analysis was performed on the raw bio-oil and resulted in the determination of C, H, O, N, and S elemental percentages. These elements were regarded as the five response factors that were statistically evaluated. The percent oxygen reported was determined by difference and was inflated because the ash percentage was not taken into consideration. For each pyrolysis experiment, three ultimate analysis trials were run, resulting in a total of 27 statistical data points for each element and 135 total data points. The data was analyzed statistically to test for a

relationship between the percentage of the individual elements produced and the pyrolysis temperature. The hypotheses tested were:

H_0: $\mu C_{400°C} = \mu C_{500°C} = \mu C_{600°C}$ (i.e. the elemental percentage of C in the raw bio-oil does not vary with pyrolysis temperature).

H_A: $\mu C_{400°C} \neq \mu C_{500°C} \neq \mu C_{600°C}$ (i.e. the elemental percentage of C in the raw bio-oil varies with pyrolysis temperature).

A similar set of hypotheses can be tested for H, N, S and O. An ANOVA was used to analyze the data. The F-statistic used to test the equality of the means was distributed as $F_{2,24}$. The rejection criteria was $F_0 > F_{0.05,2,24}$. All tests were performed at the 5% level of α.

4.1.15 Analysis of the Raw Bio-oil's Hydrogen-to-Carbon (H/C) Ratio

From the ultimate analysis, the hydrogen to carbon (H/C) ratio was calculated and statistically analyzed. The H/C ratio is related to the amount of energy released during combustion of the biofuel (Jagadish 2011). The higher the H/C ratio, the more energy is released during combustion. For each pyrolysis experiment, three ultimate analysis trials were run, resulting in a total of 27 statistical data points. The data was analyzed statistically to test for a relationship between the H/C ratio and the pyrolysis temperature. The hypotheses tested were:

H_0: $\mu H/C_{400°C} = \mu H/C_{500°C} = \mu H/C_{600°C}$ (i.e. the H/C ratio of the raw bio-oil is affected by the pyrolysis temperature).

H_A: $\mu H/C_{400°C} \neq \mu H/C_{500°C} \neq \mu H/C_{600°C}$ (i.e. the H/C ratio of the raw bio-oil is not affected by the pyrolysis temperature).

An ANOVA was used to analyze the data. The F-statistic used to test the equality of the means was distributed as $F_{2,24}$. The rejection criteria was $F_0 > F_{0.05,2,24}$. All tests were performed at the 5% level of α.

4.1.16 Energy Content Analysis of Raw Bio-oil

The raw bio-oil was analyzed using a bomb calorimeter (Manufacturer: Parr Instruments, Model:6200) to determine its energy content. Pyrolysis temperature was an input factor represented at three levels, and the HHV was the only response factor. For statistical purposes, three heating values were determined for each pyrolysis experiment and at each pyrolysis temperature for a total of 27 data points. The hypotheses tested were:

H_0: $\mu HHV_{400°C} = \mu HHV_{500°C} = \mu HHV_{600°C}$ (i.e. the HHV of the raw bio-oil is not affected by the pyrolysis temperature).

H_A: $\mu HHV_{400°C} = \mu HHV_{500°C} = \mu HHV_{600°C}$ (i.e. the HHV of the raw bio-oil is affected by the pyrolysis temperature).

An ANOVA was used to analyze the data. The F-statistic was used to test the equality of the means which was distributed as $F_{2,24}$. The rejection criteria for H_0 was $F_0 > F_{0.05,\,2,24}$. All tests were performed at the 5% level of α.

4.1.17 Density Analysis of the Raw Bio-oil

The density of the raw bio-oil was calculated by weighing one milliliter of bio-oil and dividing the weight by the volume. Pyrolysis temperature was an input factor that was represented at three levels, and the density was the only response factor. For statistical purposes, three density values were determined for each pyrolysis experiment and at each pyrolysis temperature for a total of 27 data points. The hypotheses tested were:

H_0: $\mu\rho_{400°C} = \mu\rho_{500°C} = \mu\rho_{600°C}$ (i.e. the ρ of the raw bio-oil is not affected by the pyrolysis temperature).

H_A: $\mu\rho_{400°C} = \mu\rho_{500°C} = \mu\rho_{600°C}$ (i.e. the ρ of the raw bio-oil is affected by the pyrolysis temperature).

An ANOVA was used to analyze the data. The F-statistic used to test the equality of the means was distributed as $F_{2,24}$. The rejection criteria for H_0 was $F_0 > F_{0.05,\ 2,24}$. All tests were performed at the 5% level of α.

4.1.18 Total Acid Number (TAN) Analysis of the Raw Bio-oil

The TAN of the raw bio-oil was determined according to ASTM D664. Pyrolysis temperature was an input factor represented at three levels, and the TAN was the only response factor. Again, three TAN values were determined for each pyrolysis experiment and at each pyrolysis temperature for a total of 27 data points. The hypotheses tested were:

H_0: $\mu TAN_{400°C} = \mu TAN_{500°C} = \mu TAN_{600°C}$ (i.e. the TAN of the raw bio-oil is not affected by the pyrolysis temperature).

H_A: $\mu TAN_{400°C} = \mu TAN_{500°C} = \mu TAN_{600°C}$ (i.e. the TAN of the raw bio-oil is affected by the pyrolysis temperature).

An ANOVA was used to analyze the data. The F-statistic used to test the equality of the means was distributed as $F_{2,24}$. The rejection criteria for H_0 was $F_0 > F_{0.05,\ 2,24}$. All tests were performed at the 5% level of α.

The raw bio-oil fraction collected from each pyrolysis experiment (of the same temperature), were combined to produce a collective sample. The distillation setup is pictured I figure 5. This collective sample was distilled to produce the bio-oil distillates. The tests outlined in table 8 were repeated on the bio-distillates with the exception of the UA and the energy content. Distilling the bio-oil resulted in small fractions, often with volumes less than 5 mL. The small distillate volumes limited the number of analytical tests that could be performed. For this reason, after the GCMS analysis of the distillates, a “model mixture” was created from those oxygenated compounds present in the sample at significant concentrations.

Figure 5. Distillation Setup. This figure shows the distillation setup used to distill the pyrolytic bio-oil.

4.1.19 MC Analysis of the Bio-oil Distillates

The MCs of the bio-oil distillates were determined according to ASTM D3173 using a Karl Fisher titrator (Manufacturer: Metrohm Model: 701 Titrino). The MC values were determined in triplicate resulting in a total of 39 statistical data points. The data was statistically analyzed to determine if the pyrolysis temperature affected the MC of the bio-oil distillates. The hypotheses tested were:

H_0: $\mu MC_{400°C} = \mu MC_{500°C} = \mu MC_{600°C}$ (i.e. the MC for each bio-oil distillate is not effected by pyrolysis temperature).

H_A: $\mu MC_{400°C} \neq \mu MC_{500°C} \neq \mu MC_{600°C}$ (i.e. the MC for each bio-oil distillate is effected by pyrolysis temperature).

An ANOVA was used to analyze the data. The F-statistic used to test the equality of the means was distributed as $F_{2,31}$. The rejection criteria for H_0 was $F_0 > F_{0.05,\ 2,31}$. All tests were performed at the 5% level of α.

4.1.20 Density Analysis of the Bio-oil Distillates

The densities of the bio-oil distillates were calculated by weighing one milliliter of the distillate and dividing the weight by the volume. Pyrolysis temperature was an input factor represented at three levels, and the density was the only response factor. For statistical purposes, three density values were determined for each distillate of each collective sample and at each pyrolysis temperature for a total of 39 data points. The first distillate from each temperature was not included because it was determined by KF titration to be the water fraction and was discarded. The hypotheses tested were:

H_0: $\mu\rho_{400°C} = \mu\rho_{500°C} = \mu\rho_{600°C}$ (i.e. the ρ of the bio-oil distillate is not affected by the pyrolysis temperature).

H_A: $\mu\rho_{400°C} = \mu\rho_{500°C} = \mu\rho_{600°C}$ (i.e. the ρ of the bio-oil distillate is affected by the pyrolysis temperature).

An ANOVA was used to analyze the data. The F-statistic was used to test the equality of the means which was distributed as $F_{2,31}$. The rejection criteria for H_0 was $F_0 > F_{0.05,\ 2,31}$. All tests were performed at the 5% level of α.

4.1.21 TAN Analysis of the Bio-oil Distillates

The TANs of the bio-oil distillates were determined according to ASTM D664. Pyrolysis temperature was an input factor represented at three levels, and the TAN was the only response factor. For statistical purposes, three TAN values were determined for each pyrolysis experiment and at each pyrolysis temperature for a total of 39 data points. The hypotheses tested were:

H_0: $\mu TAN_{400°C} = \mu TAN_{500°C} = \mu TAN_{600°C}$ (i.e. the TAN of the bio-oil distillate was not affected by the pyrolysis temperature).

H_A: $\mu TAN_{400°C} = \mu TAN_{500°C} = \mu TAN_{600°C}$ (i.e. the TAN of the bio-oil distillate was affected by the pyrolysis temperature).

An ANOVA was used to analyze the data. The F-statistic was used to test the equality of the means which was distributed as $F_{2,31}$. The rejection criteria for H_0 was $F_0 > F_{0.05,\,2,31}$. All tests were performed at the 5% level of α.

4.1.22 Analysis of the Bio-oil Distillates

A GCMS analysis was performed on the bio-oil distillates which rendered seven response factors including paraffins, isoparaffins, aromatics, naphthenics, olefins, oxygenates, and halogenates. The input factors were pyrolysis temperature, which was present at three levels and distillate fraction. The level of distillate fraction varied among the three pyrolysis temperatures. At 400°C, the distillate level was six, at 500°C, the distillate level was three and at 600°C the distillate level was four. The first distillate of each bio-oil fraction was discarded because it was determined by KF titration to be the

water fraction. Because of the limited amounts, the bio-oil distillates were only analyzed once, resulting in a total of 13 data points for each response factor an a total of 92 GCMS statistical data points. The data was statistically analyzed to determine if the amount of hydrocarbons produced was affected by pyrolysis temperature. The hypotheses tested were:

H_0: $\mu Paraffins_{400°C} = \mu Paraffins_{500°C} = \mu Paraffins_{600°C}$ (i.e. the percentage paraffins present in a specific bio-oil distillate is not affected by pyrolysis temperature).

H_A: $\mu Paraffins_{400°C} \neq \mu Paraffins_{500°C} \neq \mu Paraffins_{600°C}$ (i.e. the percentage paraffins present in a specific bio-oil distillate is affected by pyrolysis temperature).

The data was analyzed statistically to test for a relationship between the hydrocarbons of the bio-oil distillates and the pyrolysis temperature. An ANOVA was used to analyze the data. The F-statistic used to test the equality of the means was distributed as $F_{7,5}$. The rejection criteria for H_0 was $F_0 > F_{0.05,\,7,5}$. All tests were performed at the 5% level of α.

4.2 Procedure to Determine and Evaluate the Deoxygenation Efficiency of the Catalysts and Their Ability to Produce JP8 Hydrocarbons

While the catalysts selected are primarily used to catalyze hydrogenations, they may also be effective deoxygenation catalysts. The deoxygenation capability of the catalyst will be evaluated as well as their abililty to produce hydrocarbons in the JP8

range. The hydrogenation reactions were carried out using a model mixture of phenolic and alcoholic compounds based on the bio-oil distillates.

Prior to beginning the hydrogenation reactions, the hydrogenation apparatus was pressure tested. The setup was pressurized to 225 psi and 200°C, which represented the most caustic set of experimental conditions. The drop in H_2 pressure was recorded over a 24 hour period and the leak rate was determined. Figure 6 shows the hydrogenation setup.

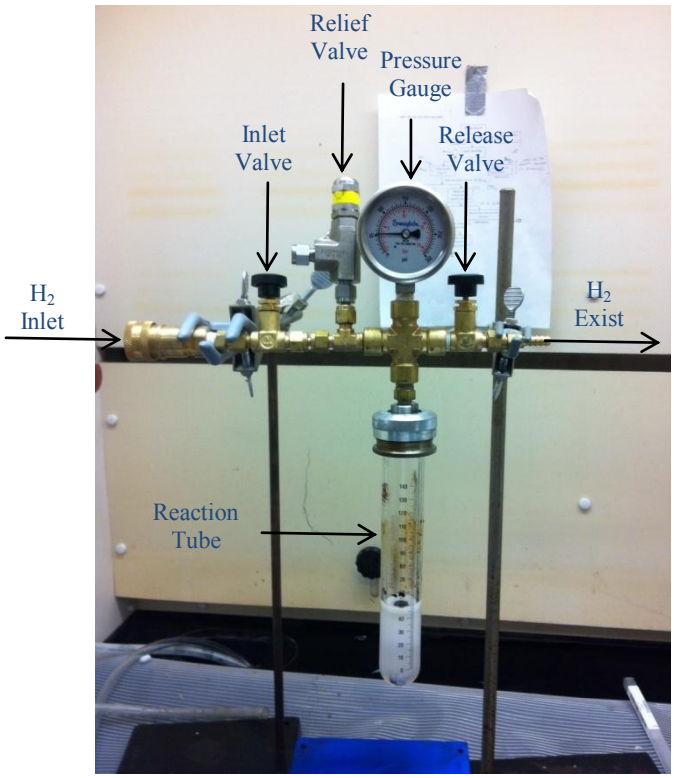

Figure 6. Hydrogenation Setup. The reaction tube was submerged in a mineral oil bath. The oil bath and subsequently the reaction mixture were heated and stirred.

Hydrodeoxygenation is a term used to describe the replacement of oxygen in oxygenated compounds with hydrogen. The hydrodeoxygenation procedure used was the same for both Pd/C and Shvo's catalysts. First, the catalyst (either Pd/C or Shvo's catalyst) was placed inside the reaction tube. Then, the pure compounds comprising the model mixture were added to the reaction tube. The model mixture consisted of o-cresol, m-cresol, 2-ethylphenol, phenol, octanoic acid, pentanoic acid, and heptadecanoic acid. The area of each compound (from each previously analyzed bio-oil distillate) was taken from the compound table and divided by the total sample area to obtain the percent of that compound present in the sample. The percentages from each sample run were averaged and used to determine the percent compositions of the model mixture. The mass percent was calculated from the percent concentration. The approximate masses were 0.039 g (pentanoic acid), 0.057 g (octanoic acid), 0.004 g (heptadecanoic acid), 0.289 g (2-ethylphenol), 1.149 g (m-cresol), 1.319 g (o-cresol) and 1.226 g (phenol). The remainder of the mixture was composed of a phosphoric acid solution for a total model mixture sample mass of 25 g.

In accordance with the procedure described by Zhao et al (2010) for the aqueous hydrogenation of phenols, a phosphoric acid solution was prepared (pH=2) and added to the reaction tube last. The reaction tube was sealed, flushed and pressurized to approximately 125 psi with H_2. Then, stirring and heating were initiated. The pressure and temperature were recorded every 15 minutes over a 12 hour period. This data was used to determine the rate of reaction characterized by a decrease in H_2 pressure.

The hydrodeoxygenation procedure used for the fluorous Pd catalyst was a modification of that used for Pd/C and Shvo's catalyst to accommodate the use of a fluorous solvent and the sensitivity of the catalyst to water. The Pd catalyst used was prepared according to the procedure described by Jurisch (2008) and had the chemical formula $Cl_2Pd(S(CH_2CH_2R_{f8})_2)_2$, where $R_{f8} = (CF_2)_7CF_3$. First, the Pd catalyst was placed inside the reaction tube followed by approximately 1mL of the fluorous oil. The fluorous oil used was manufactured by DuPont (Krytox XHT-500). The Krytox oil is fluorinated synthetic oil with a boiling point range of -20°C to 300°C and the chemical formula $F\text{-}(CF_3CFCF_2O)_n\text{-}CF_2CF_3$ where n = 10 - 60. Then, the model mixture components were each added to the reaction tube. The reaction tube was sealed, flushed and pressurized to approximately 125 psi with H_2. Then, stirring and heating were initiated. The phosphoric acid solution was not included in the reaction mixture because it was known that this particular Pd catalyst was sensitive to water. The overall procedure is pictured in figure 7.

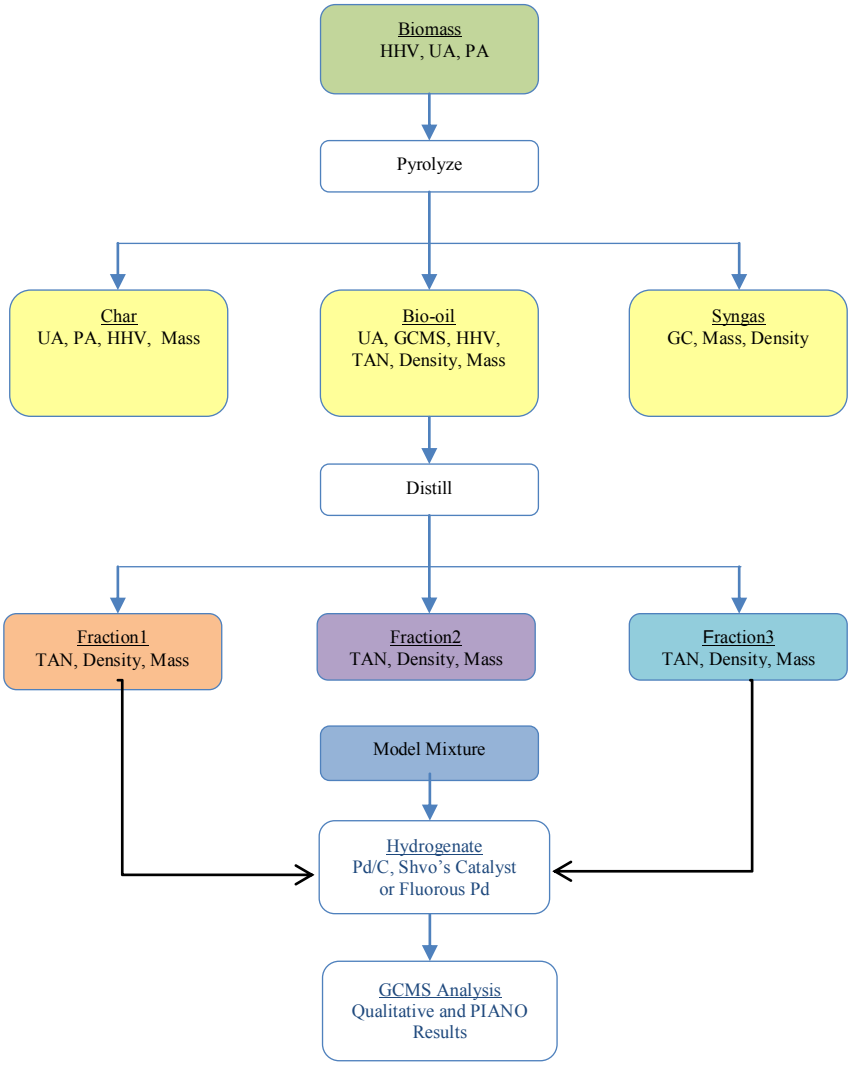

Figure 7. Procedural Diagram

4.2.1 Statistical Procedure for Evaluating the Deoxygenation Capability of Catalysts

This research effort also sought to determine and evaluate the deoxygenation efficiency of the fluorous Pd, Pd/C and the Shvo's catalysts. Given that the initial model mixture was composed entirely of oxygenated compounds, the initial percent concentration of oxygenates was 100%. After hydrogenation, the percentage of

oxygenates was expected to decrease. To statistically evaluate the deoxygenation capability of the catalysts, three hydrogenation trials were run using each of the catalysts for a total of nine statistical data points. The nine data points themselves consisted of the percent concentration of the oxygenates determined by the GCMS analysis. The hypotheses tested were:

H_0: $\mu_{\text{Fluorous Pd}} = \mu_{\text{Pd/C}} = \mu_{\text{Shvo's Catalyst}}$ (i.e. the percent concentration of the oxygenates of all catalysts were equal).

H_A: $\mu_{\text{Fluorous Pd}} \neq \mu_{\text{Pd/C}} \neq \mu_{\text{Shvo's Catalyst}}$ (i.e. the percent concentration of the oxygenates of at least one catalyst differed from the others).

The data was statistically analyzed to determine the deoxygenation capability of each catalyst and evaluated to determine if any one catalysts was better suited for deoxygenation than the others. An ANOVA was used to analyze the data. The F-statistic used to test the equality of the means was distributed as $F_{2,6}$. The rejection criteria for H_0 was $F_0 > F_{0.05,\,2,6}$. All tests were performed at the 5% level of α.

4.2.2 Statistical Procedure for Evaluating the Catalysts Tendency to JP8 Hydrocarbons

Evaluating the deoxygenation capability of the catalysts required a complete GCMS analysis of the hydrogenated product. For the hydrogenated product, the remaining six GCMS response factors (PIANO and halogenates) were statistically analyzed to determine whether a specific catalyst showed a preference for producing a certain group of hydrocarbons (i.e. paraffins, isoparaffins, etc.). The catalysts were the input factor and was present at three levels. A total of three hydrogenation trials were

run for each catalysts resulting in nine statistical data points. This resulted in a total of nine data points for each response factor and 54 data points total. The data was statistically analyzed to determine if the catalyst used affected the amount of hydrocarbons produced. The hypotheses tested were:

H_0: $\mu Paraffins_{400°C} = \mu Paraffins_{500°C} = \mu Paraffins_{600°C}$ (i.e. the percentage paraffins produced was not affected by catalyst choice).

H_A: $\mu Paraffins_{400°C} \neq \mu Paraffins_{500°C} \neq \mu Paraffins_{600°C}$ (i.e. the percentage paraffins was affected by catalyst choice).

A similar set of hypotheses can be written for the isoparaffins, aromatics, naphthenics, and olefins. An ANOVA was used to analyze the data. The F-statistic used to test the equality of the means was distributed as $F_{2,6}$. The rejection criteria for H_0 was $F_0 > F_{0.05, 2,6}$. All tests were performed at the 5% level of α.

4.3 JP8 Hydrocarbon Quality Evaluation

The quality of the JP8 produced will be based on the detection of improved TAN, MC, and oxygenate percent concentration, where the term "improved" refers to a reduction of these properties in the bio-oil distillates as compared to the raw bio-oil.

4.3.1 Statistical Procedure for Evaluating the JP8 Product Quality Based on TAN

The TAN of the raw bio-oil was determined according to ASTM D664. Pyrolysis temperature was an input factor represented at three levels, and the TAN was the only response factor. For statistical purposes, three TAN values were determined for each pyrolysis experiment and at each pyrolysis temperature for a total of 9 data points.

The TAN of the bio-oil distillate was determined according to ASTM D664. Pyrolysis temperature was an input factor represented at three levels, and the TAN was the only response factor. For statistical purposes, three TAN values were determined for each pyrolysis experiment and at each pyrolysis temperature for a total of 39 data points.

Together, the TAN analysis of the raw bio-oil and the bio-oil distillates resulted in 48 data points. The data was statistically evaluated to determine if there was a difference in the TANs of the raw bio-oil and the bio-oil distillates. This provided an indication of the effectiveness of distillation as a method of TAN reduction. The hypotheses tested were:

H_0: $\mu TAN_{raw\ bio\text{-}oil} = \mu TAN_{bio\text{-}oil\ distillates}$ (i.e. the TAN for raw bio-oil equal to the TAN for the bio-oil distillates).

H_A: $\mu TAN_{raw\ bio\text{-}oil} = \mu TAN_{bio\text{-}oil\ distillates}$ (i.e. the TAN for raw bio-oil is not equal to the TAN for the bio-oil distillates).

An ANOVA was performed on the data and the data was blocked by distillate to remove any variation caused by the individual distillates themselves. The F-statistic used to test the equality of the means was distributed as $F_{15,5}$. The rejection criteria for H_0 was $F_0 > F_{0.05,15,5}$. All tests were performed at the 5% level of α.

4.3.2 Statistical Procedure for Evaluating the JP8 Product Quality Based on MC

The MCs of the raw bio-oil fractions were determined according to ASTM D3173 using a Karl Fisher titrator (Manufacturer: Metrohm Model: 701 Titrino). The MC values were determined in triplicate resulting in a total of 9 statistical data points.

The MCs of the bio-oil distillates were determined according to ASTM D3173 using a Karl Fisher titrator (Manufacturer: Metrohm Model: 701 Titrino). The MC values were determined in triplicate resulting in a total of 39 statistical data points. The data was statistically analyzed to determine if the pyrolysis temperature affected the MC of the bio-oil distillates.

Together, the MC analysis of the raw bio-oil and the bio-oil distillates resulted in 48 data points. The data was statistically evaluated to determine if there was a difference in the MCs of the raw bio-oil and the bio-oil distillates. This provided an indication of the effectiveness of distillation as a method of moisture reduction. The hypotheses tested were:

H_0: $\mu MC_{\text{raw bio-oil}} = \mu MC_{\text{bio-oil distillates}}$ (i.e. the MC for raw bio-oil equal to the MC for the bio-oil distillates).

H_A: $\mu MC_{\text{raw bio-oil}} = \mu MC_{\text{bio-oil distillates}}$ (i.e. the MC for raw bio-oil is not equal to the MC for the bio-oil distillates).

An ANOVA was performed on the data and the data was blocked by distillate to remove any variation caused by the individual distillates themselves. The F-statistic used

to test the equality of the means was distributed as $F_{15,5}$. The rejection criteria for H_0 was $F_0 > F_{0.05,15,5}$. All tests were performed at the 5% level of α.

CHAPTER V

RESULTS AND DISCUSSION

5.1 Results for the Characterization of Miscane Feedstock and Pyrolysis Co-Products

Miscane, sugarcane and *Miscanthus* are all C4 plants. The results of their individual elemental analyses were similar for all elements. The PA showed some significant differences among the MCs of the feedstocks. These differences were explained by the fact that upon arrival, the miscane had been field dried while the others were fresh cut. The HHVs of the feedstocks appeared to be directly proportional to the MC. The UA, PA, and energy content results are displayed in table 9.

Table 9. Comparison of Miscane Properties to Other Feedstocks

Ultimate Analysis			
	Miscane	*Sugarcane*	*Miscanthus*
C	41.29±0.307	47.8±0.041	44.1±0.155
H	5.98±0.044	5.79±0.014	5.76±0.029
O	44.33±0.355	43.2±0.145	41.4±.515
N	0.559±0.009	0.187±0.025	0.675±0.035
S	0.289±0.003	0.140±0.062	0.173±0.037
Proximate Analysis (%)			
MC	8.23±0.15	58.71±0.98	49.3±.82
VCM	74.90±0.65	14.4±1.55	24.6±1.59
Ash	7.55±0.70	2.93±0.08	7.88±0.41
FC	9.32±0.69	23.9±14.8	18.25±1.29
Energy Content (Btu/lb)			
HHV	7485±6.36	8147±9.15	8278±158.45

This table compares the ultimate analyses, proximate analyses and energy contents of miscane, sugarcane, and *Miscanthus*.

The VCM constitutes the combustible components of the feedstock that vaporizes when heated. A high VCM content indicates the ease of ignition of the source. It is also an indication of the gaseous fuels present in the biomass. The FC represents free carbon that is not bound to other elements. FC acts as a heat generator during burning. Together, the amounts of VCM and FC directly contribute to the energy content of the biomass. Ash is an impurity that will not burn. The presence of ash causes slagging and fouling and reduces the burn capacity of the biomass. Generally speaking, biomass that is to be burned for fuel should have high VCM and FC contents but low ash content. Because the initial moisture contents for each of the feedstocks were different, no direct comparisons can be made from the data in table 9.

5.1.1 Results of the Miscane Syngas Analysis

While syngas is primarily composed of H_2, CO, and CH_4, other gases are present as well. The GC analysis showed that CO_2 was also a major component of miscane syngas. GC analysis of the syngas produced gave the following component percentages listed in table 10 below:

Table 10. Percent Composition of Syngas Components

	400°C	500°C	600°C
H_2	4.385±0.054	11.694±0.271	9.199±0.062
O_2	1.233±0.066	2.977±0.171	2.449±0.296
N_2	3.531±0.193	9.162±0.524	9.119±0.988
CO	11.594±0.281	4.801±0.306	5.924±0.092
CH_4	26.861±0.306	34.857±0.851	43.973±0.439
CO2	30.46±0.553	18.896±0.382	14.668±0.216
C_2H_2	0	0.005±0.001	0
C_2H_4	1.198±0.057	0.181±0.016	0.068±0.039
C_2H_6	7.115±0.117	3.675±0.093	0.218±0.028
C_3H_6	0.970±0.045	0.253±0.034	0.081±0.047
C_3H_8	2.105±0.059	0.554±0.035	0

Further investigation of the effects of pyrolysis temperature on the significant syngas components are illustrated in figure 8:

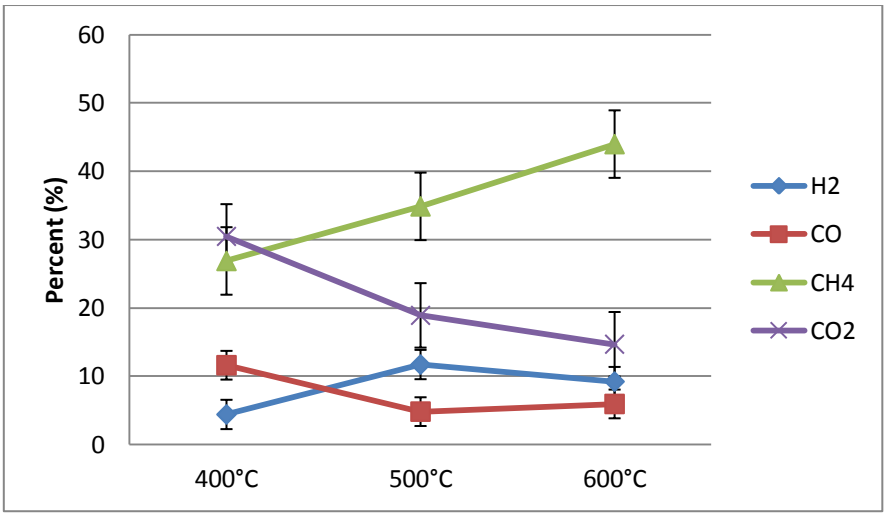

Figure 8. Primary Syngas Components as a Function of Pyrolysis Temperature. This figure graphically illustrates the percentages of the primary syngas components.

Pyrolysis temperature and CH_4 production were directly proportional, while CO_2 had an indirectly proportional relationship with the pyrolysis temperature. The maximum amount of H_2 was produced at 500°C and the minimum amount of CO was produced at 500°C. The miscane syngas was statistically analyzed and the data resides in section A1 of Appendix A. The ANOVA results imply that there is evidence to reject H_0 for each of the major syngas components which suggests that the mean percentage of gas produced is affected by pyrolysis temperature. For each gas, namely H_2, CO, CH_4 and CO_2, their respective F_0 values were greater than $F_{2,24} = 3.40$. The evidence to reject H_0 is further substantiated because the respective p-values of the component gases are less than α. All statistical tests were conducted at the 5% level of α.

The validity of the ANOVA assumptions were verified by checking the adequacy of the model. Both the equality of variance assumption and the normality assumption were verified for the four gases previously mentioned. The plot of the residual versus the fitted values of the percent CO_2 produced indicates the existance of variance inequality. The data was transformed and re-analyzed. After the Box Cox transformation, the results of the previous untransformed ANOVA remained unchanged. There is evidence to rejectt H_0 and suggest that the amount of CO_2 produced is not significantly affected by the pyrolysis temperature. This evidence is further substantiated by the fact that the p-value ($p < 0.0001$) is less than α. When ploted the transformed CO_2 residuals showed there is no evident pattern among the data which suggests that the issue of unequal variances has been corrected. This data resides in section A1 of Appendix A.

Because H_0 was rejected, a t-test of the syngas components was conducted to determine if the percentage of H_2, CO, CH_4 and CO_2 produced was affected by pyrolysis. The results showed that for H_2, the difference was not significant for the percentage of H_2 produced at 500°C and 600°C. However, there was a significant difference between the H_2 production at 400°C in relation to the other two pyrolysis temperatures. The same is true for CO and CO_2. For CH_4, the t-test results showed that the difference was not significant for the percentage of CO produced at 400°C and 500°C, but there was a significant difference between these two pyrolysis temperatures and the amount of CO produced at 600°C. This data resides in section A1 of Appendix A.

Syngas can itself be burned as fuel and is therefore considered to be a source of renewable energy. In addition to being burned as engine fuel, it can be used to produce methanol and H_2 gas. Because of the increased percentages of CH_4 and H_2, the miscane syngas might best be suited for the production of methanol and H_2. All other hydrocarbons were present in insignificant amounts.

5.1.2 Results of Miscane Char Yields

The amount of char produced from each pyrolysis experiment was weighed and statistically analyzed. The results of the char yield measurements are presented in table 11.

Table 11. Char Yield Measurements

Pyrolysis Temperature	Mass (g)
400	437.70
400	387.33
400	436.46
500	421.14
500	425.37
500	447.18
600	406.44
600	398.75
600	415.86

The data in this table represents the char yields obtained from the miscane pyrolysis experiments.

The miscane char yield was statistically analyzed and the data resides in section A2 of Appendix A. The ANOVA results show that because $F_{2,6} > F_0$ (where $F_{2,6} = 5.14$), there is evidence to accept H_0 which states the mean char yield is not affected by pyrolysis temperature. Because the p-value ($p = 0.361$) is greater than α, there is further evidence to accept H_0. The statistical analysis was conducted at the 5% level of α. The validity of the ANOVA assumptions were verified by checking the adequacy of the model. This data resides in section A2 of Appendix A.

For a slow pyrolysis process, such as that used for this research effort, char formation is favored over syngas and liquid product production. Typically, as the temperature and heating rate increase, the amount of char production decreases. The miscane char yields of this research substantiate this claim because at 400°C, 500°C, and 600°C, the respective char yields were 44%, 35% and 34%. If char production was the research goal, there are costs savings associated with producing the char at lower

temperatures. However, this research effort focused on bio-oil production. The highest bio-oil yield was obtained at 600°C.

5.1.3 Results of Miscane Char Ultimate Analysis

An ultimate analysis was conducted on the char produced from the miscane pyrolysis experiments to determine its elemental composition. The results of this analysis are presented in table 12.

Table 12. Miscane Char Elemental Analysis

Pyrolysis Temperature (°C)	%C	%H	%O	%N	%S
400	60.342	4.239	17.303	1.321	0.598
400	66.981	4.203	13.928	1.275	0.674
400	61.713	4.990	15.525	1.131	0.408
400	66.852	3.970	11.406	1.171	0.368
400	65.182	4.388	13.620	1.192	0.483
400	64.347	4.597	14.727	1.203	0.541
400	64.283	4.480	13.465	1.151	0.388
400	66.017	4.179	12.513	1.182	0.426
400	64.765	4.492	9.140	1.198	0.512
500	66.607	2.763	9.863	1.255	0.352
500	71.591	2.805	5.989	1.231	0.313
500	71.281	2.958	5.992	1.386	0.312
500	69.826	2.842	7.282	1.291	0.326
500	69.099	2.784	8.471	1.243	0.333
500	71.436	2.882	5.809	1.309	0.313
500	70.554	2.900	6.637	1.338	0.319
500	69.463	2.813	7.967	1.267	0.329
500	70.268	2.833	7.049	1.276	0.323
600	72.417	2.218	4.083	1.207	0.654
600	73.761	2.181	4.555	1.589	0.277
600	73.089	2.200	2.202	1.398	0.543
600	73.089	2.367	3.108	1.973	0.254
600	73.425	2.190	4.015	1.494	0.347

Table 12 Continued

Pyrolysis Temperature (°C)	%C	%H	%O	%N	%S
600	75.432	2.283	1.098	1.686	0.399
600	73.342	2.279	2.457	1.733	0.301
600	74.429	1.983	2.757	1.590	0.373
600	74.387	1.342	3.396	1.709	0.350

This is the raw data resulting from the elemental analysis of the miscane char. The percent O was determined by difference.

The miscane char ultimate analysis was statistically analyzed and the data resides in section A3 of Appendix A. The ANOVA results show that because $F_0 > F_{2,24}$ (where $F_{2,24} = 3.40$) for all elements, there is evidence to reject H_0 and suggest that the amount of C, H, O, N, and S produced are affected by pyrolysis temperature. Because the p-values for each of the elements are all less than α, there is further evidence to reject H_0. The statistical analysis was conducted at the 5% level of α.

The validity of the ANOVA assumptions were verified by checking the adequacy of the model. Because H_0 was rejected, a t-test was conducted on the miscane char elemental analysis data to determine if the mean percentages of C, H, O, N, and S produced was affected by pyrolysis. The results showed that the mean C, H, and O percentages were significantly different at each pyrolysis temperature. There was not a significant difference between the mean percent N produced at the 400°C and 500°C level but 600°C was significantly different from the other temperatures. There was not a significant difference between the mean percent S produced at the 500°C and 600°C

level but 400°C was significantly different from the other temperatures. This data resides in section A3 of Appendix A.

5.1.4 Results of Miscane Char Proximate Analysis

A proximate analysis was conducted on the char produced from the miscane pyrolysis experiments. The results of this analysis are presented in table 13.

Table 13. Miscane Char Proximate Analysis

Pyrolysis Temperature	MC (%)	VCM (%)	Ash (%)	FC (%)
400	0.533	30.704	16.197	52.567
400	5.045	44.630	12.939	37.386
400	8.108	29.736	16.233	45.923
400	0.423	35.023	16.233	48.321
400	4.525	36.463	15.135	43.876
400	6.577	37.183	14.586	41.654
400	4.265	32.380	16.233	47.122
400	2.474	35.743	15.684	46.098
400	1.383	17.874	19.893	60.850
500	0.721	20.935	19.160	59.185
500	0.637	19.490	18.071	61.803
500	0.035	0.820	18.071	81.075
500	0.464	13.748	18.434	67.354
500	0.336	10.155	18.071	71.439
500	0.249	7.284	18.252	74.214
500	0.400	11.952	18.252	69.396
500	0.293	8.720	18.161	72.827
500	0.325	9.618	18.252	71.805
600	2.771	20.148	17.637	59.444
600	3.375	13.760	20.569	62.296
600	2.137	17.491	19.209	61.163
600	1.518	19.356	18.529	60.596
600	3.073	16.954	19.103	60.870
600	2.756	15.625	19.889	61.729
600	1.828	18.424	18.869	60.880

Table 13 Continued

Pyrolysis Temperature	MC (%)	VCM (%)	Ash (%)	FC (%)
600	2.296	18.155	18.816	60.733

This table displays the results of the miscane char prosimate analysis. The FC was determined by difference.

The miscane char proximate analysis was statistically analyzed and the data resides in section A4 of Appendix A. The ANOVA results show that because $F_0 > F_{2,24}$ (where $F_{2,24} = 3.40$) for all parameters (MC, VCM, ash, and FC), there is evidence to reject H_0 and suggest that the percent MC, VCM, ash, and FC produced are affected by pyrolysis temperature. Because the p-values for each of the elements are all less than α, there is further evidence to reject H_0. The statistical analysis was conducted at the 5% level of α.

The validity of the ANOVA assumptions were verified by checking the adequacy of the model. The plot of the residual versus the fitted values of the percent MC data indicates the existance of variance inequality. The data was transformed and re-analyzed. After the Box Cox transformation, the results of the previous untransformed ANOVA remained unchanged. There is evidence to reject H_0 and suggest that the percent MC produced is significantly affected by the pyrolysis temperature. This evidence is further substantiated by the fact that the p-value ($p < 0.0001$) is less than α. This data resides in section A4 of Appendix A.

Because H_0 was rejected, a t-test was conducted on the miscane char proximate analysis data to determine if the mean MC, VCM, ash and FC percentages produced

were affected by pyrolysis. The results showed that for VCM, ash, and FC, there was a significant difference between their respective mean percentages produced between 400°C and 500°C as well as between 500°C and 600°C. The t-test was conducted on the transformed percent MC data. The results showed that there was no significant difference between the percent MC produced at 400C and 500C, but that 500C was significantly difference from the other temperatures. This data resides in section A4 of Appendix A.

Biochar can be burned directly for energy generation or co-fired with traditional coal. To do so, relatively high percentages of VCM and FC are desired along with low ash percentages. The VCM and FC content of the the miscane char suggest that it may burned as a stand alone fuel source. Theburn properties of the miscane char maybe improved if it were to be co-fired with a traditional coal. In this case, the miscane char would serve to supplement the existing fossil fuel supply. It is possible that the miscane char would be a clean burning fuel, but burn studies that incorporate air quality testing would need to be conducted to confirm this theory.

5.1.5 Results of Miscane Char Energy Content Analysis

The energy content of the char produced from each pyrolysis experiment was statistically analyzed to determine if there was an underlying affect of the pyrolysis temperature. The results of this analysis are presented in table 14.

Table 14. Miscane Char Energy Content Results

Pyrolysis Temperature (°C)	HHV (Btu lb^{-1})
400	11557
400	11717
400	10882
400	11637
400	11300
400	11385
400	11220
400	11301
400	10995
500	11780
500	12418
500	11729
500	11976
500	12099
500	12074
500	11755
500	12050
500	11540
600	11800
600	12969
600	11965
600	12245
600	12385
600	12467
600	11438
600	11874
600	11238

The miscane char energy content analysis was statistically analyzed and the data resides in section A5 of Appendix A. The ANOVA results show that because $F_{2,24} < F_0$ (where $F_{2,24} = 3.40$), there is evidence to reject H_0 which states the mean energy content of the char is not affected by pyrolysis temperature. Because the p-value ($p = 0.001$) is

less than α, there is further evidence to reject H_0. The statistical analysis was conducted at the 5% level of α. The validity of the ANOVA assumptions were verified by checking the adequacy of the model. This data resides in section A5 of Appendix A.

Because H_0 was rejected, a t-test was conducted on the miscane char heating values to determine if the mean heating value was affected by pyrolysis. The results showed that there was no significant difference between the 500°C and 600°C char heating values, but the 400C heating value was significantly different from the other temperatures. This data resides in section A5 of Appendix A.

The heat of combustion is the defined as the energy released during the complete combustion of a compound. It is measured by a bomb calorimeter and can be expressed in different quantities including the high heating value (HHV). The HHV is defined as the amount of energy released during the combustion of a specified amount of a substance. In this case, the energy content of the miscane char was measured using a bomb calorimeter and expressed as the HHV. On average, the energy content of the miscane char increased as the pyrolysis temperature increased. The implication is that if char were to be burned either directly or co-fired with another fuel source, the energy released from the miscane char produced at 600°C would be greater than that of the chars produced at lower pyrolysis temperatures.

5.1.6 Results of the JP8 Calibration Curve

The GCMS analysis of the JP8 standard solutions resulted in a compound table, a chromatogram and a calibration curve. Figure 9 is the JP8 chromatogram from the analysis of the 5000 ppm standard and Table 15 lists the compounds identified in JP8.

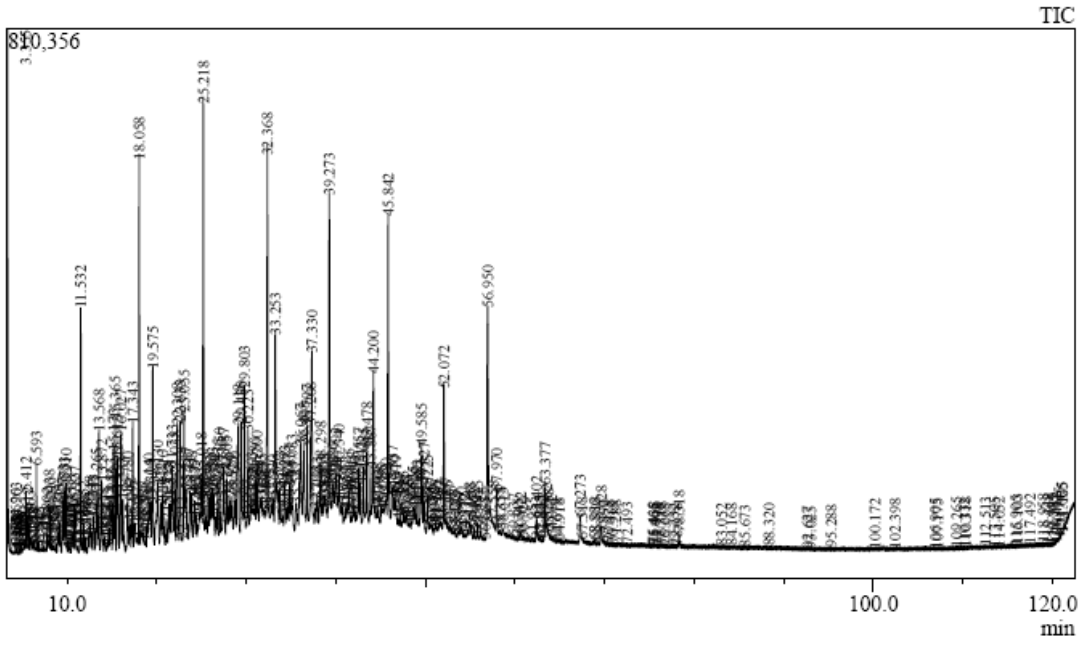

Figure 9. 5000ppm JP8 Chromatogram. This is the chromatogram for the 5000 ppm JP8 standard with retention times.

Table 15. JP8 Compound Table

Retention Time	Compound Name
3.355	Cyclohexene
3.69	Heptane
4.263	Cyclohexane, methyl-
5.612	Heptane, 3-methyl-
5.863	Cyclohexane, 1,4-dimethyl-
6.593	Octane
6.842	Cyclohexane, 1,4-dimethyl-, cis-
7.452	Heptane, 2,4-dimethyl-
7.802	Heptane, 2,6-dimethyl-
8.038	Cyclopentane, 1-ethyl-3-methyl-, cis-
8.21	Cyclohexane, 1,1,3-trimethyl-
8.972	Cyclohexane, 1,3,5-trimethyl-, (1.alpha.,3.alpha.,5.beta.)-
9.073	Heptane, 2,3-dimethyl-
9.262	Ethylbenzene
9.477	Hexane, 2,3,4-trimethyl-
9.583	Octane, 2-methyl-

Table 15 Continued

Retention Time	Compound Name
9.733	p-Xylene
9.91	Octane, 3-methyl-
10.783	Cyclohexane, 1-ethyl-4-methyl-, cis-
10.927	o-Xylene
11.532	Nonane
11.852	Cyclohexane, 1-ethyl-4-methyl-, cis-
12.37	Heptane, 3,5-dimethyl-
12.548	1,3-Cyclopentanedimethanol
12.943	Pentane, 2,2,3,3-tetramethyl-
13.265	Cyclohexane, (1-methylethyl)-
13.568	Nonane, 3-methyl-
13.872	Decane, 2,5-dimethyl-
14.227	1-Tridecyne
14.645	Benzene, propyl-
14.863	Octane, 4-ethyl-
15.613	Nonane, 2-methyl-
15.725	Benzene, 1,2,3-trimethyl-
16.027	Nonane, 3-methyl-
16.78	Cyclopentane, 1,2-dimethyl-3-(1-methylethyl)-
17.042	1,1'-Bicycloheptyl
17.343	Benzene, 1,2,3-trimethyl-
17.607	Cyclohexane, 1-ethyl-2-methyl-, cis-
18.058	Decane
18.777	Isooctane, (ethenyloxy)-
18.938	1-Octanol, 2-butyl-
19.14	Benzene, (1-methylethyl)-
19.305	1-Octanol, 2-butyl-
19.575	Decane, 4-methyl-
20.13	Cyclohexane, (2-methylpropyl)-
20.472	Hexadecane, 3-methyl-
20.71	Decane, 3-methyl-
21.377	Benzene, 1-methyl-3-propyl-
21.538	1-Pentanol, 4-methyl-2-propyl-
22.038	Nonane, 2,5-dimethyl-
22.633	Decane, 2-methyl-
23.055	Decane, 3-methyl-
23.287	Benzene, 1-methyl-2-(1-methylethyl)-
23.717	Benzene, 1-methyl-2-(1-methylethyl)-

Table 15 Continued

Retention Time	Compound Name
23.908	Cyclopentane, 1,2-dimethyl-3-(1-methylethyl)-
24.235	1-Decene, 5-methyl-
24.423	(2-Methylbutyl)cyclohexane
25.018	Benzene, 1,3-diethyl-5-methyl-
25.218	Undecane
25.408	1-Undecene, 4-methyl-
25.767	5-Hexadecyne
26.203	Benzene, 4-ethyl-1,2-dimethyl-
26.382	Octane, 3,4,5,6-tetramethyl-
26.592	3-Eicosene, (E)-
26.835	1-Hexadecyne
27.05	Decane, 3,7-dimethyl-
27.487	n-Amylcyclohexane
28.323	Benzene, 1-ethyl-2,3-dimethyl-
29.43	Octane, 2,3,6,7-tetramethyl-
29.803	Hexadecane
30.223	Undecane, 3-methyl-
31.2	trans-1,3-Diethylcyclopentane
32.368	Tridecane
33.253	Undecane, 2,6-dimethyl-
33.773	Decane, 2,3,5,8-tetramethyl-
34.293	Hexadecane, 1-chloro-
34.857	Cyclohexane, (1-methylethyl)-
35.083	1-Octanol, 2-butyl-
36.067	1-Heptanol, 2-propyl-
36.408	Heptadecane, 4-methyl-
36.797	Hexadecane
37.208	Oxalic acid, isobutyl undecyl ester
37.33	Octane, 2,3,7-trimethyl-
39.273	Tridecane
39.68	Decane, 1,1'-oxybis-
40.34	Tridecane, 6-methyl-
40.685	2-Hexyl-1-octanol
41.057	1-Iodo-2-methylundecane
41.918	Cyclohexane, (2-methylpropyl)-
42.08	Cyclopentane, pentyl-
42.557	Tridecane, 6-methyl-
42.742	Undecane, 4-ethyl-

Table 15 Continued

Retention Time	Compound Name
43.085	Decane, 2,3,5,8-tetramethyl-
43.478	Nonadecane, 2-methyl-
43.887	Dodecane, 3-methyl-
44.2	Dodecane, 2,6,11-trimethyl-
45.842	Dodecane
48.625	Cyclohexane, (1-methylethyl)-
48.89	Octane, 2,4,6-trimethyl-
49.083	Sulfurous acid, hexyl pentadecyl ester
49.437	Undecane, 4,8-dimethyl-
49.585	Hexadecane
49.827	Tetradecane
50.225	Nonane, 3,7-dimethyl-
52.072	Hexadecane
55.825	Hexadecane
56.95	Diethyl Phthalate
57.97	Dodecane
67.273	1-Chloro-2-methyl-2-phenylpropane

This table lists the compounds identified in the JP8 standard and their retention times.

Table 16 displays the results of the PIANO analysis for JP8.

Table 16. PIANO Analysis Results for the JP8 Standard

Chemical Grouping	JP8
Paraffins	31.96
Iso-paraffins	43.44
Aromatics	6.23
Naphthenics	8.25
Olefins	1.06
Oxygenates	6.34
Halogenates	2.72

The group sum percentages for each chemical category are reported for JP8.

5.1.7 Results of the Miscane Raw Bio-oil Analysis

The raw bio-oil refers to unprocessed bio-oil that was collected immediately after each pyrolysis experiment and separated from the aqueous phase. An ultimate analysis was performed on the raw bio-oil and the unprocessed data is displayed in table 17. Figure 10 graphically displays the relationship between the average C, H, O, N, and S values and pyrolysis temperature.

Table 17. Raw Miscane Bio-oil Ultimate Analysis Results

Pyrolysis Temperature (°C)	C(%)	H(%)	O(%)	N(%)	S(%)
400	59.728	6.999	32.112	0.785	0.376
400	74.238	8.448	16.203	0.970	0.141
400	53.107	5.909	39.795	0.839	0.350
400	62.358	7.119	29.370	0.865	0.289
400	66.983	7.724	24.158	0.878	0.259
400	63.673	7.179	27.999	0.905	0.246
400	57.732	6.514	34.583	0.852	0.320
400	64.670	7.421	26.764	0.871	0.274
400	65.328	7.451	26.078	0.891	0.252
500	76.307	8.598	14.077	0.906	0.112
500	68.888	7.758	22.376	0.901	0.077
500	71.808	8.243	19.039	0.817	0.093
500	46.521	5.297	46.897	0.829	0.456
500	47.580	5.309	46.096	0.803	0.212
500	55.122	6.328	37.673	0.749	0.128
500	72.334	8.200	18.497	0.875	0.094
500	62.406	7.099	29.437	0.849	0.209
500	55.303	6.283	37.344	0.816	0.254
600	67.321	7.577	24.210	0.794	0.098
600	68.120	7.564	23.173	1.028	0.115
600	40.126	4.553	54.636	0.589	0.096
600	44.344	4.985	49.802	0.783	0.086
600	50.863	5.701	42.537	0.800	0.099

Table 17 Continued

Pyrolysis Temperature (°C)	C(%)	H(%)	O(%)	N(%)	S(%)
600	42.235	4.769	52.219	0.686	0.091
600	47.604	5.343	46.170	0.792	0.093
600	46.549	5.235	47.378	0.743	0.095
600	44.919	5.056	49.194	0.739	0.092

This table displays the ultimate analysis results of the raw miscane bio-oil. The percent oxygen was determined by difference.

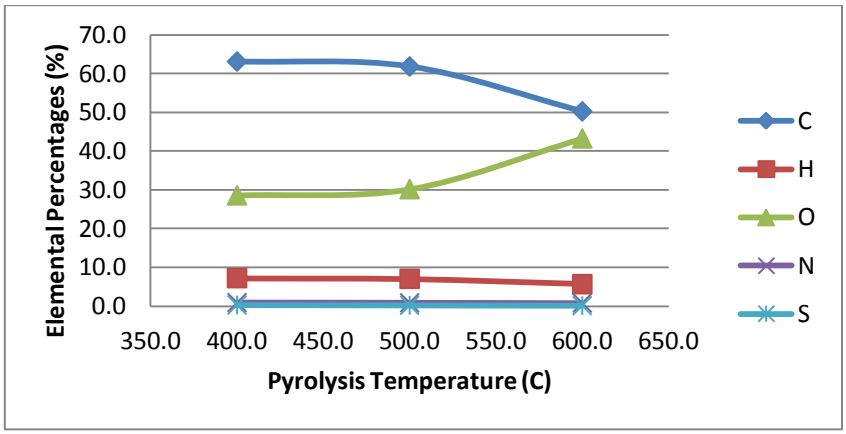

Figure 10. Elemental Analysis of Bio-oil As a Function of Pyrolysis Temperature.

The maximum values of C and H were obtained at 400°C while the minimum value of O was evident at this same pyrolysis temperature. In comparison to the other elements, N and S were present in insignificant amounts. The decreased S content is considered to be an advantage of bio-oil over traditional crude oil. The presence of S and other impurities has been associated with the deactivation of hydrogenation catalysts. Conversely, the elevated O levels of bio-oil indicate the need for bio-oil to be upgraded, and the O content lowered before it can be used as a drop-in biofuel. Traditional crude

oil does not have the elevated O levels that have come to be associated with bio-oil. Catalyst deactivation can be an expensive problem considering many hydrogenation catalysts are precious metal catalysts.

Raw bio-oil samples were analyzed for MC, TAN, HHV, and density. The results are listed in table 18. Variations among MC percentages of bio-oil were dependent upon the ability of the operator to sufficiently separate the aqueous phase from the bio-oil phase. It is certainly possible that the increased MC of the 500°C and 600°C bio-oil samples could have affected the other properties such as the TAN or HHV.

Table18. Properties of Raw Bio-oil

	400°C	500°C	600°C
MC (%)	6.348±0.037	24.98±0.239	21.93±0.050
TAN (mg KOH g bio-oil^{-1})	26.64±0.111	19.55±0.148	13.37±2.084
HHV (BTU lb^{-1})	13513±164	12762±93	12131±96
Density @ 25°C (g mL^{-1})	1.274±0.004	1.305±0.013	1.419±0.013

Various properties of raw bio-oil are reported as a function of pyrolysis temperature.

5.1.8 Results of Miscane Raw Bio-oil Moisture Content (MC) Analysis

The moisture content of the raw miscane bio-oil produced from each pyrolysis experiment was statistically analyzed to determine if there was an underlying affect of the pyrolysis temperature. The raw bio-oil MC data is presented in table 19.

Table 19. Raw Bio-oil Moisture Content

Pyrolysis Temperature	MC (%)
400	5.612
400	6.822
400	6.467
400	6.300
400	6.217
400	6.645
400	6.384
400	6.259
400	6.431
500	28.650
500	24.910
500	21.380
500	24.980
500	26.780
500	23.145
500	23.180
500	25.880
500	24.963
600	21.945
600	22.348
600	22.126
600	21.978
600	21.922
600	22.764
600	21.222
600	21.459
600	22.037

The MC of the raw bio-oil was determined using the KF titreation method.

The MC of the raw miscane bio-oil was statistically analyzed and the data resides in section A6 of Appendix A. The ANOVA results show that because $F_{2,24} < F_0$ (where $F_{2,24} = 3.40$), there is evidence to reject H_0 which states the mean MC of the raw

miscane bio-oil is not affected by pyrolysis temperature. Because the p-value ($p < 0.001$) is less than α, there is further evidence to reject H_0. The statistical analysis was conducted at the 5% level of α. The validity of the ANOVA assumptions were verified by checking the adequacy of the model and this data resides in section A6 of Appendix A.

Because H_0 was rejected, a t-test was conducted on the miscane raw bio-oil MC to determine if there was a significant difference between the mean MC values. The results showed that there was a significant difference between all MC values from each of the pyrolysis temperatures. This was an expected conclusion considering the vast difference between the MCs of each bio-oil sample. This data resides in section A6 of Appendix A.

The MC of the bio-oil samples in part varied based on the ability of the operator to sufficiently separate the aquaeous phase products from the bio-oil phase. Care was taken during th MC analysis to ensure the sample was well mixed. The MC is an indication of the amount of water present in the sample. The presence of water could also be an indication of the presence of other polar compounds with similar chemical functional groups. It was expected that a decreased TAN would be assoiated with lower MC values, but the data of table 18 demonstrates the contrary. Similarly, it was expected that increased MC would have lowered the density values of the bio-oil samples, but again, the data illisutrated the contrary.

5.1.9 Results of Miscane Raw Bio-oil Ultimate Analysis

The elemental analysis of the raw miscane bio-oil produced from each pyrolysis experiment and was analyzed to determine the affect of pyrolysis temperature. The elemental analysis data is presented in table 20.

Table 20. Raw Bio-oil Elemental Analysis Data

Pyrolysis Temperature	C(%)	H(%)	O(%)	N(%)	S(%)
400	59.728	6.999	32.112	0.785	0.376
400	74.238	8.448	16.203	0.970	0.141
400	53.107	5.909	39.795	0.839	0.350
400	62.358	7.119	29.370	0.865	0.289
400	66.983	7.724	24.158	0.878	0.259
400	63.673	7.179	27.999	0.905	0.246
400	57.732	6.514	34.583	0.852	0.320
400	64.670	7.421	26.764	0.871	0.274
400	65.328	7.451	26.078	0.891	0.252
500	76.307	8.598	14.077	0.906	0.112
500	68.888	7.758	22.376	0.901	0.077
500	71.808	8.243	19.039	0.817	0.093
500	46.521	5.297	46.897	0.829	0.456
500	47.580	5.309	46.096	0.803	0.212
500	55.122	6.328	37.673	0.749	0.128
500	72.334	8.200	18.497	0.875	0.094
500	62.406	7.099	29.437	0.849	0.209
500	55.303	6.283	37.344	0.816	0.254
600	67.321	7.577	24.210	0.794	0.098
600	68.120	7.564	23.173	1.028	0.115
600	40.126	4.553	54.636	0.589	0.096
600	44.344	4.985	49.802	0.783	0.086
600	50.863	5.701	42.537	0.800	0.099
600	42.235	4.769	52.219	0.686	0.091
600	47.604	5.343	46.170	0.792	0.093
600	46.549	5.235	47.378	0.743	0.095
600	44.919	5.056	49.194	0.739	0.092

The data was statistically analyzed to determine if there was an underlying affect of the pyrolysis temperature on the percent C, H, (O + Ash), S, and N, and the data resides in section A7 of Appendix A. The ANOVA results show that because $F_{2,24} < F_0$ (where $F_{2,24} = 3.40$) for all elements there is evidence to reject H_0 for each corresponding element which states the mean elemental percentage of the raw miscane bio-oil is not affected by pyrolysis temperature. Because the bio-oil was not ashed, the percent O_2 could not be determined. As a result, the percent O_2 + ash was reported. Because the p-values for C ($p = 0.014$), H ($p = 0.009$), O_2 + ash ($p = 0.012$), N ($p = 0.039$) and S ($p = 0.003$) were each less than α, there is further evidence to reject H_0. The statistical analysis was conducted at the 5% level of α. The validity of the ANOVA assumptions were verified by checking the adequacy of the model.

Because H_0 was rejected, a t-test was conducted on the miscane raw bio-oil ultimate analysis results to determine if there was a significant difference between the mean percentages of C, H, (O + Ash), N, and S values. The results showed that for the C, the mean percentage produced was not significantly different at the 400°C and 500°C levels of pyrolysis temperature, but the 600°C pyrolysis temperature level was significantly different from both of the other temperature levels. The same was observed for H and (O_2 + Ash). The results for N showed that there was a significant difference for the mean percentage of N produced at the 400°C and 600°C levels of pyrolysis temperature. However, there was not a significant difference between the mean percentage of N produced between the 400°C and 500°C levels of pyrolysis temperature or the 500°C and 600°C levels of pyrolysis temperature. The results for S showed that all

levels of pyrolysis temperature produced significantly different mean percentages of S. This data resides in section A7 of Appendix A.

5.1.10 Results of Miscane Raw Bio-oil H/C Ratio

The H/C ratio was calculated using the results of the ultimate analysis, the sample masses and the molecular weights of C and H. The data is presented in table 21.

Table 21. H/C Ratio for Raw Miscane Bio-oil

Pyrolysis Temperature	Sample Mass (mg)	H/C
400	2.70	1.393
400	1.50	1.353
400	3.50	1.323
400	3.30	1.357
400	1.80	1.371
400	3.89	1.341
400	3.81	1.342
400	4.23	1.365
400	4.08	1.356
500	4.58	1.340
500	3.54	1.339
500	4.42	1.365
500	4.26	1.354
500	3.72	1.327
500	3.00	1.365
500	4.37	1.348
500	4.96	1.353
500	3.90	1.351
600	4.46	1.338
600	3.67	1.320
600	3.20	1.349
600	2.85	1.337
600	4.05	1.333
600	2.23	1.343
600	4.07	1.335
600	3.44	1.337

Table 21 Continued

Pyrolysis Temperature	Sample Mass (mg)	H/C
600	3.02	1.338

The H/C ratio of the raw miscane bio-oil was calculated using the elemental analysis results.

The H/C ratio data was statistically analyzed for the raw miscane bio-oil produced from each pyrolysis experiment to determine if there was an underlying affect of the pyrolysis temperature. The data resides in section A8 of Appendix A. The ANOVA results show that because $F_{2,24} < F_0$ (where $F_{2,24} = 3.40$), there is evidence to reject H_0 which states the mean H/C ratio of the raw miscane bio-oil is not affected by pyrolysis temperature. Because the p-value ($p = 0.029$) is less than α, there is further evidence to reject H_0. The statistical analysis was conducted at the 5% level of α. The validity of the ANOVA assumptions were verified by checking the adequacy of the model. This data can be found in section A8 of Appendix A.

Because H_0 was rejected, a t-test was conducted on the miscane raw bio-oil H/C ratio to determine if there was a significant difference between the mean H/C ratios. The results showed that there was a significant difference between the mean H/C ratios of the 400°C and 600°C raw bio-oil.

The ignition temperature for burning fuel is related to the H/C ratio, which is in turn related to the amount of energy released during burning. The higher the H/C ratio, the more energy is released during combustion. Although the t-test indicated that the difference between the mean H/C ratios of the 400°C and 600°C pyrolysis bio-oil, the

difference between the actual values is relatively small with the average H/C ratio at 400°C being 1.356 and the average H/C ratio at 600°C being 1.337. These values are lower than the H/C ratio for JP8 which is approximately 1.91 (Unknown unknown). The increased H/C ratio is associated with decreased formation of CO_2 but the increased formation of C-H bonds is associated with a increased toxicity levels (Phelps unknown). The data from the miscane bio-oil suggest that it requires upgrading before the JP8 hydrocarbons can be recognized. The 400°C bio-oil has the highest H/C ratio of the pyrolysis temperatures tested and is therefore closer to the JP8 H/C ratio than the other bio-oil samples.

5.1.11 Results of Miscane Raw Bio-oil Energy Content

The energy content of the raw bio-oil was measured and the data is displayed in table 22.

Table 22. Raw Bio-oil Energy Content

Pyrolysis Temperature	HHV (Btu lb^{-1})
400	14970.634
400	14867.970
400	14897.067
400	14911.890
400	11557.314
400	11717.753
400	11882.793
400	13543.632
400	13271.006
500	12952.401
500	11738.595
500	14575.246

Table 22 Continued

Pyrolysis Temperature	HHV (Btu lb^{-1})
500	11780.588
500	12418.569
500	12688.126
500	13088.747
500	12698.143
500	12924.801
600	11872.097
600	10186.131
600	12859.308
600	12964.000
600	12615.000
600	12231.000
600	11639.179
600	12003.146
600	12812.769

The raw miscane bio-oil was analyzed to determine its energy content.

The energy content data was statistically analyzed to determine if there was an underlying affect of the pyrolysis temperature. This data can be foud in section A9 of Appendix A. The ANOVA results show that because $F_{2,24} < F_0$ (where $F_{2,24} = 3.40$), there is evidence to reject H_0 which states the mean heating value of the raw miscane bio-oil is not affected by pyrolysis temperature. Because the p-value ($p = 0.045$) is less than α, there is further evidence to reject H_0. The statistical analysis was conducted at the 5% level of α.The validity of the ANOVA assumptions were verified by checking the adequacy of the model.

Because H_0 was rejected, a t-test was conducted on the miscane raw bio-oil heating values to determine if there was a significant difference between the mean

heating values. The results showed that there was a significant difference between the mean heating values of the 400°C and 600°C raw bio-oil with those average values being 13,513 Btu lb^{-1} and 12,131 Btu lb^{-1} respectively. This data can be found in section A9 of Appendix A.

On average, the HHV of the raw miscane bio-oil decreases with increasing pyrolysis temperature. The indication is that if the raw bio-oil were to be burned as fuel, the 400°C raw bio-oil would be prefereable to the other temperatures because it contains the highest energy content. This supports the results of the H/C ratio analysis considering that the 400°C bio-oil sample had the highest H/C ratio of all the bio-oil samples. It also contained the lowest MC which suggests could be more stable than the other bio-oil samples produced at 500°C and 600°C. While the increased H/C ratio and HHV of the 400°C bio-oil sample imply the need for further upgrading, it is the most suitable among the bio-oil samples collected as a fuel subsidy.

5.1.12 Results of Miscane Raw Bio-oil Density Determination

The density of the raw bio-oil was measured and the results are presented in table 23.

Table 23. Raw Bio-oil Density Data

Pyrolysis Temperature	Density (g/mL)
400	1.175
400	1.273
400	1.293
400	1.305
400	1.281

Table 23 Continued

Pyrolysis Temperature	Density (g/mL)
400	1.265
400	1.283
400	1.299
400	1.293
500	1.351
500	1.467
500	1.075
500	1.297
500	1.409
500	1.271
500	1.186
500	1.353
500	1.340
600	1.458
600	1.496
600	1.252
600	1.555
600	1.432
600	1.509
600	1.437
600	1.222
600	1.412

The density of the raw miscane bio-oil was determined using gravimetric methods.

The density data was statistically analyzed to determine if there was an underlying affect of the pyrolysis temperature. The data can be foud in section A10 of Appendix A. The results of the ANOVA suggest that because $F_{2,24} < F_0$ (where $F_{2,24} = 3.40$), there is evidence to reject H_0 which states the mean density of the raw miscane bio-oil is not affected by pyrolysis temperature. Because the p-value ($p = 0.010$) is less than α, there is further evidence to reject H_0. The statistical analysis was conducted at the

5% level of α. The validity of the ANOVA assumptions were verified by checking the adequacy of the model.

Because H_0 was rejected, a t-test was conducted on the miscane raw bio-oil density values to determine if there was a significant difference between the mean densities. The results showed that there was a significant difference between the mean heating values of the 400°C and 600°C and also 500°C and 600°C density values.

As the pyrolysis temperature increased, the density of the bio-oil increased. While the 400°C and 500°C bio-oil samples were viscous, they remained pourable. However, the 600°C bio-oil sample had the consistency of tar and had to be heated before it could be poured. Bridgwater et al. (2001) suggests that bio-oil becomes more unstable with increasing temperature and tends to undergo such chemical processes as polymerization and/or agglomeration(Bridgwater 2001). It could be that the increased residence time with the hot pyrolysis gases of the 500°C and 600°C bio-oil samples favored the aforementioned chemical processes, leading to the increased densities recognized in the data. This increased density is undesirable when JP8 hydrocarbons are the desired end product. JP8 has an approximate density of 0.81 g mL^{-1} so that the much higher densities of the raw miscane bio-oil indicate the need to be upgraded.

5.1.13 Results of Miscane Raw Bio-oil Total Acid Number (TAN) Determination

The TANs of the raw bio-oil were measured and the data is in table 24.

Table 24. Raw Bio-oil TAN Data

Pyrolysis Temperature	TAN (mg KOH/g sample)
400	28.13
400	25.92
400	26.86
400	25.64
400	25.47
400	26.23
400	26.95
400	28.23
400	26.34
500	18.59
500	20.05
500	17.34
500	20.56
500	19.96
500	20.23
500	17.67
500	20.73
500	20.78
600	20.03
600	19.96
600	21.05
600	19.95
600	19.34
600	18.12
600	18.44
600	19.38
600	21.02

The TAN data was statistically analyzed to determine if there was an underlying affect of the pyrolysis temperature. This data resides in section A11 of Appendix A. The results of the ANOVA show that because $F_{2,24} < F_0$ (where $F_{2,24} = 3.40$), there is evidence to reject H_0 which states the mean TAN of the raw miscane bio-oil is not

affected by pyrolysis temperature. Because the p-value ($p < 0.0001$) is less than α, there is further evidence to reject H_0. The statistical analysis was conducted at the 5% level of α.The validity of the ANOVA assumptions were verified by checking the adequacy of the model.

Because H_0 was rejected, a t-test was conducted on the miscane raw bio-oil TAN values to determine if there was a significant difference between the mean TANs. The results showed that there was a significant difference between the mean TAN values of the 400°C and 600°C and also 400°C and 500°C TAN values.

The TAN is an important measurement of quality for bio-oil and is defined as the amount of KOH needed to neutralize the acids in one gram of bio-oil. Increased TAN values are associated with instability and corrosion problems. As such, before bio-oil can be utilized as a drop-in biofuel, the TAN needs to be reduced to an acceptable value. For the raw miscane bio-oil, the average TANs for 500°C and 600°C were relatively close in value being 19.32 and 20.15 mg KOH g bio-oil^{-1} respectively. The TAN for the 400°C bio-oil sample (27.02 mg KOH g bio-oil^{-1}) was significantly higher than both of these values. The implication here is that the 400°C bio-oil sample is more corrosive than the other samples. Overall, with the elevated TANs associated with the raw miscance bio-oil of each pyrolysis temperature, there is a need to upgrade the bio-oil. As it stands, no one raw bio-oil sample was directly applicable as a drop-in bio-fuel without first being upgraded.

5.1.14 Results of the Miscane Bio-oil Distillate Analysis

The raw bio-oil from each pyrolysis treatment was distilled and the distillate fractions were analyzed. The results of the characterization tests are listed in table 25. During each distillation, the first fraction collected was identified as the water fraction. No GCMS analysis was performed on this fraction. The remaining fractions each contained less than 5% water and in most cases less than 2% water thereby meeting the objective to produce samples with a MC near zero.

Table 25. Properties of Bio-oil Distillates

	400°C Bio-oil Distillates						
	Fraction 1	**Fraction 2**	**Fraction 3**	**Fraction 4**	**Fraction 5**	**Fraction 6**	**Fraction 7**
MC (%)	75.63	0.424	0.332	0.153	0.07	0.323	0.862
TAN (mg KOH g bio-oil $^{-1}$)	35.12	20	19.66	21.4	19.8	18.8	18.6
Density @ 25°C (g mL^{-1})	1.03	1.005	1.22	1.386	1.302	1.358	1.38
	500°C Bio-oil Distillates						
	Fraction 1	**Fraction 2**	**Fraction 3**	**Fraction 4**			
MC (%)	73.89	4.03	0.654	1.818			
TAN (mg KOH g bio-oil^{-1})	32.04	19.57	21.5	20.8			
Density @ 25°C (g mL^{-1})	1.19	1.26	1.272	1.244			
	600°C Bio-oil Distillates						
	Fraction 1	**Fraction 2**	**Fraction 3**	**Fraction 4**	**Fraction 5**		
MC (%)	89.27	1.003	1.485	0.342	0.271		
TAN (mg KOH g bio-oil^{-1})	43.6	19.3	21.1	20.4	19.7		
Density @ 25°C (g mL^{-1})	1.352	1.174	1.306	1.258	1.258		

The TANs and the densities of the bio-oil distillates were also determined. In each case, the TAN was improved with distilliation, but the density was not. Generally speaking, distillation was an effective method for improving the MC and TAN of the bio-oil but not the density.

5.1.15 Results of Miscane Bio-oil Distillate Moisture Content (MC) Analysis

The moisture content of the miscane bio-oil distillates produced from each pyrolysis experiment was determined by KF titration. The data is in table 26.

Table 26. Bio-oil Distillate Moisture Content Data

Pyrolysis Temperature	Distillate #	MC (%)
400	2	0.439
400	2	0.444
400	2	0.389
400	3	0.345
400	3	0.299
400	3	0.351
400	4	0.153
400	4	0.178
400	4	0.133
400	5	0.07
400	5	0.101
400	5	0.074
400	6	0.323
400	6	0.355
400	6	0.4
400	7	0.854
400	7	0.867
400	7	0.901
500	2	4.34
500	2	4.484
500	2	4.72

Table 26 Continued

Pyrolysis Temperature	Distillate #	MC (%)
500	3	0.657
500	3	0.684
500	3	0.62
500	4	1.892
500	4	1.727
500	4	1.813
600	2	0.94
600	2	0.945
600	2	1.125
600	3	1.458
600	3	1.329
600	3	1.668
600	4	0.363
600	4	0.273
600	4	0.391
600	5	0.265
600	5	0.278
600	5	0.271

The bio-oil distillate was statistically analyzed to determine if there was an underlying affect of the pyrolysis temperature. The data is displayed in section A12 of Appendix A. The ANOVA results suggest that because $F_{7,31} < F_0$ (where $F_{7,31} = 2.30$), there is evidence to reject H_0 which states the mean MC of the miscane bio-oil distillates is not affected by pyrolysis temperature. Because the p-value ($p < 0.001$) is less than α, there is further evidence to reject H_0. The statistical analysis was conducted at the 5% level of α. The validity of the ANOVA assumptions were verified by checking the adequacy of the model.

Because H_0 was rejected, a t-test was conducted on the miscane bio-oil distillate MCs to determine if there was a significant difference between the mean MC values produced at each pyrolysis temperature and for each corresponding distillate. The results showed that there was a significant difference between all 500°C and 600°C MC values as well as between 400°C and 500°C MC values.

Moisture is a source of corrosion and instability and must be maintained at minimal levels if a biofuel is to be blended with traditional fuels or utilized as drop-in biofuel. The data suggests that vacuum distillation is an effective method for removing moisture from bio-oil. After distillation, in most cases, the MC of the bio-oil distillate was only a fraction of a percent. The highest MC result belonged to the second distillate of 500C bio-oil with an average MC of 4.51%. All other distillates associated with all other pyrolysis temperatures were below 2%. With the removal of water, it was expected that some of the polar compounds with similar boiling points would be removed as well. Testing the TAN of the bio-oil distillates would verify this theory.

5.1.16 Results of Miscane Bio-oil Distillate Density Determination

The densities of the miscane bio-oil distillates produced from each pyrolysis experiment and the data is displayed in table 27.

Table 27. Bio-oil Distillate Density Data

Pyrolysis Temperature	Distillate #	Density (g/mL)
400	2	1.344
400	2	1.450
400	2	1.278

Table 27 Continued

Pyrolysis Temperature	Distillate #	Density (g/mL)
400	3	1.264
400	3	1.299
400	3	1.257
400	4	1.222
400	4	1.238
400	4	1.245
400	5	1.386
400	5	1.421
400	5	1.399
400	6	1.358
400	6	1.402
400	6	1.268
400	7	1.380
400	7	1.451
400	7	1.210
500	2	1.285
500	2	1.261
500	2	1.153
500	3	1.272
500	3	1.430
500	3	1.371
500	4	1.244
500	4	1.029
500	4	1.247
600	2	1.174
600	2	1.005
600	2	1.204
600	3	1.306
600	3	1.169
600	3	1.278
600	4	1.256
600	4	1.014
600	4	1.150
600	5	1.258
600	5	1.262
600	5	1.270

The miscane distillate density data was statistically analyzed to determine if there was an underlying affect of the pyrolysis temperature. This data can be found in section A13 of Appendix A. The results of the ANOVA suggest that because $F_{7,31} < F_0$ (where $F_{7,31} = 2.30$), there is evidence to reject H_0 which states the mean density of the miscane bio-oil distillates is not affected by pyrolysis temperature. Because the p-value ($p < 0.001$) is less than α, there is further evidence to reject H_0. The statistical analysis was conducted at the 5% level of α. The validity of the ANOVA assumptions were verified by checking the adequacy of the model.

Because H_0 was rejected, a t-test was conducted on the miscane bio-oil distillate densities to determine if there was a significant difference between the mean density values produced at each pyrolysis temperature and for each corresponding distillate. The results showed that there was a significant difference between all 500°C and 600°C density values as well as between 400°C and 600°C density values.

With the removal of water and other polar compounds after distillation, it was expected that the density of the bio-oil distillates would be less than that of the raw bio-oil. However, thee density of the distillate fractions remained near that of the raw bio-oil fraction from which it was derived. The average density of the 500°C bio-oil was 1.296 g mL^{-1}. The densities for the second, third, and fourth distillate fractions were 1.260, 1.272, and 1.244 g mL^{-1} respectively. In some cases, the density increased for a specific distillate fraction when compared to that of the raw bio-oil. The density of JP8 is approximately 0.81 g mL^{-1}. In all cases, the densities of the distillate fractions were all

significantly higher than that of JP8. This indicates the need for further upgrading to produce hydrocarbons in the JP8 range.

5.1.17 Results of Miscane Bio-oil Distillate Total Acid Number (TAN) Determination

The TANs of the miscane bio-oil distillates produced from each pyrolysis experiment were measured and the data is displayed in table 28.

Table 28. Bio-oil Distillate TAN Data

Pyrolysis Temperature	Distillate #	TAN
400	2	20
400	2	21.03
400	2	20.54
400	3	19.66
400	3	20.21
400	3	20.65
400	4	21.4
400	4	25.12
400	4	19.33
400	5	19.8
400	5	19.22
400	5	19.98
400	6	18.8
400	6	19.63
400	6	19.21
400	7	18.6
400	7	18.02
400	7	19.78
500	2	19.57
500	2	17.43
500	2	17.98
500	3	21.5
500	3	28.99
500	3	20.05

Table 28 Continued

Pyrolysis Temperature	Distillate #	TAN
500	4	20.8
500	4	19.44
500	4	19.69
600	2	19.2
600	2	18.04
600	2	19.44
600	3	21.1
600	3	21.98
600	3	21.67
600	4	20.4
600	4	20.12
600	4	19.11
600	5	19.7
600	5	20.55
600	5	20.15

The TAN data for the distillates was statistically analyzed to determine if there was an underlying affect of the pyrolysis temperature. This data resides in section A14 of Appendix A. The results of the ANOVA suggest that because $F_{7,31} < F_0$ (where $F_{7,31} = 2.30$), there is evidence to accept H_0 which states the mean TAN of the miscane bio-oil distillates is not affected by pyrolysis temperature. Because the p-value ($p = 0.127$) is greater than α, there is further evidence to accept H_0. The statistical analysis was conducted at the 5% level of α. The validity of the ANOVA assumptions were verified by checking the adequacy of the model.

As with the density, it was expected that after distillation, the TAN of the bio-oil distillates would decrease. However, in most cases the TAN of the distillate fractions remained near that of the raw bio-oil from which was derived. The elevated TAN

number of the raw bio-oil indicated the need for further upgrading as did that of the bio-oil distillate. The next logical step would be to catalytically treat the distillate fractions to remove any undesired compounds leading to the increased TANs. However, because the distillate fractions were small in volume, they were first qualitatively and quantitatively analyzed. Then, from this analysis a model mixture of the undesired compounds was hydrotreated using different catalysts to study the impact on biofuel properties.

5.1.18 GCMS Analysis Results of 400C Bio-oil Distillates

The chromatogram and the spectrum process table for the second distillate of the 400°C bio-oil can be found in section B1 of Appendix B. The PIANO analysis for each of the 400°C distillate fractions is displayed in table 29. Please refer to Appendix B for all chromatograms and spectrum process tables for each 400°C distillate.

Table 29. PIANO Analysis for All 400°C Bio-oil Distillates

Chemical Grouping	JP8	Distillate #2 Percent (%)	Distillate #3 Percent (%)	Distillate #4 Percent (%)	Distillate #5 Percent (%)	Distillate #6 Percent (%)	Distillate #7 Percent (%)
Paraffins	31.96	0.58	0.44	13.31	9.15	44.21	22.62
Iso-paraffins	43.44	56.87	45.40	65.00	70.46	49.88	74.05
Aromatics	6.23	1.44	1.39	0.00	0.00	0.03	0.07
Naphthenics	8.25	0.68	0.51	0.10	0.28	0.44	0.09
Olefins	1.06	0.41	0.30	0.00	0.05	0.00	0.81
Oxygenates	6.34	40.01	51.95	21.24	19.95	4.95	1.39
Halogenates	2.72	0	0.00	0.35	0.11	0.48	0.97

Fractions resulting from the distillation of 400°C bio-oil were surprisingly similar to JP8 in terms of their high isoparaffins composition. These percentages of paraffins

and isoparaffins satisfied the objective to produce hydrocarbons within the JP8 range from miscane.

The oxygenates and halogenates needed to be separated from the existing JP8 hydrocarbons. This could have been achieved via a second distillation or a solvent fractionation. However, because of the small amounts of the distillates, neither of these were viable options. Instead, a model mixture of oxygenated compounds was created from pure reactants based on those phenolic and acidic compounds significantly present in the bio-oil distillates. Because the model mixture was composed solely of oxygenated compounds, the initial percentage of oxygenate percentage was 100%. The percent deoxygenation was calculated bu subtracting the remaining oxygenate percentage from 100%.

It should be noted that while two inernal standards were added to the distilled samples analyzed by GCMS, the standards did not appear in the spectrum process table as expected. The absence of the α-androstane and Tetracosane could be equated to the GCMS quantification parameters. Because peaks with areas less than 40,000 were not identified or quantified, it is likely that the internal standards were not indentified based on this criteria. This issue could have ben further exaserbated by the increased split ratio that was utilized at the beginning of the GC program.

5.1.19 GCMS Analysis Results of 500°C Bio-oil Distillates

The chromatograms and the spectrum process tables for the distillates of the 500°C bio-oil can be found in section B2 of Appendix B. The PIANO analysis for each of the 500°C distillate fractions is displayed in table 30.

Table 30. PIANO Analysis for All 500°C Bio-oil Distillates

Chemical Grouping	JP8	Distillate #2 Percent (%)	Distillate #3 Percent (%)	Distillate #4 Percent (%)
Paraffins	31.96	28.67	24.25	26.01
Iso-paraffins	43.44	29.32	48.00	71.98
Aromatics	6.23	0.78	0.00	0.03
Naphthenics	8.25	0.28	0.30	0.06
Olefins	1.06	0.18	0.00	0.36
Oxygenates	6.34	40.77	27.45	1.55
Halogenates	2.72	0.00	0.00	0.00

As with the 400°C distillate fractions, the 500°C distillates contained a significant amout of existing JP8 hydrocarbons, especially the paraffin and isoparaffin composition. These percentages of paraffins and isoparaffins satisfied the objective to produce hydrocarbons within the JP8 range from miscane.

The oxygenates and halogenates needed to be separated from the existing JP8 hydrocarbons. This could have been achieved via a second distillation or a solvent fractionation. However, because of the small amounts of the distillates, neither of these were viable options. Instead, a model mixture of oxygenated compounds was created from pure reactants based on those phenolic and acidic compounds significantly present in the bio-oil distillates.

5.1.20 GCMS Analysis Results of 600°C Bio-oil Distillates

The chromatograms and spectrum process tables for the distillates of the 600°C bio-oil can be found in section B3 of Appendix B. The PIANO analysis for each of the 600°C distillate fractions is displayed in table 31.

Table 31. PIANO Analysis for All 600°C Bio-oil Distillates

Chemical Grouping	JP8	Distillate #2 Percent (%)	Distillate #3 Percent (%)	Distillate #4 Percent (%)	Distillate #5 Percent (%)
Paraffins	31.96	5.71	34.23	38.54	6.96
Iso-paraffins	43.44	57.98	23.96	27.52	72.37
Aromatics	6.23	2.32	1.34	0.00	0.00
Naphthenics	8.25	1.19	0.63	0.83	0.84
Olefins	1.07	0.00	0.35	0.27	0.10
Oxygenates	6.34	32.79	39.48	32.53	19.63
Halogenates	2.72	0.00	0.00	0.31	0.10

The group sum percentages of the chemical groupings are listed for each of the 600C bio-oil distillates.

As with the 400°C and 500°C distillates, the 600°C distillates were similar to JP8 in terms of their high paraffins and isoparaffin composition. These percentages of paraffins and isoparaffins satisfied the objective to produce hydrocarbons within the JP8 range from miscane.

The oxygenates and halogenates needed to be separated from the remaining distillate components. This could have been achieved via either a second distillation or a solvent fractionation. However, because of the small amounts of the distillates, neither of these were viable options. Instead, a model mixture of oxygenated compounds was created from pure reactants based on those phenolic and acidic compounds significantly present in the bio-oil distillates.

It should also be noted that, regardless of the pyrolysis temperature, immediately after the distillates were collected, they all ranged from clear to bright yellow in color.

However, they soon began to darken which may be indicative of an oxidation reaction taking place. Figures 11 and 12 show the change in color.

Figure 11. Initial Bio-oil Distillate Color. This figure shows the color of the bio-oil distillated fractions immediately after distillation. Initially, most fractions ranged from light yellow to light orange in color.

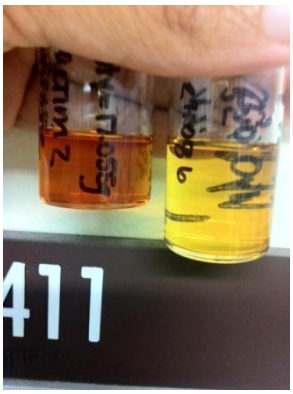

Figure 12. Bio-oil Distillate Color Change. This figure shows the color of the bio-oil distillates about two hours after distillation. Notice, that the fractions have already begin to darken in color.

5.1.21 Results of Miscane Bio-oil Distillate GCMS Analysis

The GMCS analysis produced seven quantitative responses namely the summed grouped concentrations of the paraffins, isoparaffins, aromatics, naphthenics, olefins (PIANO), oxygenates, and halogenates found in a sample. The GCMS results of the miscane bio-oil distillates produced from each pyrolysis experiment were statistically analyzed to determine if there was an underlying affect of the pyrolysis temperature. The data resides in section A15 of Appendix A. The results of the ANOVA suggest that because $F_{7,5} > F_0$ (where $F_{7,5} = 4.88$) for the paraffins, isoparaffins, aromatics, olefins and oxygenates, there is evidence to accept H_0 which states the mean percent concentration of the respective GCMS responses of the miscane bio-oil distillates is affected by pyrolysis temperature. Because the p-values for the paraffins ($p = 0.219$) isoparaffins ($p = 0.256$), aromatics ($p = 0.057$), olefins ($p = 0.362$) and oxygenates ($p = 0.076$) are greater than α, there is further evidence to accept H_0 for these GCMS responses. Because $F_{7,5} < F_0$ (where $F_{7,5} = 4.88$) for the naphthenics and halogenates there is evidence to reject H_0 which states the mean percent concentration of the respective GCMS responses of the miscane bio-oil distillates is not affected by pyrolysis temperature. Because the p-values for the naphthenics ($p = 0.033$) and halogenates ($p = 0.005$) are less than α, there is further evidence to reject H_0 for these GCMS responses. The statistical analysis was conducted at the 5% level of α. The validity of the ANOVA assumptions were verified by checking the adequacy of the model.

Because H_0 was rejected for the naphthenics and halogenates, a t-test was conducted on the miscane bio-oil distillate naphthenic and halogenate data sets to

determine if there was a significant difference between their mean respective grouped summed concentration percentage values produced at each pyrolysis temperature and for each corresponding distillate. The results showed that there was no significant difference between the halogenate means based on pyrolysis temperature. However, the percent concentration of naphthenics produced at 400°C was significantly different from the percentages produced at both 500°C and 600°C.

The results of the PIANO statistical analysis suggest that the percentage of paraffins, isoparaffins, aromatics, olefins and oxygenates is not dependent on the pyrolysis temperature. A t-test of the GCMS data suggests that their percentage changes depending on the distillate fraction obtained. This is expected considering that the distillate fractions are separated by boiling point and the varying molecular weights of the compound groupings affect the hydrocarbon boiling points. In general, if a specific range of hydrocarbons is desired, the pyrolysis temperature at which the raw bio-oil was produced is not as important as the distillation process that follows. To the contrary, the percentage of naphthenics and halogenates were affected by both the pyrolysis temperature and the distillate fraction.

5.2 Results of Hydrogenation/Deoxygenation Catalyst Experiments

Distilling the bio-oil resulted in volumetrically small fractions. While there was enough of each fraction to conduct characterization tests, afterwards, there was not enough to hydrogenate. Consequently, a model mixture of phenolic and acidic compounds were selected for the hydrogenation reactions. The pure compounds chosen were those oxygenated compounds identified at significant concentration levels within

the bio-oil. The model mixture was composed of m-cresol, o-cresol, 2-ethylphenol, phenol, pentanoic acid, octanoic acid, and heptadecanoic acid.

All experiments were run for 12 hours. The temperature and pressure were recorded every 15 minutes. A hydrogen pressure drop was expected for all catalysts, but only observed for Pd/C. The hydrogen pressure for both the fluorous Pd catalyst and Shvo's catalyst increased as the temperature increased until they reached steady state. The reason why the H_2 pressure did not decline for these catalysts may be associated with the water production during hydrogenation experiments. Water is produced as a byproduct and the rate of production of the water vapor may have exceeded the hydrogen consumption rate, thereby masking the declining H_2 pressure. The GCMS results clearly indicate that hydrogenation reactions occurred.

5.2.1 GCMS Analysis of Hydrogenated Product Using a Fluorous Pd Catalyst

The fluorous catalyst used was prepared according to the procedure outlined by (Jurisch 2008). The amount of catalyst used was based on the total mass of the model mixture and equated to five weight percent of the total mass. The chromatogram for the first trial of the fluorous Pd hydrogenation is displayed in figure 13. Table 32 is the resulting spectrum process table for the hydrogenation trial. The PIANO analysis for each of the fluorous Pd hydrogenation reactions is displayed in table 33. Table 33 also includes the percent deoxygenation for all trials. Please refer to section C4 of Appendix B for all chromatograms and spectrum process tables for each hydrogenation experiment.

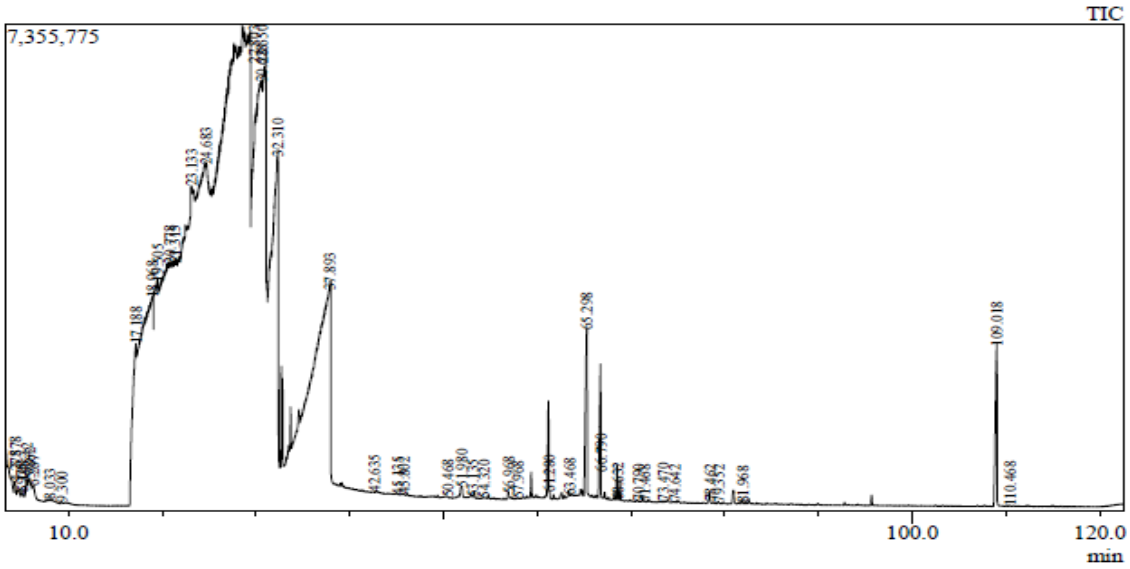

Figure 13. Chromatogram for Hydrogenated Product Using Fluorous Pd Catalyst. This is the resulting chromatogram for the first trial of the fluorous Pd hydrogenation of the model mixture compounds. The ill-defined peaks that range between 17.188 and 37.893 minutes are the unreacted compounds of the model mixture. The hydrocarbon peaks appearing after 37.89 minutes are better defined, Gaussian shaped peaks.

The peaks that show up between 17.188 and 37.893 minutes are the polar, phenolic compounds there were not converted during the hydrogenation experiment. Because the DB5-MS column is a non-polar column designed for the analysis of hydrocarbons, it is not suited for the analysis of polar compounds like those that appear before 37.893 minutes. This is why the resulting peaks in this area of the chromatogram are non-Gaussian in shape and this is also why they were not sufficiently separated.

Table 32. Spectrum Process Table for Trial#1 of the Fluorous Pd Hydrogenations

Retention Time	Compound Name
4.278	Cyclohexane, methyl-
4.975	Cyclohexane, methyl-
5.108	Cyclohexane, methyl-
8.033	Cyclohexane, ethyl-
9.3	Ethylbenzene
17.188	Phenol
19.505	Phenol
24.683	Phenol
27.643	Cyclohexane, 1,2-dimethyl-, cis-
30.628	Phenol, 2-methyl-
32.31	Phenol, 2-ethyl-
37.408	4-Decene, 3-methyl-, (E)-
37.893	Octanoic Acid
51.98	Hexadecane
57.899	Tridecane, 6-methyl-
63.656	Oxalic acid, isobutyl hexadecyl ester
64.631	Tridecane, 2,5-dimethyl-
65.298	Oxalic acid, heptyl 2-methylphenyl ester
66.79	Oxalic acid, heptyl 2-methylphenyl ester

The resulting compounds of the hydrogenation of the model mixture using the fluorous Pd catalyst are listed along with their retention times.

The spectrum process table shows that while the acids were not completely converted to hydrocarbons, they were esterified. The hydrogenation of organic acids is difficult to achieve under the mild experimental conditions employed (i.e. 125 psi H_2 and 200°C) but they can be esterified in the presence of an alcohol (Elliott 2007; Xiong, Fu et al. 2011). It appears that alcoholic species were sufficiently present to promote the esterification of the acids.

Table 33. PIANO Analysis for Fluorous Pd Hydrogenations

Chemical Grouping	Fluorous Pd Trial 1 Percentage (%)	Fluorous Pd Trial 2 Percentage (%)	Fluorous Pd Trial 3 Percentage (%)	Average (%)	Standard Deviation (%)
Paraffins	0.00	0.29	0.00	0.10	0.06
Iso-paraffins	21.15	20.17	24.38	21.90	0.73
Aromatics	0.00	0.00	0.00	0.00	0.00
Naphthenics	48.03	52.12	63.40	54.52	2.65
Olefins	24.88	22.92	5.68	17.83	3.52
Oxygenates	5.94	4.79	6.54	5.75	0.30
Halogenates	0.00	0.00	0.00	0.00	0.00
Deoxygenation Results	94.06	95.21	93.46	94.25	0.30

The group sum percentages of the chemical groupings are listed for each of fluorous Pd hydrogenation trials. The deoxygenation results represent the percentage of oxygen removed from the model mixture.

On average, the fluorous Pd catalyst successfully converted 94.25±0.30% of the oxygenated compounds to hydrocarbons.

During the trials using the fluorous Pd, the significance of this method was not realized. The significance resides in the ability to recover homogeneous catalysts due to the solubility properties of the fluorous system. However during the experiments, the fluorous catalyst was transformed into Pd nanoparticles between 80°C and 90°C rendering the catalyst in its original form unrecoverable. The Pd nanoparticles can themselves be catalytically active and able to convert the model mixture to hydrocarbons.

5.2.2 GCMS Analysis of Hydrogenated Product Using Pd/C Catalyst

The total mass of the mixture determined the amount of catalyst to be used. A total of five weight percent of catalyst was used. The chromatogram for the first trial of

the Pd/C hydrogenation is displayed in figure 14. Table 34 is the resulting spectrum process table for the hydrogenation trial. The PIANO analysis for each of the Pd/C hydrogenation reactions is displayed in table 35. Table 35 also includes the percent deoxygenation for all trials. Please refer to section B5 of Appendix B for all chromatograms and spectrum process tables for each hydrogenation experiment.

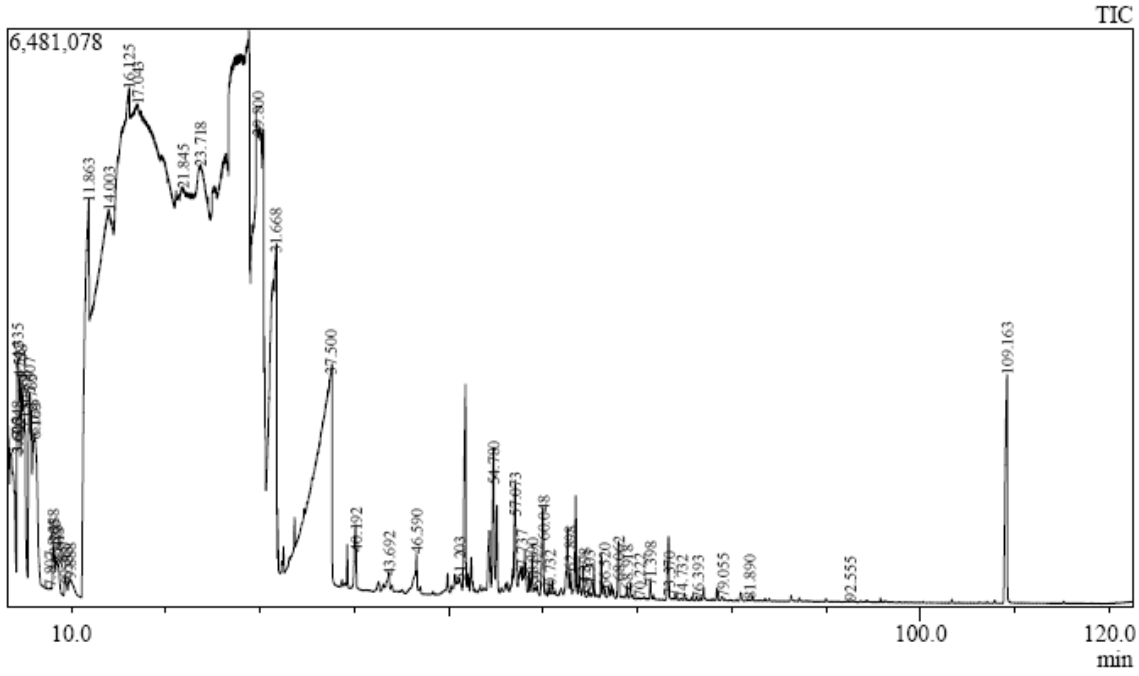

Figure 14. Chromatogram for Hydrogenated Product Using Pd/C Catalyst. This is the resulting chromatogram for the first trial of the Pd/C hydrogenation of the model mixture compounds. The ill-defined peaks that range between 11.86 and 37.50 minutes are the unreacted compounds of the model mixture. The hydrocarbon peaks appearing after 37.50 minutes are better defined, Gaussian shaped peaks.

The peaks that show up between 11.863 and 37.500 minutes are the polar, phenolic compounds there were not converted during the hydrogenation experiment. Because the DB5-MS column is a non-polar column designed for the analysis of

hydrocarbons, it is not suited for the analysis of polar compounds like those that appear before 37.500 minutes. This is why the resulting peaks in this area of the chromatogram are non-Gaussian in shape and this is also why they were not sufficiently separated.

Table 34. Spectrum Process Table for Trial#1 of the Pd/C Hydrogenations

Retention Time	Compound Name
3.348	Benzene
4.335	Cyclohexane, methyl-
4.527	Cyclohexane, methyl-
4.758	Cyclohexane, methyl-
4.968	Cyclohexane, methyl-
5.132	Cyclohexane, methyl-
5.607	1,3,5-Cycloheptatriene
5.765	1,3,5-Cycloheptatriene
6.165	Toluene
7.807	Pentanoic acid, methyl ester
8.088	Cyclohexane, ethyl-
8.255	Cyclohexane, ethyl-
8.473	Cyclohexane, ethyl-
8.618	Cyclohexane, ethyl-
9.367	Ethylbenzene
9.533	Ethylbenzene
11.863	Cyclohexanone
14.003	Cyclohexanone
17.043	Cyclohexanone, 2-methyl-
23.718	Phenol, 2-methyl-
26.755	Cyclopentane, 1-methyl-3-(2-methylpropyl)-
31.668	Phenol, 2-ethyl-
37.252	4-Decene, 3-methyl-, (E)-
37.5	Octanoic Acid
39.274	C11
40.192	Benzene, cyclohexyl-
42.579	Cyclopentane, 1,2-dimethyl-3-(1-methylethyl)-
46.59	Benzene, 1-cyclohexyl-3-methyl-
52.065	Dodecane, 3-methyl-
54.78	Bicyclo[8.2.0]dodecan-11-one, 12-chloro-

Table 34 Continued

Retention Time	Compound Name
58.723	Hexadecane
60.048	Phenol, 2-cyclohexyl-4-methyl-
63.599	Oxalic acid, isobutyl hexadecyl ester
68.062	Phenol, 4-(phenylmethyl)-

The resulting compounds of the hydrogenation of the model mixture using Pd/C as the catalyst are listed along with their retention times.

The spectrum process table shows that while the acids were not completely converted to hydrocarbons, they were esterified.

Table 35. PIANO Analysis for Pd/C Hydrogenations

Chemical Grouping	Pd/C Trial 1 Percentage (%)	Pd/C Trial 2 Percentage (%)	Pd/C Trial 3 Percentage (%)	Average (%)	Standard Deviation (%)
Paraffins	17.15	7.03	4.03	9.41	2.29
Iso-paraffins	18.98	12.90	12.79	14.89	1.18
Aromatics	32.92	41.20	19.26	31.13	3.69
Naphthenics	13.17	24.92	51.33	29.81	6.51
Olefins	10.46	9.09	9.09	9.55	0.26
Oxygenates	7.32	4.85	3.50	5.22	0.65
Halogenates	0.00	0.00	0.00	0.00	0.00
Deoxygenation Results	92.68	95.15	96.50	94.78	0.65

The group sum percentages of the chemical groupings are listed for each Pd/C hydrogenation trials. The deoxygenation results represent the percentage of oxygen removed from the model mixture.

On average, the Pd/C catalyst successfully converted 94.78±0.65% of the oxygenated compounds to hydrocarbons.

5.2.3 GCMS Analysis of Hydrogenated Product Using Shvo's Catalyst

The total mass of the mixture determined the amount of catalyst to be used. A total of five weight percent of catalyst was used. The chromatogram for the first trial of the Shvo's catalyst hydrogenation is displayed in figure 15. Table 36 is the resulting spectrum process table for the hydrogenation trial. The PIANO analysis for each of the Shvo's catalyst hydrogenation reactions is displayed in table 37. Table 37 also includes the percent deoxygenation for all trials. Please refer to section B6 of Appendix B for all chromatograms and spectrum process tables for each hydrogenation experiment.

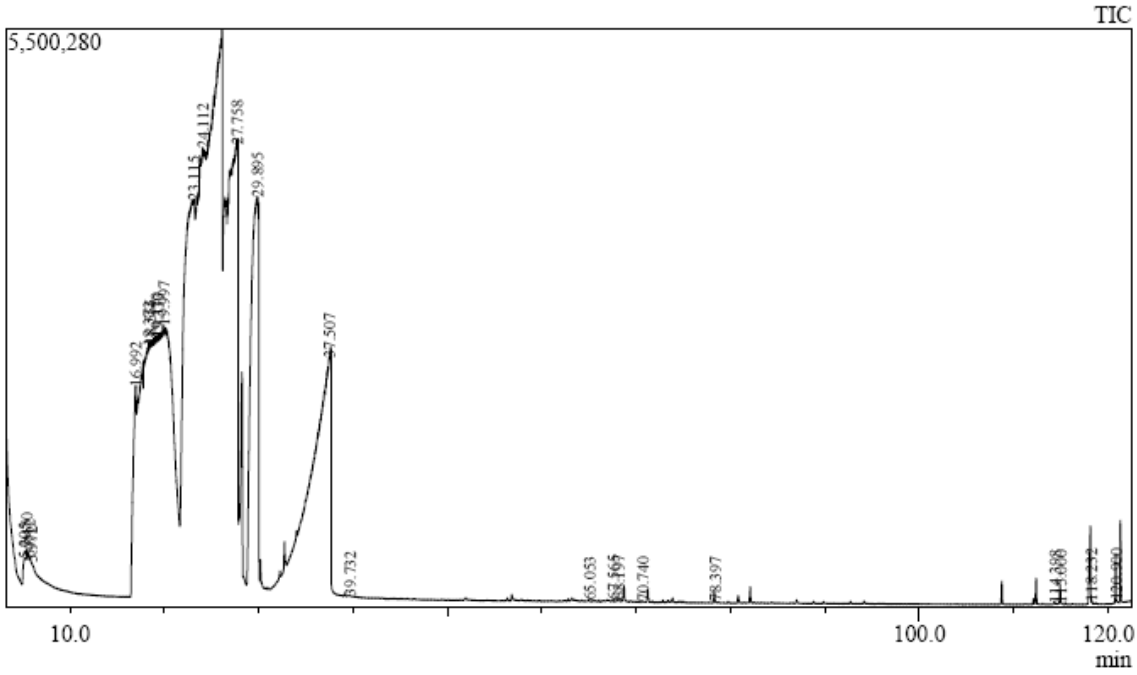

Figure 15. Chromatogram for Hydrogenated Product Using Shvo's Catalyst. This is the resulting chromatogram for the first trial of the Shvo's catalyst hydrogenation of the model mixture compounds. The ill-defined peaks that range between 16.99 and 37.51 minutes are the unreacted compounds of the model mixture. The hydrocarbon peaks appearing after 37.51 minutes are better defined, Gaussian shaped peaks.

The peaks that show up between 16.99 and 37.51 minutes are the polar, phenolic compounds there were not converted during the hydrogenation experiment. Because the DB5-MS column is a non-polar column designed for the analysis of hydrocarbons, it is not suited for the analysis of polar compounds like those that appear before 37.51 minutes. This is why the resulting peaks in this area of the chromatogram are non-Gaussian in shape and this is also why they were not sufficiently separated.

Table 36. Spectrum Process Table for Trial#1 of the Shvo's Catalyst Hydrogenation

Retention Time	Compound Name
5.205	Methylene Chloride
5.47	Toluene
16.992	Phenol
19.997	Phenol
23.115	Phenol, 2-methyl-
27.758	Phenol, 3-methyl-
29.895	Phenol, 2-ethyl-
37.33	4-Decene, 3-methyl-, (E)-
37.507	Octanoic Acid
39.128	C11
51.943	Undecane, 2,10-dimethyl-
57.848	Tridecane, 6-methyl-
63.451	Oxalic acid, isobutyl hexadecyl ester

The spectrum process table shows that while the acids were not completely converted to hydrocarbons, they were esterified.

Table 37. PIANO Analysis for Shvo's Catalyst Hydrogenations

Chemical Grouping	Shvo's Catalyst Trial 1 Percentage (%)	Shvo's Catalyst Trial 2 Percentage (%)	Shvo's Catalyst Trial 3 Percentage (%)	Average (%)	Standard Deviation (%)
Paraffins	6.39	6.57	4.52	5.83	0.38
Iso-paraffins	13.45	16.71	14.42	14.86	0.56
Aromatics	0.00	0.00	0.00	0.00	0.00
Naphthenics	0.00	0.00	0.00	0.00	0.00
Olefins	74.24	69.84	76.88	73.65	1.19
Oxygenates	5.92	6.88	4.18	5.66	0.46
Halogenates	0.00	0.00	0.00	0.00	0.00
Deoxygenation Results	94.08	93.12	95.82	94.34	0.46

The group sum percentages of the chemical groupings are listed for each Shvo's catalyst hydrogenation trials. The deoxygenation results represent the percentage of oxygen removed from the model mixture.

On average, Shvo's catalyst successfully removed 94.34±0.46% of the oxygen from the model mixture.

5.2.4 Statistical Analysis Results for Hydrogenation/Deoxygenation Catalysts

In order to assess the hydrogenation/deoxygenation capability of the catalysts used, the percent oxygenates remaining after hydrogenating the model mixture was statistically evaluated. The data resides in section A16 of Appendix A. The resulting ANOVA for the model mixture oxygenate response data suggests that because $F_{2,6} < F_0$ where ($F_{2,6} = 5.14$) there is evidence to reject H_0 which states the amount of remaining oxygenates is not affected by the choice of catalyst. This could also be restated to say that the amount of oxygen removed during the hydrogenation reaction is not affected by the choice of catalyst. The validity of the ANOVA assumptions were verified by checking the adequacy of the model.

Because H_0 was rejected, a t-test was conducted on the remaining model mixture oxygenates to determine if there was a significant difference between their mean grouped summed concentration percentage values produced by each catalyst. The results showed that there was no significant difference between the mean percentages of remaining oxygenates.

The statistical analysis suggests that if the goal of the catalytic hydrogenation is to saturate oxygenated compounds, the choice among the catalysts tested is irrelevant. Each of the catalysts tested effectively removed similar amounts of oxygen from the model mixture. When considering a cost effective conversion process, the least expensive catalyst should be the tool of choice for upgrading bio-oil to biofuel.

5.2.5 Statistical Analysis Results for JP8 Hydrocarbon Production

The GMCS analysis of the model mixture hydrogenation product produced seven quantitative responses namely the summed grouped concentrations of the paraffins, isoparaffins, aromatics, naphthenics, olefins (PIANO), oxygenates, and halogenates found in a sample. The GCMS results of the hydrogenated product generated from each pyrolysis experiment were statistically analyzed to determine if there was an underlying affect of the catalyst choice. The data resides in section A16 of Appendix A. The resulting ANOVA for the hydrogenated product or the PIANO analysis suggests that because $F_{2,6} < F_0$ where ($F_{2,6} = 5.14$) for the paraffins produced, there is evidence to accept H_0 which states that the mean percentage of paraffins produced is not affected by catalyst choice. This evidence is further substantiated because the p-value for the paraffins ($p = 0.076$) is greater than α. However, because $F_{2,6}$ is less than the

corresponding F_0 values for the isoparaffins (F_0 = 7.327), aromatics (F_0 = 23.648), naphthenics (F_0 = 15.060), and olefins (F_0 = 87.614), there is evidence to reject H_0 and suggest that the mean percentage of the respective hydrocarbon groups produced is affected by the catalyst choice. This evidence is further substantiated because the p-values for the isoparaffins (p = 0.024), aromatics (p = 0.001), naphthenics (p = 0.004) and olefins ($p < 0.0001$) are less than α. The validity of the ANOVA assumptions were verified by checking the adequacy of the model.

Because H_0 was rejected for the isoparaffins, aromatics, naphthenics, and olefins, a t-test was conducted on the hydrogenated product IANO data to determine if there was a significant difference between their mean respective grouped summed concentration percentage values produced based on catalyst choice. For isoparaffins, there is a significant difference between the amount produced from the use of the fluorous Pd and the other catalysts. For the aromatics, naphthenics, and olefins, the results were the same. There was a significant difference between the amount of each corresponding group of hydrocarbons produced as a result of using the Pd/C instead of either the fluorous Pd or the Shvo's catalyst. The resulting data is displayed in section A16 of Appendix A.

The results of this data implicate the production of a specific group of hydrocarbons is possible depending on the choice of catalyst. While each catalyst tested has similar deoxygenation capabilities, they each have the propencity to produce a different group of hydrocarbons. On average, the fluorous Pd catalysts rendered a higher percentage of isoparaffins than either the Pd/C or Shvo's catalyst. There was no

significant difference between the percentage of isoparaffins produced by the Pd/C or Shvo's catalysts. No aromatics resulted from the use of the fluorous Pd or Shvo's catalysts. Therefore, if the goal was to produce aromatic compounds, Pd/C would need to be the catalyst used. Likewise, the use of Shvo's catalyst also produced no naphthenics. The percentage of naphthenics produced by the fluorous Pd catalyst (54.52%) was almost twice that produced by Pd/C (29.81%). If olefin production was the goal, Shvo's catalyst far out performed the other catalysts, rendering 73.65% olefins in comparison to 17.83% and 9.55% produced by the fluorous Pd and Pd/C respectively. Generally speaking, specific catalysts have a tendency to produce a specific range of hydrocarbons and the choice of catalyst could in part be based on the desired end product.

5.3 Results for JP8 Hydrocarbon Product Evaluation

5.3.1 Statistical Analysis Results for JP8 Hydrocarbon Product Quality Based on TAN

The raw bio-oil and distillate fractions were statistically analyzed to determine whether or not the TAN was improved after distilling the raw bio-oil. The data was analyzed according to the specific distillate fraction and the pyrolysis temperature. This data can be foud in section A17 of Appendix A. The resulting ANOVA for the TAN analysis suggests that because $F_{15,50} < F_0$ (where $F_{15,50} = 1.87$) there is evidence to reject H_0 which states that the mean TAN is not affected by distillation. This can be restated to say that the TAN of the raw bio-oil is not equal to the TAN of the bio-oil distillate. This evidence is further substantiated because the p-value ($p < 0.0001$) is less than α. The

validity of the ANOVA assumptions were verified by checking the adequacy of the model.

Because H_0 was rejected, a t-test was conducted on the TAN data to determine if there was a significant difference between the TAN of the raw bio-oil and that of the resulting distillate fractions. An additional t-test was conducted on the TAN data to determine if there was significant difference between the TAN of the raw bio-oil and distillate fractions when pyrolysis temperature was an input factor.

The result of this analysis is that the TAN is affected by the pyrolysis temperature and also by distillation. T-test results indicate that there were significant differences among the varying distillate levels. These results are best described by the tables in section A17 of Appendix A.

5.3.2 Statistical Analysis Results for JP8 Hydrocarbon Product Quality Based on MC

The raw bio-oil and distillate fractions were statistically analyzed to determine whether or not the MC was improved after distilling the raw bio-oil. The data was analyzed according to the specific distillate fraction and the pyrolysis temperature. This data resides in section A18 of Appendix A. The resulting ANOVA for the MC analysis suggests that because $F_{15,50} < F_0$ (where $F_{15,50} = 1.87$) there is evidence to reject H_0 which states that the mean MC is not affected by distillation. This can be restated to say that the MC of the raw bio-oil is equal to the MC of the bio-oil distillate. This evidence is further substantiated because the p-value ($p < 0.0001$) is less than α.

The validity of the ANOVA assumptions were verified by checking the adequacy of the model. The plot of the residual versus the fitted values of the percent MC data

indicates the existance of variance inequality. The data was transformed and re-analyzed. After employing a Box Cox transformation, the results of the previous untransformed ANOVA remained unchanged. There is evidence to reject H_0 and suggest that the percent MC is significantly affected by the pyrolysis temperature and by distillation. This evidence is further substantiated by the fact that the p-value ($p < 0.0001$) is less than α.

Because H_0 was rejected, a t-test was conducted on the MC data to determine if there was a significant difference between the MC of the raw bio-oil and that of the resulting distillate fractions. An additional t-test was conducted on the MC data to determine if there was significant difference between the MC of the raw bio-oil and distillate fractions when pyrolysis temperature was an input factor. The results suggest that the MC of the raw bio-oil and bio-oil distillates varied both with pyrolysis temperature and distillate fraction. T-test results indicate that there were significant differences among the varying distillate levels. These results are best described by the tables in section A18 of Appendix A.

5.4 Mass and Energy Balances

5.4.1 Mass Balance Resulting From Miscane Pyrolysis at 400°C

Three pyrolysis experiments were run at 400°C. Each of the pyrolysis co-products were weighed. The density of the gas was determined by gravimetric means and when multiplied by the volume of gas produced, yielded the mass of the gas. Figure 16 shows the resulting mass balance.

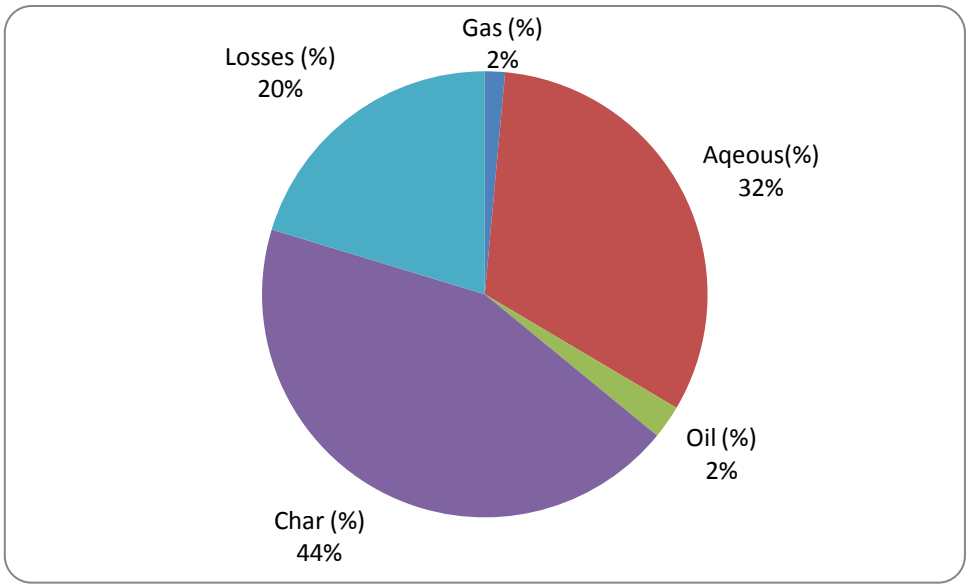

Figure 16. 400°C Pyrolysis Co-Product Mass Percentages. This figure shows the distribution of the mass percentages of the pyrolysis co-products and the losses.

Figure 17 shows the resulting energy balance for the pyrolysis co-products produced at 400°C. 10.5%, 64.50% and 6.14% of the energy input was captured in the syngas, char, and bio-oil respectively. At 400°C, the energy losses were 18.87%. Included in these losses was the heat energy lost to the surroundings during pyrolysis.

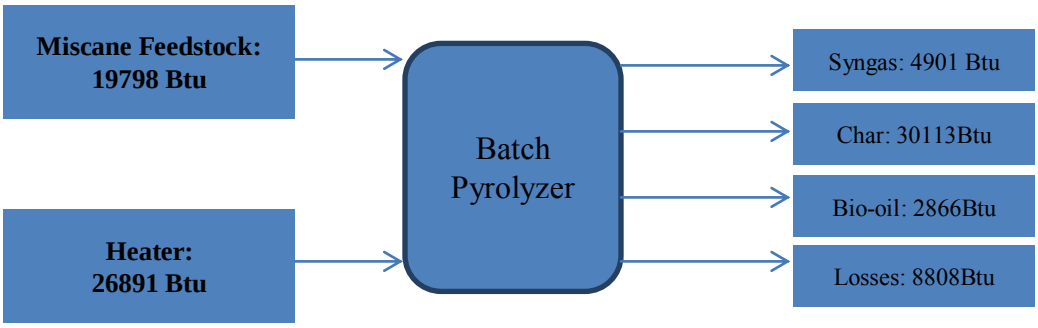

Figure 17. 400°C Pyrolysis Co-Product Energy Balance. This figure shows inputs (miscane feedstock and heater) and outputs (pyrolysis co-products and losses) for the pyrolysis process.

The distillation of the bio-oil often resulted in fractions of less than 10mL. The mass of the bio-oil distilled was about 75g. Initially, there was more bio-oil, but the distillation had to be restarted twice because of the volatility of the bio-oil. Figure 18 displays the mass balance resulting from the distillation of the 75g of bio-oil that was distilled at 400°C.

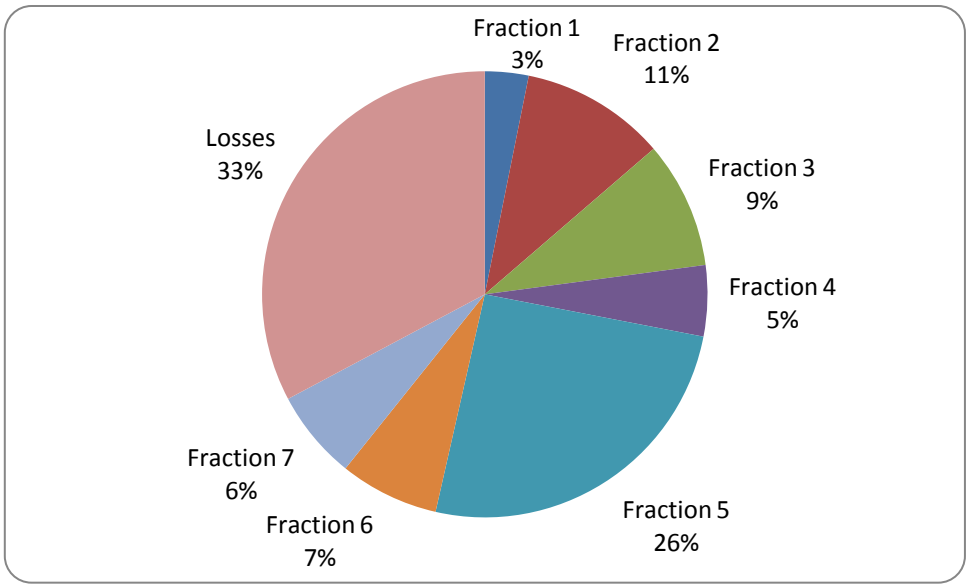

Figure 18. 400°C Bio-oil Distillate Yields. This figure shows the mass percentage distribution of the resulting distillates from the 400C bio-oil. The losses were comprised of a tar like substance remaining in the flask after the distillation process.

The distillation was stopped at 300°C because this is close to the melting poing of glass. A tar –like substance remained in the distillation flask, the mass of which was used to calculate the losses. Attempts were made to dissolve the remaining residual tar in several solvents, but it was insoluble in both polar and nonpolar solvents alike. The tar had to be soaked repeatedly for weeks in acetone to remove it from the distillation flask. The first fraction was the water fraction and was not upgraded.

5.4.2 Mass Balance Resulting From Miscane Pyrolysis at 500°C

Three pyrolysis experiments were run at 500°C. Each of the pyrolysis co-products were weighed. The density of the gas was determined by gravimetric means

and when multiplied by the volume of gas produced, yielded the mass of the gas. Figure 19 shows the resulting mass balance.

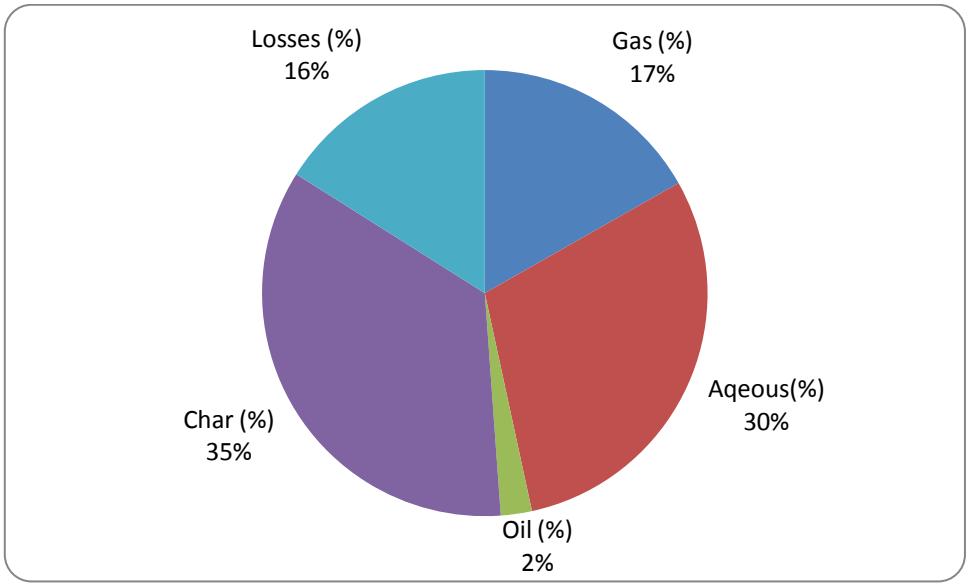

Figure 19. 500°C Pyrolysis Co-Product Mass Percentages. This figure shows the distribution of the mass percentages of the pyrolysis co-products and the losses.

Approximately 92 grams of bio-oil produced at 500°C was distilled resulting in the mass balance of figure 20.

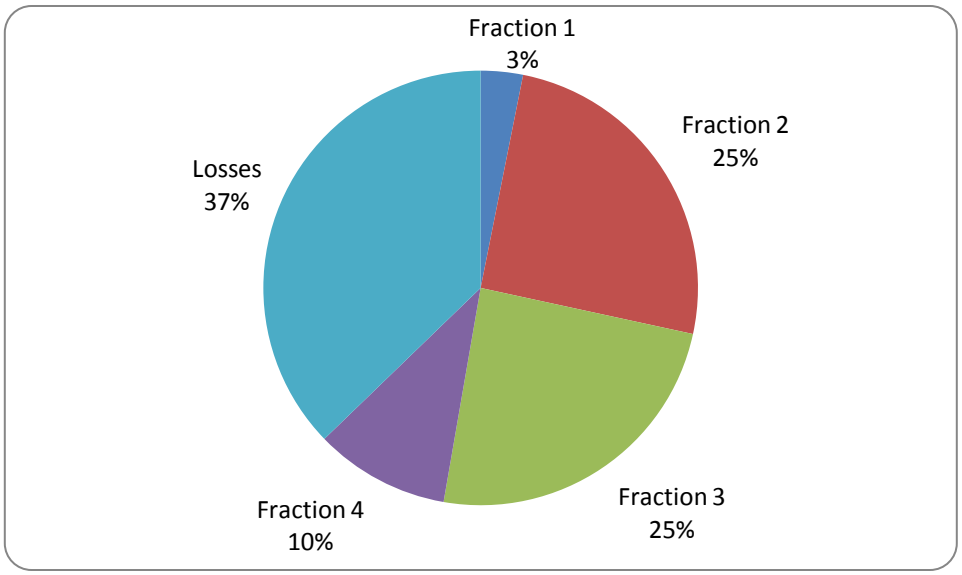

Figure 20. 500°C Bio-oil Distillate Yields. This figure shows the mass percentage distribution of the resulting distillates from the 500C bio-oil. The losses were comprised of a tar like substance remaining in the flask after the distillation process.

Figure 21 shows the resulting energy balance for the pyrolysis co-products produced at 500°C. 13.66%, 51.69% and 5.38% of the energy input was captured in the syngas, char, and bio-oil respectively. At 500°C, the losses accounted for 29.28%. Included in these losses was the heat lost to the surroundings during pyrolysis.

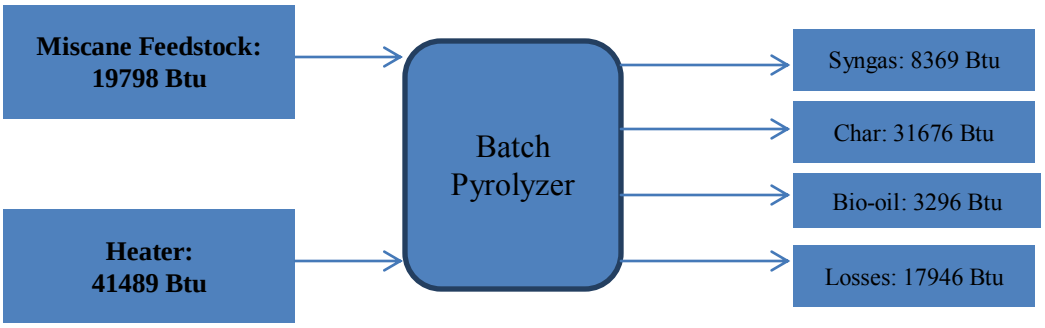

Figure 21. 500°C Pyrolysis Co-Product Energy Balance. This figure shows the energy inputs (miscane feedstock and heater) and outputs (pyrolysis co-products and losses) for the pyrolysis process.

Again, the first fraction was the water fraction and it was not upgraded. The distillation was stopped at 300°C and a tar-like substance remained. Attempts were made to dissolve the remaining residual tar in several solvents, but it was insoluble in both polar and nonpolar solvents alike. The tar had to be soaked repeatedly for weeks in acetone to remove it from the distillation flask.

5.4.3 Mass Balance Resulting From Miscane Pyrolysis at 600°C

Four pyrolysis experiments were run at 600°C. Each of the pyrolysis co-products were weighed. The density of the gas was determined by gravimetric means and when multiplied by the volume of gas produced, yielded the mass of the gas. Figure 22 shows the resulting mass balance.

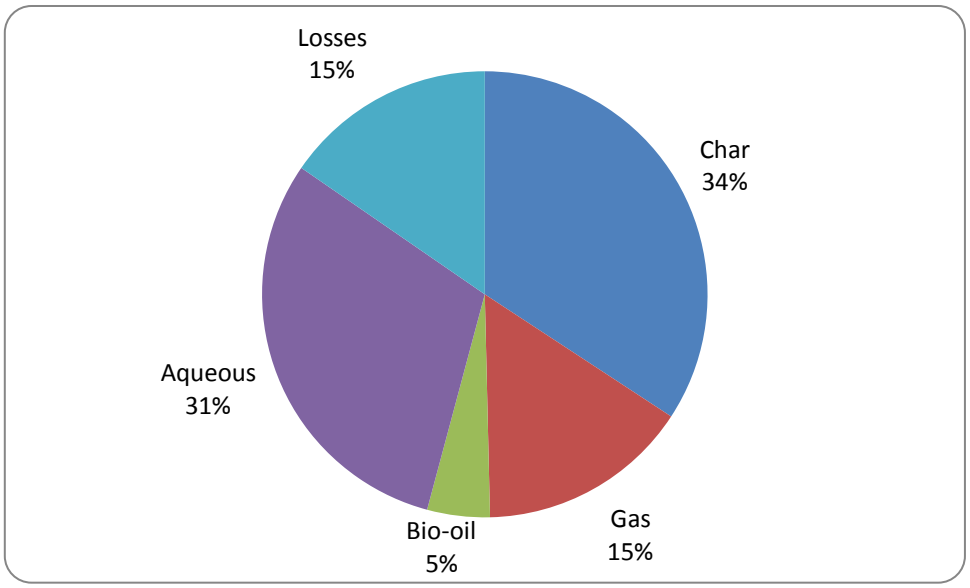

Figure 22. 600°C Pyrolysis Co-Product Mass Percentages. This figure shows the distribution of the mass percentages of the pyrolysis co-products and the losses.

Figure 23 shows the resulting energy balance for the pyrolysis co-products produced at 600°C. 3.18%, 52.19% and 4.39% of the energy input was captured in the syngas, char, and bio-oil respectively. At 600°C, the losses accounted for 40.24%. Included in these losses was heat lost to the surroundings during pyrolysis. As the temperature increased, the percent losses increased.

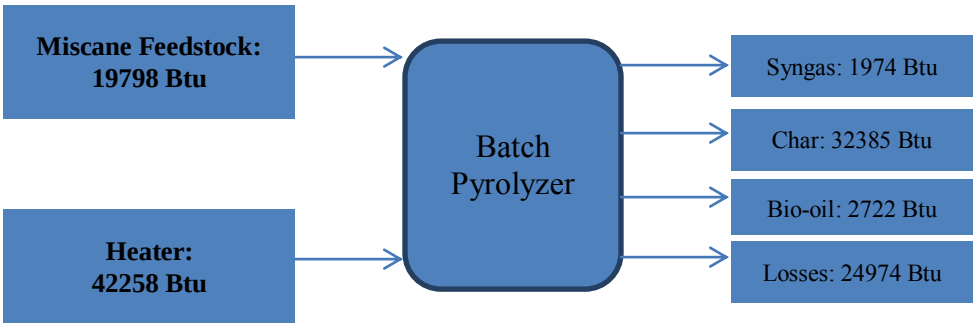

Figure 23. 600°C Pyrolysis Co-Product Energy Balance. This figure shows the energy inputs (miscane feedstock and heater) and outputs (pyrolysis co-products and losses) for the pyrolysis process.

Unlike the bio-oil produced at 400°C and 500°C, a thick tar-like bio-oil was produced at 600°C. When heated, the tar was able to be distilled. Distillation of an 82g sample resulted in the mass balance of figure 24.

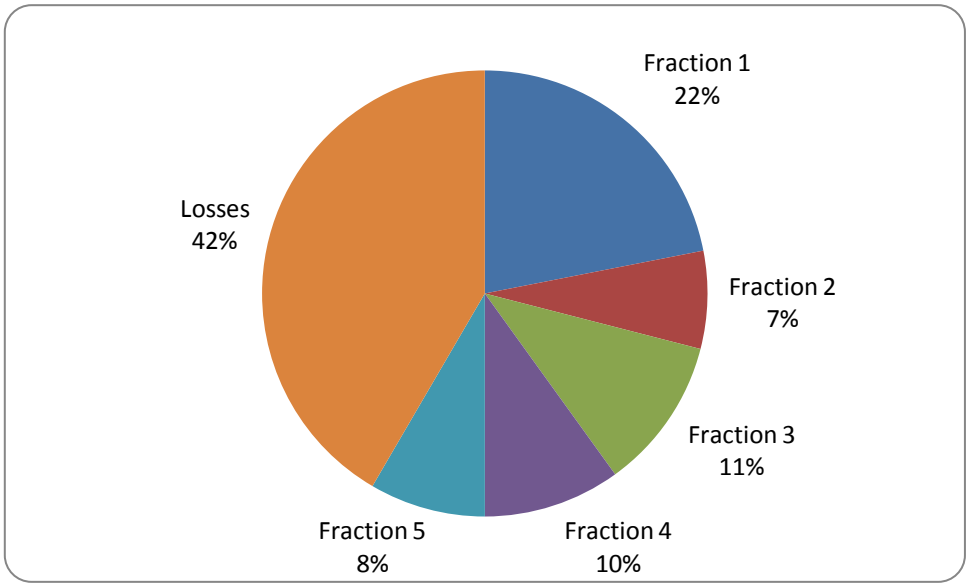

Figure 24. 600°C Bio-oil Distillate Yields. This figure shows the mass percentage distribution of the resulting distillates from the 500C bio-oil. The losses were comprised of a tar like substance remaining in the flask after the distillation process.

Also, during the distillation of the tar produced at 600°C, the water fraction was biphasic. The top layer was decanted and upgraded while the lower layer was realized to be the water fraction. The biphasic nature of this first fraction was evident at the other pyrolysis treatment temperatures as well, but in the previous cases, was not enough to upgrade. After the distillation, a tar-like substance remained in the distillation flask. The mass of the tar accounts for the distillation losses. Attempts were made to dissolve the remaining residual tar in several solvents, but it was insoluble in both polar and nonpolar solvents alike. The tar had to be soaked repeatedly for weeks in acetone to remove it from the distillation flask. Figure 25 illustrates the typical mass yields throughout the process:

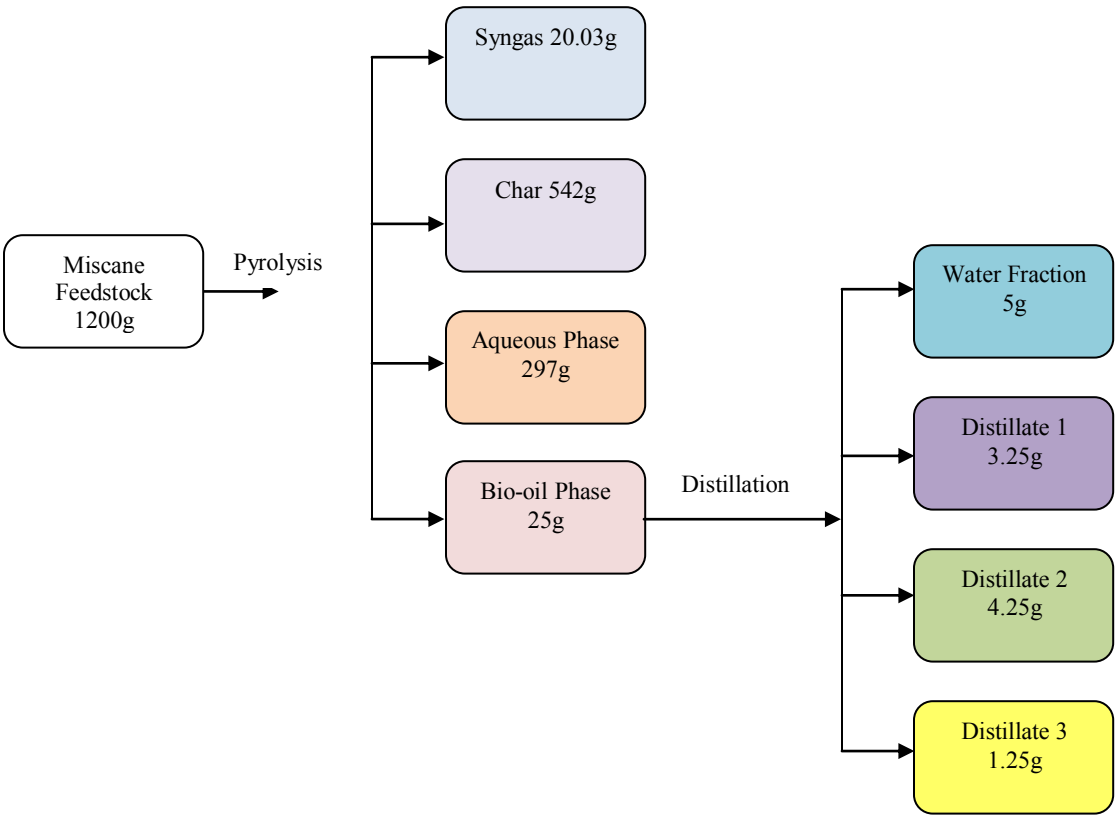

Figure 25. Exemplary Mass Yields of Pyrolysis Co-Products and Bio-oil Distillates.

CHAPTER VI

CONCLUSIONS AND FUTURE RESEARCH

6.1 Summary

Based on the comparison of the distillates to the hydrocarbons found in the JP8 standard, no hydrogenation is necessary to isolate the majority of JP8 hydrocarbon compounds in the bio-oil. This increased number of hydrocarbons may be a result of the elevated pressure maintained in the reactor during pyrolysis. A well-planned solvent separation could be instrumental in isolating hydrocarbons within the JP8 range from the miscane bio-oil.

The first objective of this research was satisfied by completing the tests in table 8 to characterize the miscane feedstock and pyrolysis co-products. Characterization tests were also performed on sugarcane and *Miscanthus* feedstocks for comparison purposes. It is difficult to draw any direct conclusions from these comparisons because of variation in the moisture content among the feedstocks during the analyses.

The second objective was to determine the deoxygenation efficiency of the fluorous Pd, Pd/C and Shvo's catalysts. Catalytic hydrogenation reactions on a model mixture composed of phenolic and alcoholic compounds yielded various percentages of JP8 hydrocarbons depending on the catalyst used. While the hydrocarbon product mixture varied among the catalysts, the deoxygenation efficiencies were similar. The original model mixtue had and oxygenate percentage of 100%. The deoxygenation efficiency was calculated by subtracting the percentage of oxygenates after hydrogenation from 100%. Thus, the second objective was satisfied.

Having determined the deoxygenation efficiencies of each catalyst, these efficiencies were statistically evaluated to identify the catalyst best suited for mild hydrogenation reactions. The statistical analysis implicated that there was no significant difference among the deoxygenation abilities of the catalysts. This is important when considering input costs for biofuel production, and the implication is that there is no added benefit to using a more expensive catalyst.

To address the problem of expensive catalysts and diminish their contribution to input costs, fluorous catalysis was explored as a regenerative catalytic technique that would allow for catalyst recovery and reuse. However, because the fluorous Pd catalyst was unstable in the presence if H_2O (which is produced as a byproduct during hydrogenation reactions), the significance of this regenerative system was not realized. Unlike the Pd/C and Shvo's catalyst, the fluorous Pd was a homogeneous catalyst. Homogeneous catalysts are not subject to the mass transport issues associated with heterogeneous catalysts. To take advantage of the solubility/recoverability properties of the fluorous catalytic system, the stability of the Pd catalyst will need to be addressed. Again, the degradation of the catalyst may have been caused by the production of H_2O produced during the hydrogenation reaction. This degradation led to the formation of Pd nanoparticles, altering the structure of the catalyst. This type of catalyst denaturation can be addressed by replacing the thiol ligand with a phosphine ligand and altering the number of methylene spacers.

The final objective was to evaluate the product quality of the JP8 hydrocarbons produced. This objective must be discussed from the perspective the relationship

between the raw bio-oil and bio-oil dsitillates as well as that of the hydrocarbon product produced as a result of the model mixture hydrogenation experiments. Distilling the bio-oil resulted in distillate fractions that were high in JP8 hydrocarbons while it simultaneously reduced the MC. The GCMS analysis results confirmed the significant presence of hydrocarbons but also showed a significant amount of oxygenated compounds that would need further catalytic upgrading. Distillation did not much improve the TAN of the raw bio-oil if at all. However, this does not negate the fact that greater than 70% JP8 hydrocarbons existed within the distillate fractions without any further upgrading. The hydrogenated fractions of the model mixture resulted in the production of JP8 hydrocarbons with significant reduction in oxygenated compounds. The implication here was that because the oxygenated compounds were reduced, there was a corresponding reduction in TAN. The noteworthy outcome was that the hydrocarbons were produced in substantial concentrations in both the distillates and the hydrogenated model mixture.

6.*2 Recommendations*

While this research focused on the production of JP8 hydrocarbons from miscane, it is recommended that the process developed within this research effort be carried out on sugarcane and *Miscanthus* as a means of evaluating those hydrocarbons produced as well. During the pyrolysis of these feedstocks, the pyrolysis pressure should be varied as a means of studying the effects of pressure on hydrocarbon production. Increased pressure and temperature could affect the hydrocarbon product obtained. Because the pyrolysis experiments take place at elevated temperature and pressure, it

may be advantageous to add a catalyst during this process thereby taking advantage of these conditions which are suitable for the conversion of alcoholic compounds. Alcoholic can be difficult to convert to hydrocarbons, often requiring temperatures above 250°C.

Future research efforts should explore the development of a more stable fluorous catalyst specifically, modifying the ligands so that they are phosphine based or maybe adjusting the length of the methylene spacers to increase the solubility of the catalyst. During the hydrogenation experiments, the fluorous solvent never became miscible with the model mixture. Instead, an emulsion was formed and sufficient stirring was used to ensure contact of the catalyst and the model mixture. This indicates the catalyst properties should be modified based on the fluorous solvent used. After designing a stable catalyst, experiments should be conducted, first on model compounds and then on mixtures that allow for the recovery and reuse of the fluorous catalyst. Data on catalyst turnover numbers and life cycle should be gathered and analyzed. It is also recommended that inexpensive metal catalysts such as Fe, Cu, or Ni be explored as potential fluorous catalytic candidates.

The pyrolytic production of bio-oil and the catalytic conversion of the oxygenates to hydrocarbons were done using batch systems. Future research efforts should explore the use of a continuous system for these processes. Of the two processes, it may be more beneficial to consider a continuous catalytic system that would allow for in-line GCMS sampling and analysis. Experiments were run for 12 hours and no conclusions can be made about the product conversion prior to the completion of the

experimental runs. However, it is possible that 12 hours is not required to achieve the conversion percentages obtained. In such case, the experimental time could be reduced and resources better managed. In-line GCMS sampling could provide insight into the catalytic conversion rate.

Also, the pyrolysis liquids produced are biphasic. This research effort did not explore the analysis of the aqueous phase products. It is recommended that a rotovap be used to evaporate the water from the aqueous phase liquids, allowing for the isolation of water soluble bio-oil compounds. Assuming that the characteristics of water soluble compounds are similar to those of water, it is expected that this layer will contain significant amounts of phenolic, acidic and other oxygenated compounds. If so, this research has shown that the mild catalytic conditions used are sufficient for the conversion of those compounds to hydrocarbons and esters. Isolating and converting the aqueous phase compounds could increase the hydrocarbon production efficiency.

Finally, it was concluded that distillation is an inefficient process for bio-oil production because it is energy intensive and promotes bio-oil instability. Because bio-oil is unstable at elevated temperatures, the distillation process encouraged polymerization reactions which rendered approximately 50% of the bio-oil remaining in the distillation flask as a coal-like brick. This residue was insoluble and was included in the lossess calculated for the mass balance. For industrial applications, solvent fractionations should be used to isolate the hydrocarbon product from the raw bio-oil.

REFERENCES

Boas, N. C., Kim; Cox, Carol; Hendon, Jim; Johnson, Russell; Marren, Mike; Marks, Harvey; and Slocum, Mike (2010). Investing in Renewable Energy. San Raomon, CA**:** 28-33.

Bridgwater, A. (1994). "Catalysis in thermal biomass conversion." *Applied Catalysis A: General* 116(1-2): 5-47.

Bridgwater, A. (1996). "Production of High Grade Fuels and Chemicals From Catalytic Pyroltsis of Biomass." *Catalysis Today* 29: 285-296.

Bridgwater, A. V. (1994). "Catalysis in thermal biomass conversion." *Applied Catalysis A: General* 116(1-2): 5-47.

Bridgwater, A. V. (2001). *An overview of fast pyrolysis Progress in thermochemical biomass conversion.* Wiley and Sons. p. 977.

Bridgwater, A. V., D. Meier, et al. (1999). "An overview of fast pyrolysis of biomass." *Organic Geochemistry* 30(12): 1479-1493.

Carroll, A. and C. Somerville (2009). "Cellulosic Biofuels." *Annual Review of Plant Biology* 60(1): 165-182.

Chen, G., J. Andries, et al. (2003). "Biomass pyrolysis/gasification for product gas production: the overall investigation of parametric effects." *Energy conversion and management* 44(11): 1875-1884.

Chen, G., J. Andries, et al. (2003). "Catalytic pyrolysis of biomass for hydrogen rich fuel gas production." *Energy conversion and management* 44(14): 2289-2296.

Council, N. R. (2009). Catalysis for Energy: Fundamental Science and Long-Term Impacts of the US Department of Energy Basic energy Sciences Catalysis Science Program. Washington, DC, National Academies Press.

da Costa, R. C. and J. A. Gladysz (2007). "Syntheses and Reactivity of Analogues of Grubbs' Second Generation Metathesis Catalyst with Fluorous Phosphines: A New Phase-Transfer Strategy for Catalyst Activation." *Advanced Synthesis & Catalysis* 349(1-2): 243-254.

de Jong, W., A. Pirone, et al. (2003). "Pyrolysis of Miscanthus Giganteus and wood pellets: TG-FTIR analysis and reaction kinetics." *Fuel* 82(9): 1139-1147.

de Wolf, E. and B.-J. Deelman (2008). Fluorous Catalysts and Fluorous Phase Catalyst Separation for Hydrogenation Catalysis, Wiley-VCH Verlag GmbH.

de Wolf, E., G. van Koten, et al. (1999). "Fluorous phase separation techniques in catalysis." *Chemical Society Reviews* 28(1): 37-41.

Dinh, L. a. D., JA (2005). "Monophasic and biphasic hydrosilylations of enones and ketones using a fluorous rhodium catalyst that is easily recycled under fluorous–organic liquid–liquid biphasic conditions." *New Journal of Chemistry* 29: 173-181.

Elliott, D. C. (2007). "Historical Developments in Hydroprocessing Bio-oils." *Energy & Fuels* 21(3): 1792-1815.

Feride, T. and G. Hasan Ferdi (2004). "Production and Characterization of Pyrolysis Oils from Euphorbia Macroclada." *Energy Sources* 26(8): 761-770.

Garcia-Perez, M., T. T. Adams, et al. (2007). "Production and Fuel Properties of Pine Chip Bio-oil/Biodiesel Blends." *Energy & Fuels* 21(4): 2363-2372.

Gladysz, J. A. (2011). Disadvantages of Fluorous Catalysis. Personal communication with A. Lovelady. College Station, TX.

Gladysz, J. A. a. T., Verona (2008). "Temperature-Controlled Catalyst Recycling: new Protocols Based upon Temperature-Dependent Solubilities of Fluorous Compounds and Solid/Liquid Phase Seperations." *Topics in Organometallic Chemistry* 23: 67-89.

Heichel, G. H. (1973). Comparative efficiency of energy use in crop production.

Hope, E. G. and A. M. Stuart (1999). "Fluorous biphase catalysis." *Journal of Fluorine Chemistry* 100(1-2): 75-83.

Horváth, I. T. (1998). "Fluorous Biphase Chemistry." *Accounts of Chemical Research* 31(10): 641-650.

Jakob, K., F. Zhou, et al. (2009). "Genetic improvement of C4 grasses as cellulosic biofuel feedstocks." *In Vitro Cellular & Developmental Biology - Plant* 45(3): 291-305.

Jason, H., E. Nelson, et al. (2006). "Environmental, Economic, and Energetic Costs and Benefits of Biodiesel and Ethanol Biofuels." *Proceedings of the National Academy of Sciences of the United States of America* 103(30): 11206-11210.

Jones, J. M., M. Kubacki, et al. (2005). "Devolatilisation characteristics of coal and biomass blends." *Journal of Analytical and Applied Pyrolysis* 74(1-2): 502-511.

Jurisch, M. (2008). Highly Fluorinated Catalysts and Compounds: Advanced Immobilization Strategies for the Recycling of Catalysts.

Lam, E., J. Shine, et al. (2009). "Improving sugarcane for biofuel: engineering for an even better feedstock." *GCB Bioenergy* 1(3): 251-255.

Mascia, P. N. 2010. Designing Plants To Meet Feedstock Needs Plant Biotechnology for Sustainable Production of Energy and Co-products. *Biotechnology in Agriculture and Forestry*(66):57-84.

Matar, S. M., MJ; Tayim, HA (1989). Catalysis in Petrochemical Processes. Dordrecht, Holland, Kluwer Academic Publishers.

Mullen, C. A. B., Akwasi A; Goldberg, Neil M; Lima, Isabel M; Laird, David A; Hicks, Kevin B (2010). "Bio-oil and Bio-char Production From Corn Cobs and Stover by Fast Pyrolysis." *Biomass and Bioenergy* 34: 67-74.

Ozlem, O. and O. Mete Koçkar (2004). "Fixed-bed pyrolysis of rapeseed (Brassica napus L.)." *Biomass and Bioenergy* 26(3): 289-299.

Phelps, J. (unknown). "Chemtrails and JP8." Retrieved March 1, 2012, from http://saba.fateback.com/articoli/chemtrails.html.

Richter, B. S., Anthony L; van Koten, Gerard; and deelman, Berth-Jan (2000). "Fluorous Versions of Wilikinson's Catalyst. Activity in Fluorous Hydrogenation of 1-Alkenes and Recycling by Fluorous Biphasic Seperation." *Journal of American Chemical Society* 122: 3945-3951.

Rocaboy, C. a. G., JA (2002). "Syntheses, Oxidations, and Palladium Complexes fo Fluorous Dialkly Sulfides: New Precursors To Highly Active Catalysts For the Suzuki Coupling." *Tetrahedron* 58: 4007-4014.

Rubin, E. M. (2008). "Genomics of cellulosic biofuels." *Nature* 454(7206): 841-845.

Rutherford, D., J. J. J. Juliette, et al. (1998). "Transition metal catalysis in fluorous media: application of a new immobilization principle to rhodium-catalyzed hydrogenation of alkenes." *Catalysis Today* 42(4): 381-388.

Sheu, Y.-H. E. A., Rayford G. and Soltes, Ed J. (1988). "Kinetic Studies of Upgrading Pine Pyrolytic Oil by Hydrotreatment." *Fuel Processing Technology* 19: 31-50.

Sinou, D., D. Maillard, et al. (2003). "- Rhodium-Catalyzed Hydrogenation of Alkenes by Rhodium/Tris(fluoroalkoxy)phosphane Complexes in Fluorous Biphasic System." - 345(-5): 603- 611.

Tahir, M. T. B. M. (2009). The Production of Bio Oil Through Batch Pyrolysis Process. Undergraduate Thesis. University of Malaysia Pahang. BS Chemical Engineering.

Unknown (unknown). "Fuel Properties." Retrieved March 1, 2012, from http://alternativefuels9.tpub.com/5948/59480013.htm.

Vermerris, W. (2008). Genetic Improvement of Bioenergy Crops. *Annals of Botany* 6(3):450.

Wang, Z. D., K and Uozumi, Y. (2008). An Overview of Heterogeneous Asymmetric Catalysis. Weinheim: Wiley-VCH.

Weerachanchai, P., C. Tangsathitkulchai, et al. "Characterization of products from slow pyrolysis of palm kernel cake and cassava pulp residue." *Korean Journal of Chemical Engineering*: (In press)1-13.

Williams, P. a. B., S (1992). "Pyrolysis of Municipal Solid Waste." *Journal of the Institute of Energy* 65: 192-200.

Williams, P. T. and S. Besler (1996). "The influence of temperature and heating rate on the slow pyrolysis of biomass." *Renewable Energy* 7(3): 233-250.

Williams, P. T. and P. A. Horne (1994). "The role of metal salts in the pyrolysis of biomass." *Renewable Energy* 4(1): 1-13.

Xiong, W.-M., Y. Fu, et al. (2011). "An in situ reduction approach for bio-oil hydroprocessing." *Fuel Processing Technology* 92(8): 1599-1605.

APPENDIX A

STATISTICAL ANALYSIS RESULTS

A1. Syngas Statistical Analysis Results

Table 38. Syngas ANOVA

Percent H_2					
Source	**DF**	**Sum of Squares**	**Mean Square**	**F Ratio**	**Prob > F**
Model	2	183.502	91.751	321.835	<.0001*
Error	24	6.842	0.285		
C. Total	26	190.344			
Percent CO					
Source	**DF**	**Sum of Squares**	**Mean Square**	**F Ratio**	**Prob > F**
Model	2	138.239	69.120	6.404	0.0059*
Error	24	259.018	10.792		
C. Total	26	397.258			
Percent CH_4					
Source	**DF**	**Sum of Squares**	**Mean Square**	**F Ratio**	**Prob > F**
Model	2	1233.137	616.569	10.752	0.0005*
Error	24	1376.210	57.342		
C. Total	26	2609.347			
Percent CO_2					
Source	**DF**	**Sum of Squares**	**Mean Square**	**F Ratio**	**Prob > F**
Model	2	1051.618	525.809	49.790	<.0001*
Error	24	253.451	10.560		
C. Total	26	1305.069			

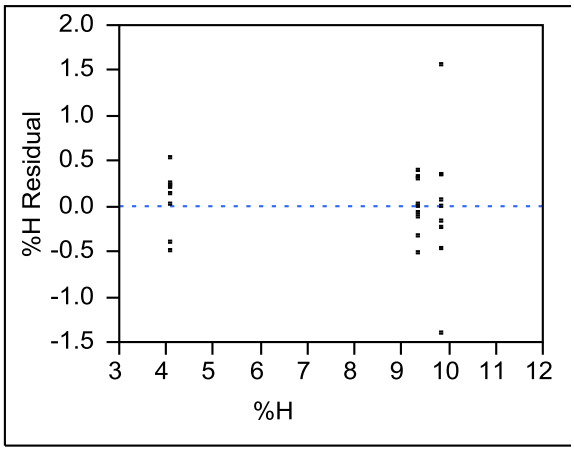

Figure 26. Syngas H2 Variance Verification.

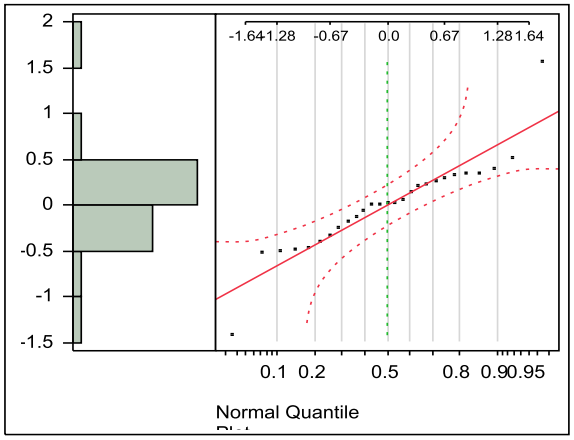

Figure 27. Syngas H2 Normality Plot.

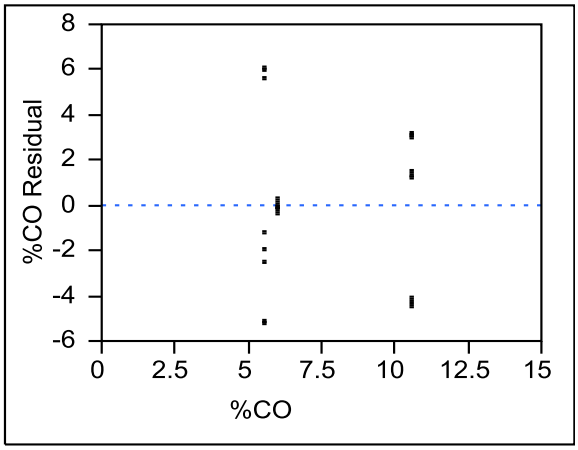

Figure 28. Syngas CO Variance Verification.

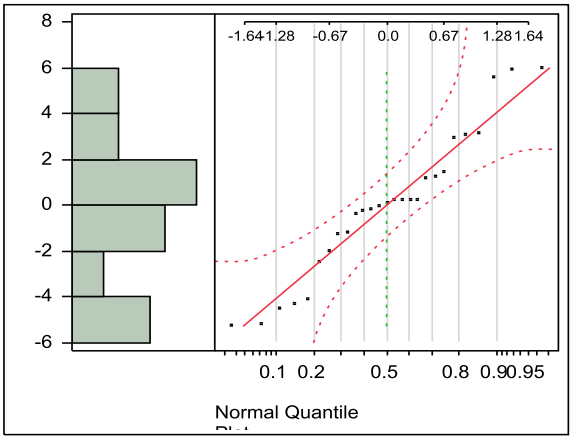

Figure 29. Syngas CO Normality Plot.

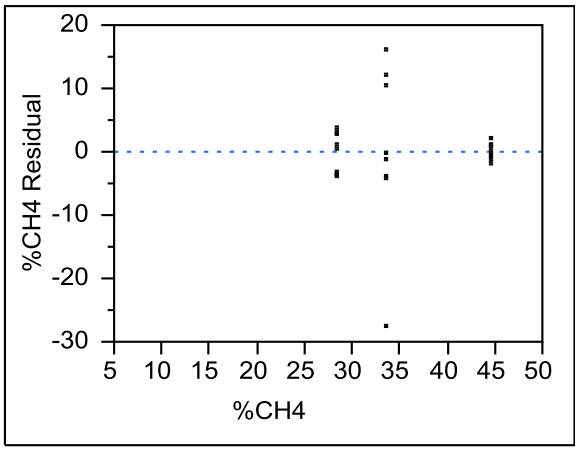

Figure 30. Syngas CH4 Variance Verification.

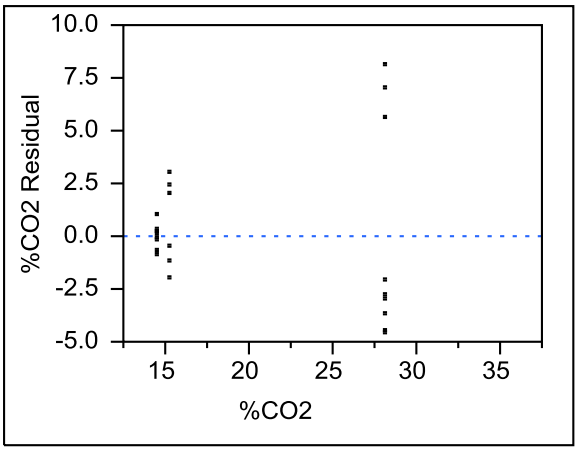

Figure 32. Syngas CO2 Variance Verification.

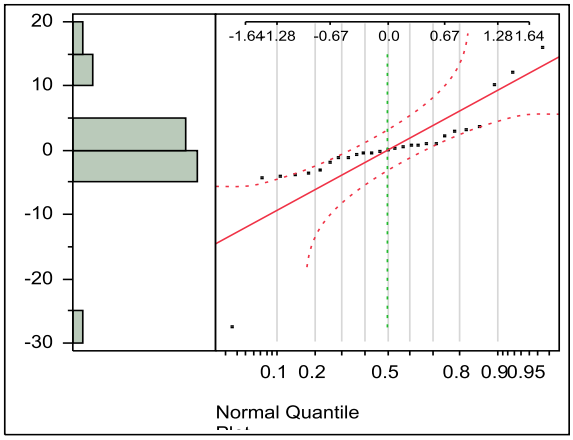

Figure 31. Syngas CH4 Normality Plot.

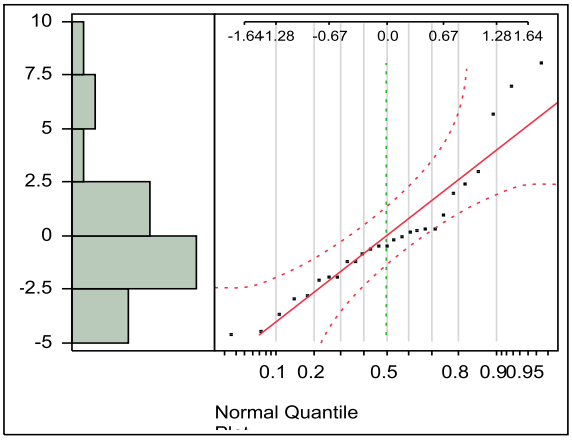

Figure 33. Syngas CO2 Normality Plot.

Table 39. Percent CO_2 Transformed ANOVA

Percent CO2

Source	DF	Sum of Squares	Mean Square	F Ratio	Prob > F
Model	2	632.438	316.219	80.554	<.0001*
Error	24	94.212	3.926		
C. Total	26	726.650			

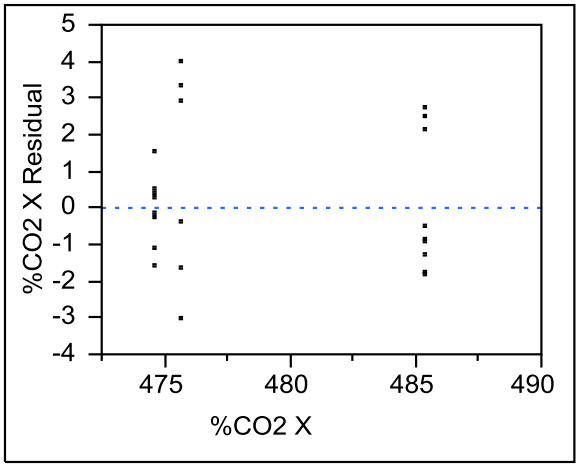

Figure 34. Syngas Transformed CO2 Variance Verification.

Table 40. t-test Results Mean Percentages of H_2, CO and CH_4

Percent H			
Level			**Least Squares Mean**
500	A		9.837
600	A		9.326
400		B	4.069
Percent CO			
Level			**Least Squares Mean**
400	A		10.578
600		B	6.006
500		B	5.578
Percent CH_4			
Level			**Least Squares Mean**
600	A		44.590
500		B	33.620
400		B	28.369
**Percent CO_2*			
Level			**Least Squares Mean**
400	A		485.357
500		B	475.620
600		B	474.632

Levels not connected by the same letter are significantly different.

A2. Char Yield Statistical Analysis Results

Table 41. Char Yield ANOVA

Source	DF	Sum of Squares	Mean Square	F Ratio	Prob > F
Model	2	883.200	441.600	1.210	0.361
Error	6	2188.235	364.706		
C. Total	8	3071.435			

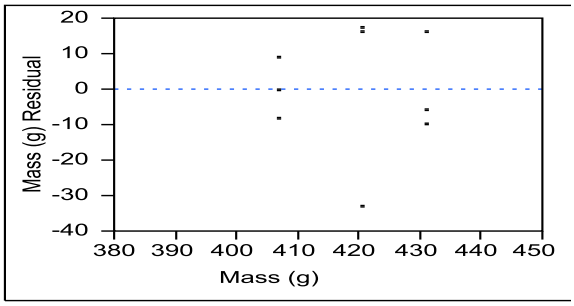

Figure 35. Char Yield Variance Verification.

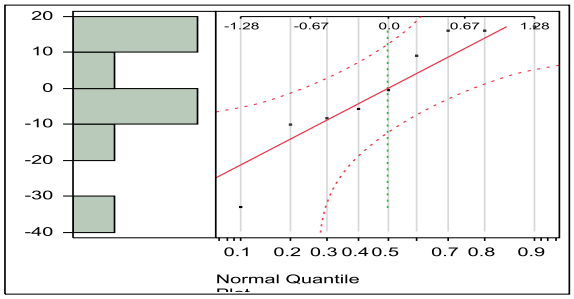

Figure 36. Char Yield Normality Plot.

A3. Miscane Char Ultimate Analysis Statistical Results

Table 42. Miscane Char Ultimate Analysis ANOVA

Percent Carbon					
Source	**DF**	**Sum of Squares**	**Mean Square**	**F Ratio**	**Prob > F**
Model	2	386.678	193.339	70.833	<.0001*
Error	24	65.507	2.729		
C. Total	26	452.186			
Percent Hydrogen					
Source	**DF**	**Sum of Squares**	**Mean Square**	**F Ratio**	**Prob > F**
Model	2	24.355	12.177	195.934	<.0001*
Error	24	1.491	0.062		
C. Total	26	25.847			
Percent Oxygen					
Source	**DF**	**Sum of Squares**	**Mean Square**	**F Ratio**	**Prob > F**
Model	2	497.244	248.622	87.139	<.0001*
Error	24	68.475	2.853		
C. Total	26	565.719			
Percent Nitrogen					
Source	**DF**	**Sum of Squares**	**Mean Square**	**F Ratio**	**Prob > F**
Model	2	0.777	0.388	21.640	<.0001*
Error	24	0.430	0.017		
C. Total	26	1.207			
Percent Sulfur					
Source	**DF**	**Sum of Squares**	**Mean Square**	**F Ratio**	**Prob > F**
Model	2	0.123	0.061	6.659	0.0050*
Error	24	0.222	0.009		
C. Total	26	0.345			

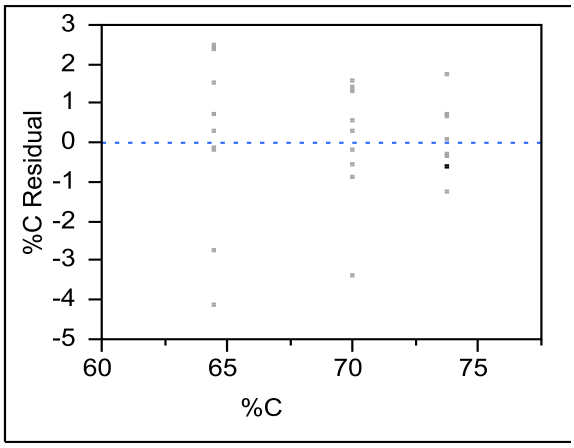

Figure 37. Char Percent C Variance Vericifation.

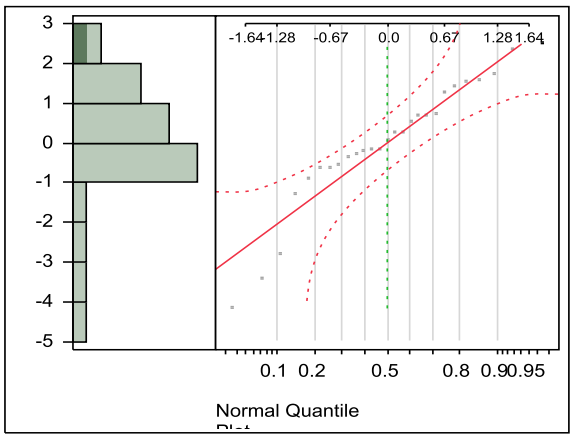

Figure 38. Char Percent C Normality Plot.

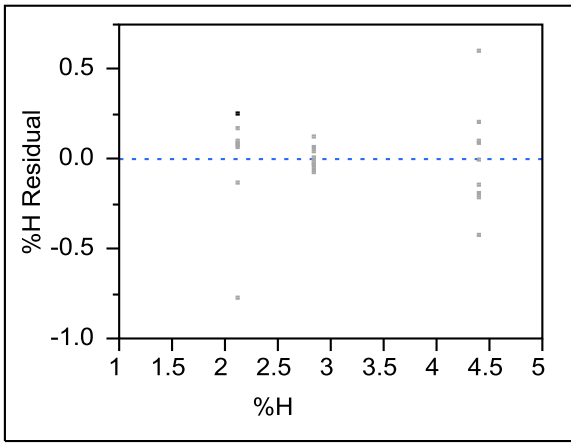

Figure 39. Char Percent H Variance Vericifation.

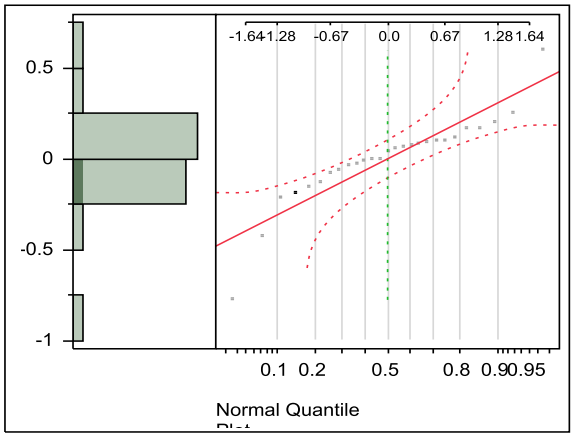

Figure 40. Char Percent H Normality Plot.

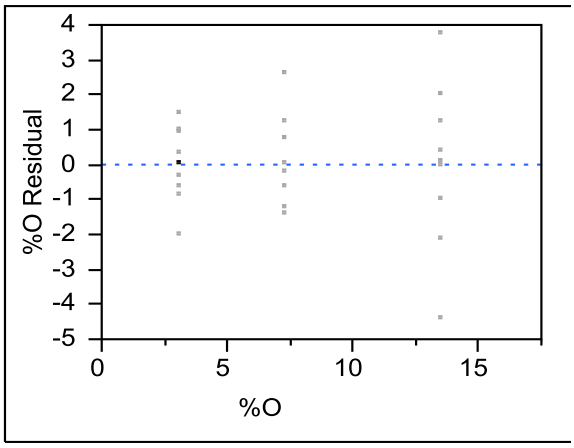

Figure 41. Char Percent O Variance Vericifation.

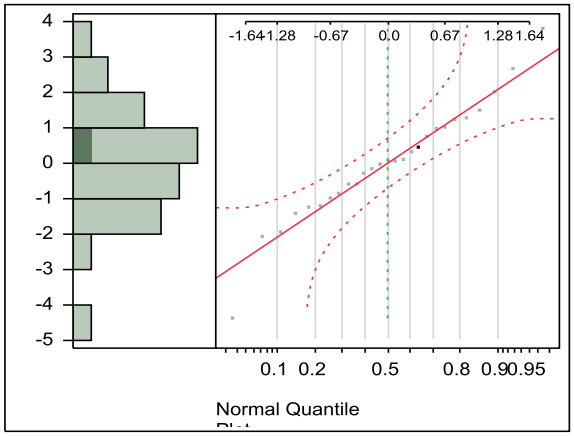

Figure 42. Char Percent O Normality Plot.

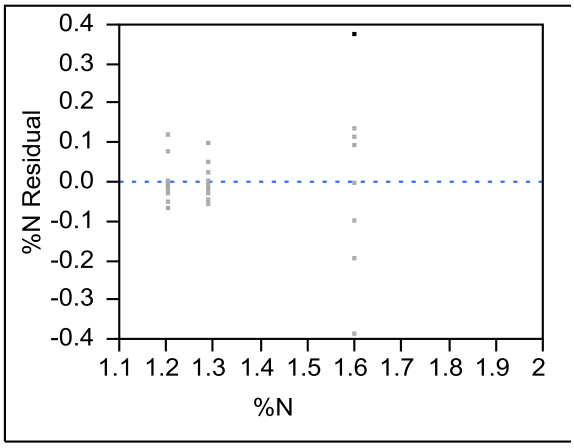

Figure 43. Char Percent N Variance Vericifation.

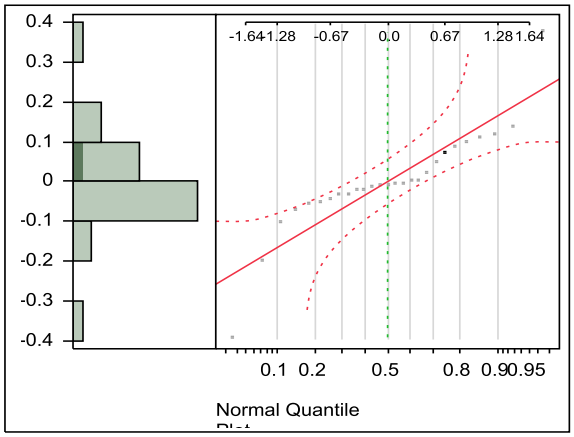

Figure 44. Char Percent N Normality Plot.

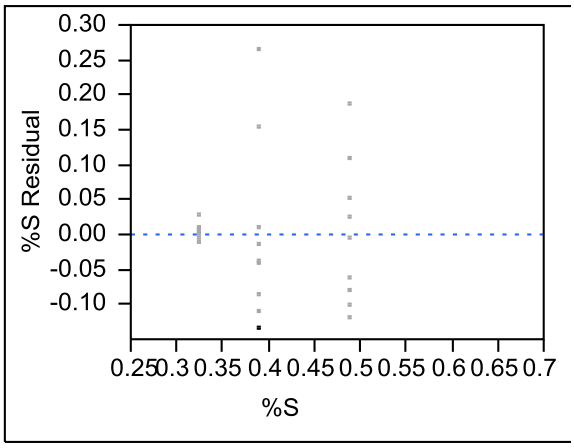

Figure 45. Char Percent S Variance Vericifation.

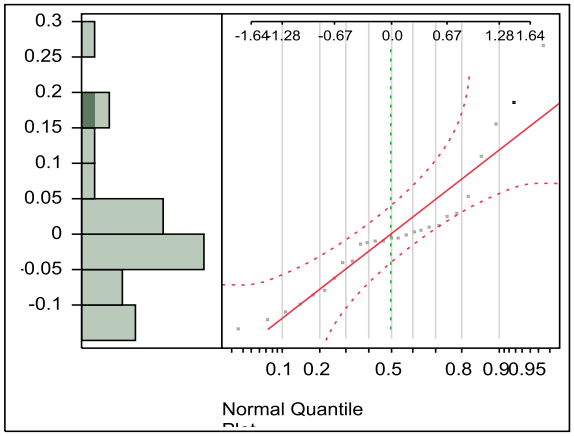

Figure 46. Char Percent S Normality Plot.

Table 43. t-test Results for Miscane Char Elemental Analysis

%C Student's t-Test Results			
Level			**Least Squares Mean**
600	A		73.707
500		B	70.013
400			C 64.498
%H Student's t-Test Results			
Level			Least Squares Mean
400	A		4.393
500		B	2.842
600			C 2.115
%O Student's t-Test Results			
Level			Least Squares Mean
400	A		13.514
500		B	7.229
600			C 3.074
%N Student's t-Test Results			
Level			Least Squares Mean
600	A		1.597
500		B	1.288
400		B	1.202
%S Student's t-Test Results			
Level			Least Squares Mean
400	A		0.488
600		B	0.388
500		B	0.324

Levels not connected by the same letter are significantly different.

A4. Miscane Char Proximate Analysis Statistical Results

Table 44. Miscane Char Proximate Analysis ANOVA

Percent MC ANOVA					
Source	**DF**	**Sum of Squares**	**Mean Square**	**F Ratio**	**Prob > F**
Model	2	49.771	24.885	9.100	0.001*
Error	23	65.626	2.734		
C. Total	25	115.398			
Percent VCM ANOVA					
Source	**DF**	**Sum of Squares**	**Mean Square**	**F Ratio**	**Prob > F**
Model	2	2291.739	1145.87	36.464	<.0001*
Error	24	754.173	31.42		
C. Total	26	3045.912			
Percent Ash ANOVA					
Source	**DF**	**Sum of Squares**	**Mean Square**	**F Ratio**	**Prob > F**
Model	2	50.202	25.101	17.757	<.0001*
Error	24	33.925	1.413		
C. Total	26	84.127			
Percent FC ANOVA					
Source	**DF**	**Sum of Squares**	**Mean Square**	**F Ratio**	**Prob > F**
Model	2	2380.804	1190.40	40.360	<.0001*
Error	24	707.859	29.49		
C. Total	26	3088.664			

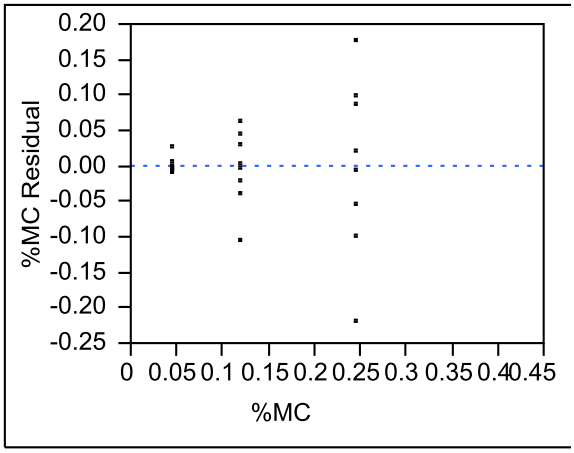

Figure 47. Char MC Variance Verificaiton.

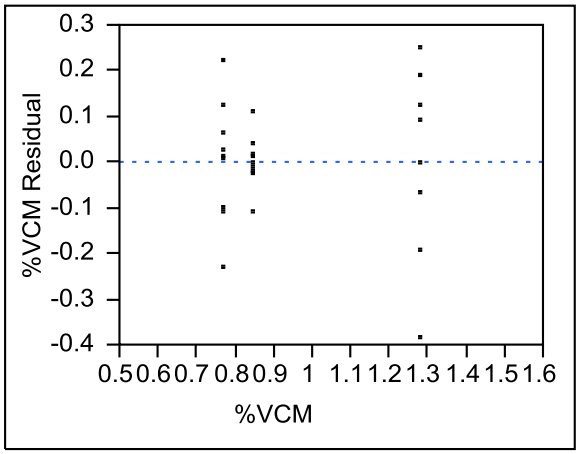

Figure 49. Char VCM Variance Verification.

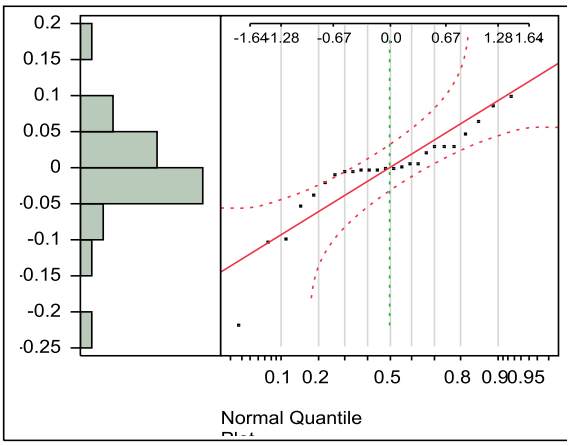

Figure 48. Char MC Normality Plot.

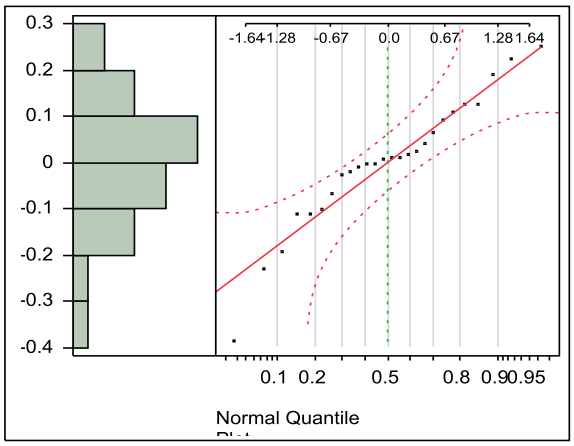

Figure 50. Char VCM Normality Plot.

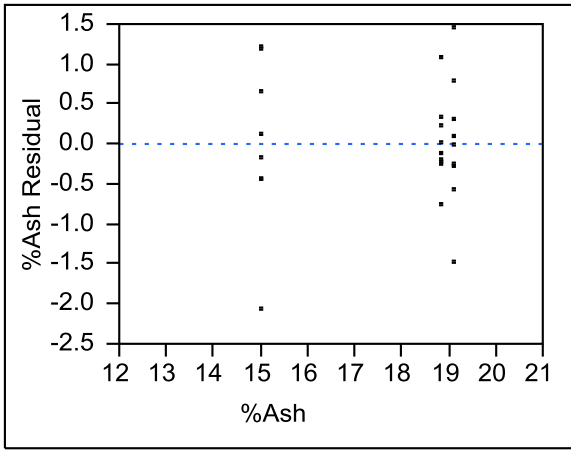

Figure 51. Char Ash Variance Verification.

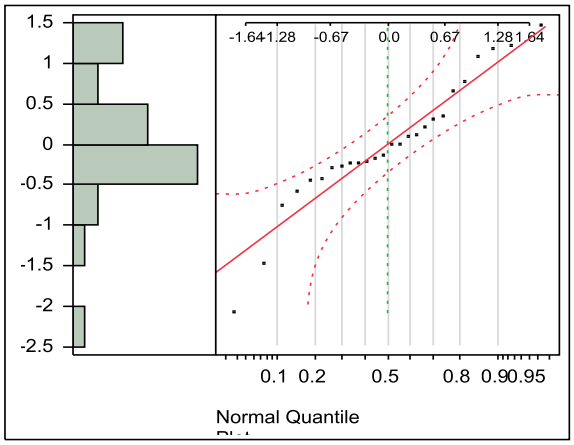

Figure 52. Char Ash Normality Plot.

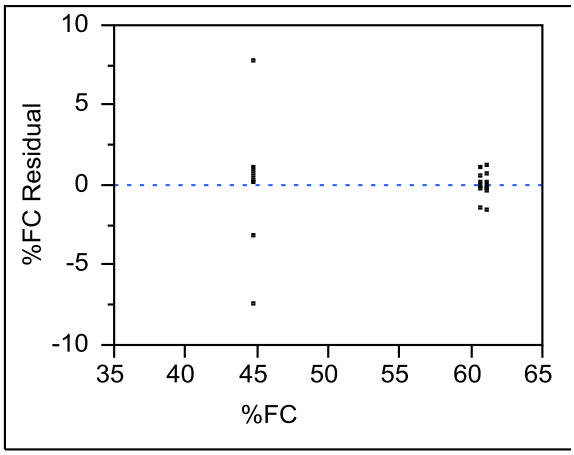

Figure 53. Char FC Variance Verification.

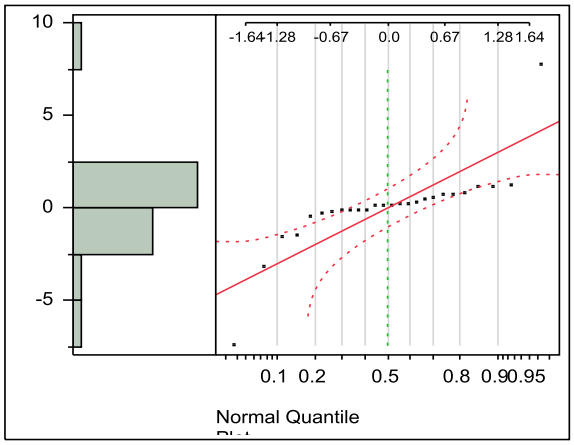

Figure 54. Char FC Normality Plot.

Table 45. Percent MC Transformed ANOVA

Percent MC Transformed ANOVA

Source	DF	Sum of Squares	Mean Square	F Ratio	Prob > F
Model	2	28.143	14.071	13.963	<.0001*
Error	24	24.187	1.007		
C. Total	26	52.330			

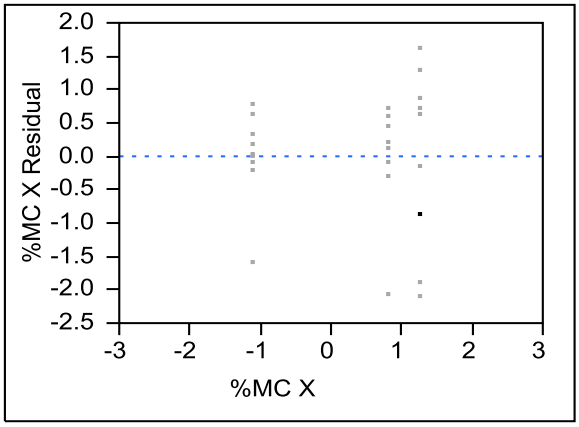

Figure 55. Char Transformed MC Variance Verification.

Table 46. t-test Results for Miscane Char Proximate Analysis

*%MC Student's t-Test Results		
Level		**Least Squares Mean**
400	A	1.248
600	A	0.799
500	B	-1.106
%VCM Student's t-Test Results		
400	A	1.280
500	B	0.847
600	B	0.770
% Ash Student's t-Test Results		
Level		Least Squares Mean
600	A	19.115
500	A	18.826
400	B	15.021
%FC Student's t-Test Results		
Level		Least Squares Mean
600	A	61.051
500	A	60.715
400	B	44.817

Levels not connected by the same letter are significantly different. * Indicates that the t-test for %MC was performed on transformed data.

A5. Miscane Char Energy Content Statistical Analysis Results

Table 47. Char Energy Content ANOVA

Source	DF	Sum of Squares	Mean Square	F Ratio	Prob > F
Model	2	2635565.9	1317783	9.095	0.0011*
Error	24	3477053.8	144877		
C. Total	26	6112619.7			

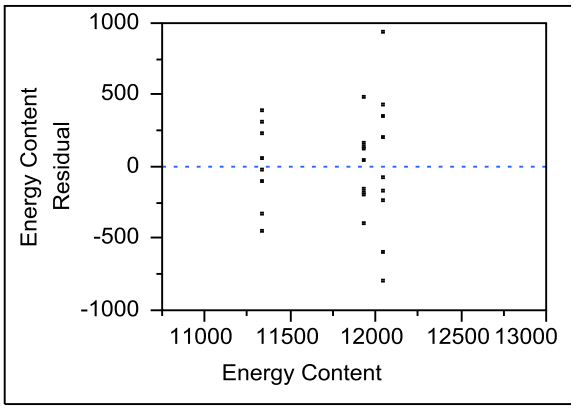

Figure 56. Char Energy Content Variance Verification.

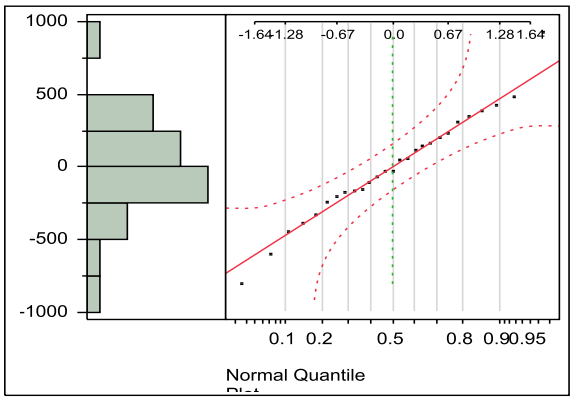

Figure 57. Char Energy Content Normality Plot.

Table 48. Char Energy Content Student t-Test Results

Level		Least Squares Mean
600	A	12042.241
500	A	11935.519
400	B	11332.588

Levels not connected by the same letter are significantly different.

A6. Raw Bio-oil MC Statistical Analysis Results

Table 49. Miscane Raw Bio-oil MC ANOVA

Source	DF	Sum of Squares	Mean Square	F Ratio	Prob > F
Model	2	1787.5954	893.798	542.7904	<.0001*
Error	24	39.5201	1.647		
C. Total	26	1827.1155			

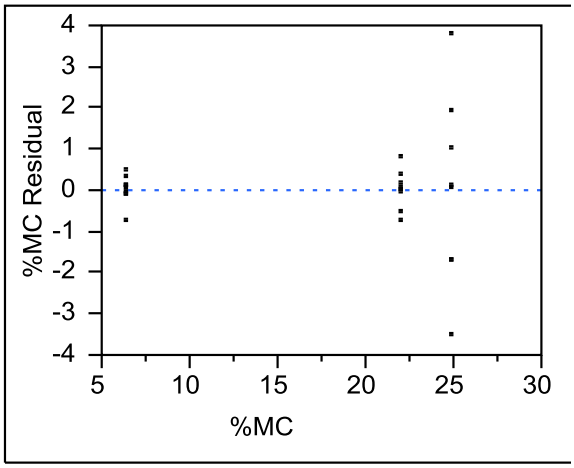

Figure 58. Raw Bio-oil MC Variance Verification.

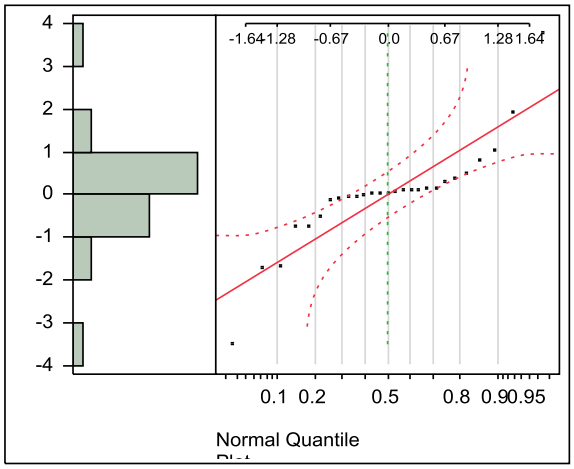

Figure 59. Raw Bio-oil MC Normality Plot.

Table 50. Raw Bio-oil %MC Student t-Test Results

Level			Least Squares Mean
500	A		24.874
600		B	21.977
400			6.348

All levels not connected by the same letter are significantly different.

A7. Raw Bio-oil Ultimate Analysis Statistical Results

Table 51. Miscane Raw Bio-oil Ultimate Analysis ANOVA

%C

Source	DF	Sum of Squares	Mean Square	F Ratio	Prob > F
Model	2	903.085	451.543	5.054	0.014*
Error	24	2143.996	89.333		
C. Total	26	3047.082			

%H

Source	DF	Sum of Squares	Mean Square	F Ratio	Prob > F
Model	2	12.972	6.486	5.682	0.009*
Error	24	27.395	1.141		
C. Total	26	40.368			

%O + Ash

Source	DF	Sum of Squares	Mean Square	F Ratio	Prob > F
Model	2	1170.182	585.091	5.280	0.012*
Error	24	2659.190	110.800		
C. Total	26	3829.373			

%N

Source	DF	Sum of Squares	Mean Square	F Ratio	Prob > F
Model	2	0.046	0.023	3.718	0.039*
Error	24	0.150	0.006		
C. Total	26	0.197			

%S

Source	DF	Sum of Squares	Mean Square	F Ratio	Prob > F
Model	2	0.149	0.074	11.653	0.0003*
Error	24	0.154	0.006		
C. Total	26	0.304			

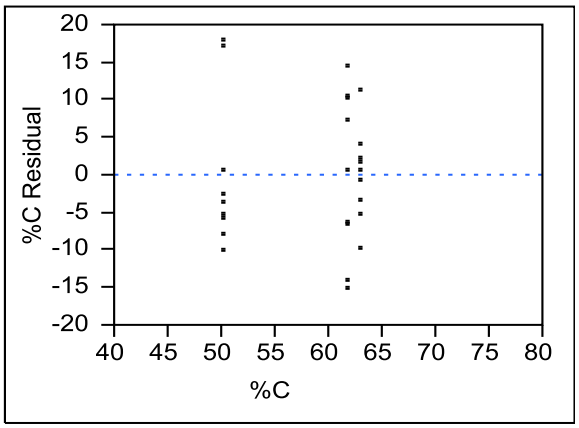

Figure 60. Raw Bio-oil Percent C Variance Verification.

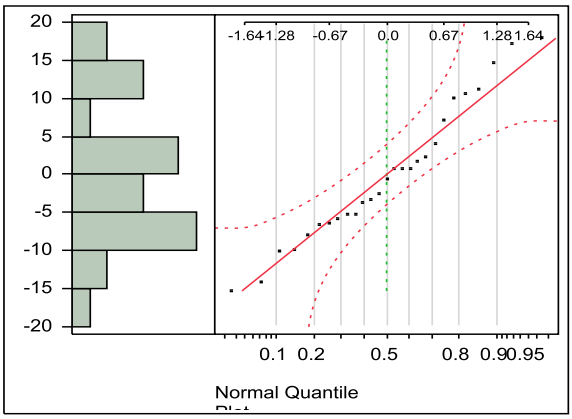

Figure 61. Raw Bio-oil Percent C Normality Plot.

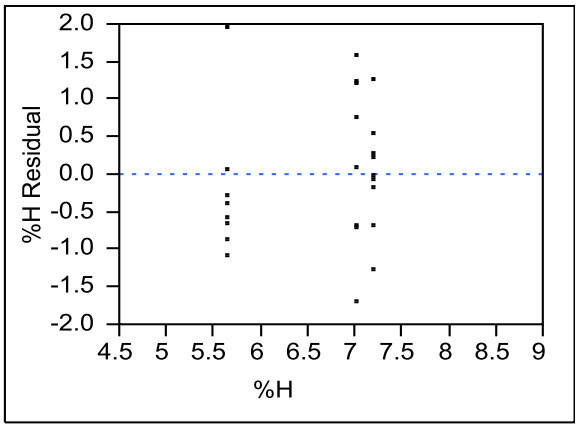

Figure 62. Raw Bio-oil Percent H Variance Verification.

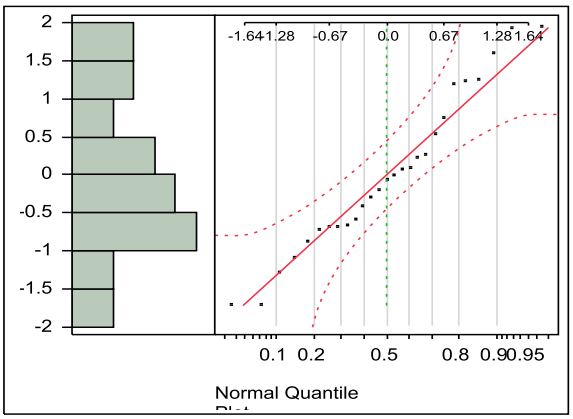

Figure 63. Raw Bio-oil Percent H Normality Plot.

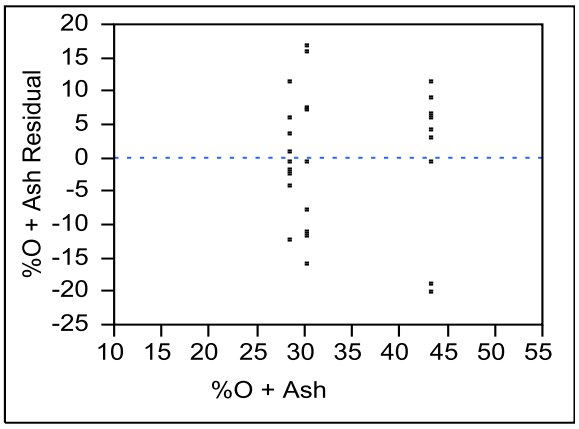

Figure 64. Raw Bio-oil Percent (O2 + Ash) Variance Verification.

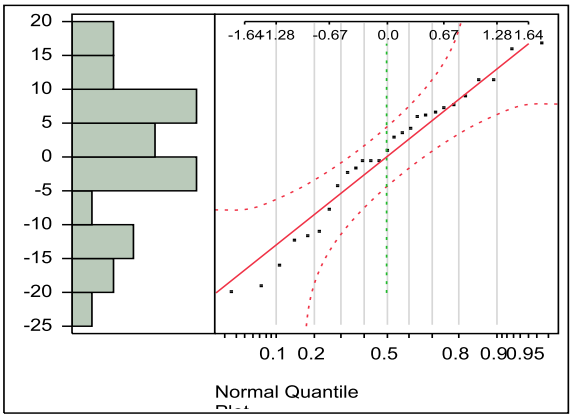

Figure 65. Raw Bio-oil Percent (O2 + Ash) Normality Plot.

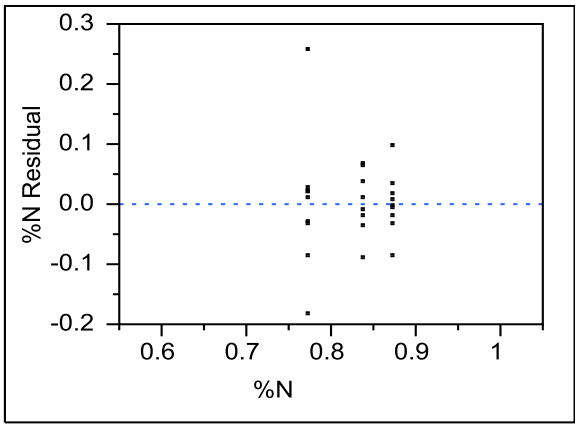

Figure 66. Raw Bio-oil Percent N Variance Verification.

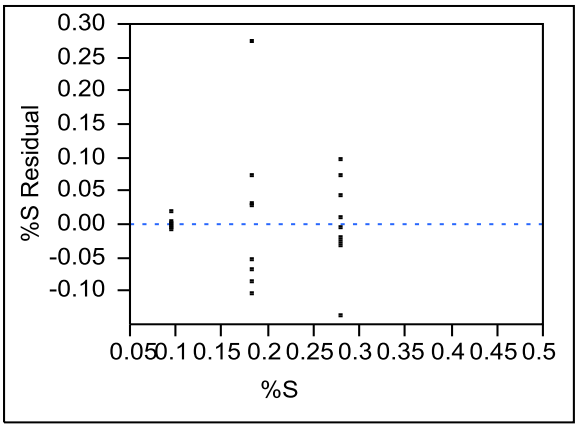

Figure 68. Raw Bio-oil Percent S Variance Verification.

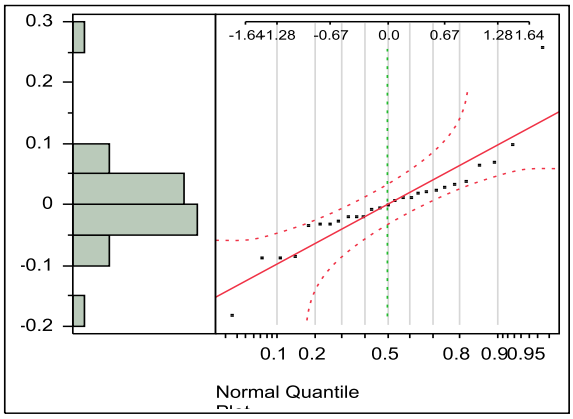

Figure 67. Raw Bio-oil Percent N Normality Plot

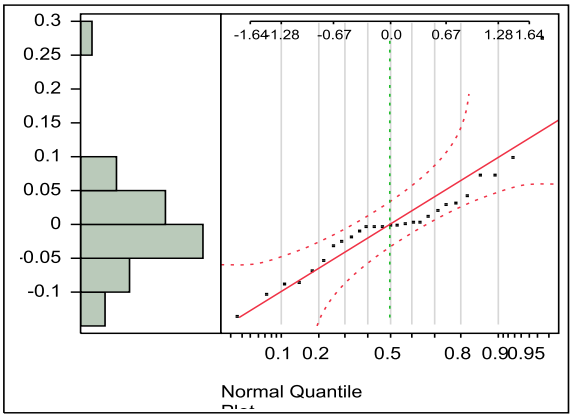

Figure 69. Raw Bio-oil Percent S Normality Plot.

Table 52. Raw Bio-oil Ultimate Analysis Student t-Test Results

Percent C				
Level			**Least Mean**	**Squares**
400	A		63.090	
500	A		61.807	
600		B	50.231	
Percent H				
Level			**Least Mean**	**Squares**
400	A		7.196	
500	A		7.012	
600		B	5.642	
Percent (O2+Ash)				
Level			**Least Mean**	**Squares**
600	A		43.257	
500		B	30.159	
400		B	28.562	
Percent N				
Level			**Least Mean**	**Squares**
400	A		0.872	
500	A	B	0.838	
600		B	0.772	
Percent S				
Level			**Least Mean**	**Squares**
400	A		0.278	
500		B	0.181	
600			C	0.096

All levels not connected by the same letter are significantly different.

A8. Results of H/C Ratio Statistical Analysis

Table 53. H/C Ratio ANOVA

Source	DF	Sum of Squares	Mean Square	F Ratio	Prob > F
Model	2	0.001	0.0008	4.100	0.029*
Error	24	0.004	0.0002		
C. Total	26	0.006			

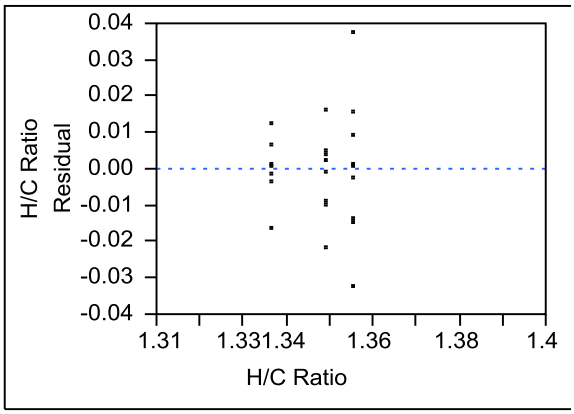

Figure 70. Raw Bio-oil H/C Ratio Variance Verification.

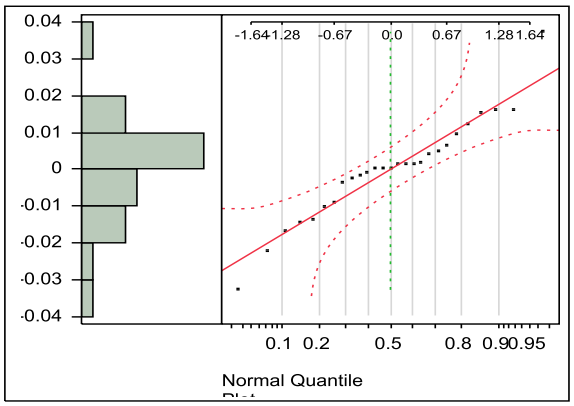

Figure 71. Raw Bio-oil H/C Ratio Normality Plot.

Table 54. Raw Bio-oil H/C Ratio Student t-Test Results

Level			Least Squares Mean
400	A		1.355
500	A	B	1.349
600		B	1.336

All levels not connected by the same letter are significantly different.

A9. Results of Raw Bio-oil Energy Content Statistical Analysis

Table 55. Raw Bio-oil Energy Content ANOVA

Source	DF	Sum of Squares	Mean Square	F Ratio	Prob > F
Model	2	8615160	4307580	3.536	0.045*
Error	24	29234417	1218101		
C. Total	26	37849577			

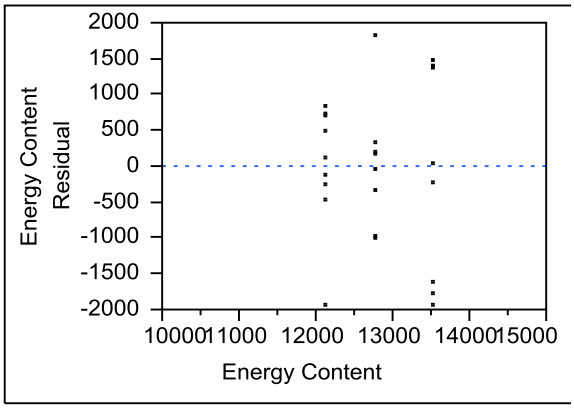

Figure 72. Raw Bio-oil Energy Content Normality Plot.

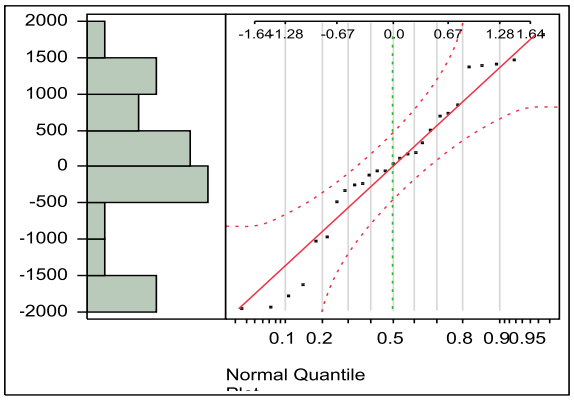

Figure 73. Raw Bio-oil Energy Content Ratio Normality Plot.

Table 56. Raw Bio-oil Energy Content Student t-Test Results

Level			Least Squares Mean
400	A		13513.340
500	A	B	12762.802
600		B	12131.403

Table 1. Levels not connected by the same letter are significantly different.

A10. Raw Bio-oil Density Statistical Analysis Results

Table 57. Raw Bio-oil Density ANOVA

Source	DF	Sum of Squares	Mean Square	F Ratio	Prob > F
Model	2	0.104	0.052	5.607	0.010*
Error	24	0.224	0.009		
C. Total	26	0.329			

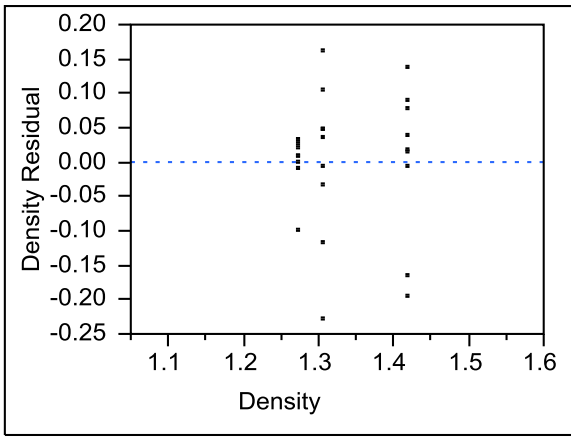

Figure 74. Raw Bio-oil Density Variance Verification.

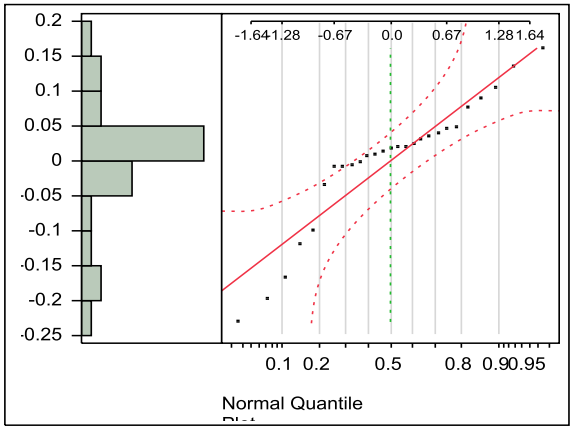

Figure 75. Raw Bio-oil Density Normality Plot.

Table 58. Raw Bio-oil Density Student t-Test Results

Level			Least Mean	Squares
600	A		1.419	
500		B	1.305	
400		B	1.274	

Levels not connected by the same level are significantly different.

A11. Raw Bio-oil TAN Statistical Analysis

Table 59. Raw Bio-oil TAN ANOVA

Source	DF	Sum of Squares	Mean Square	F Ratio	Prob > F
Model	2	403.77461	201.887	113.2331	<.0001*
Error	24	42.79047	1.783		
C. Total	26	446.56507			

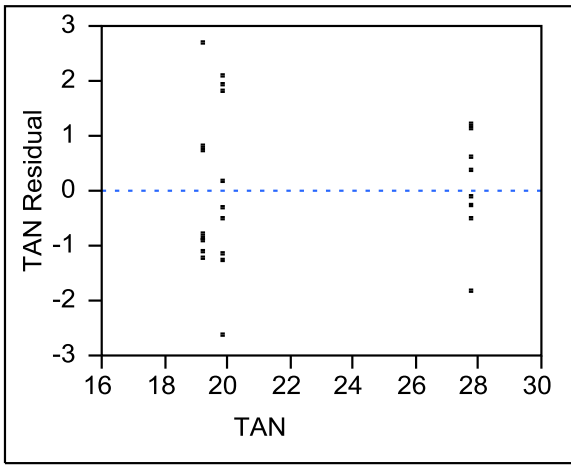

Figure 76. Raw Bio-oil TAN Variance Verification.

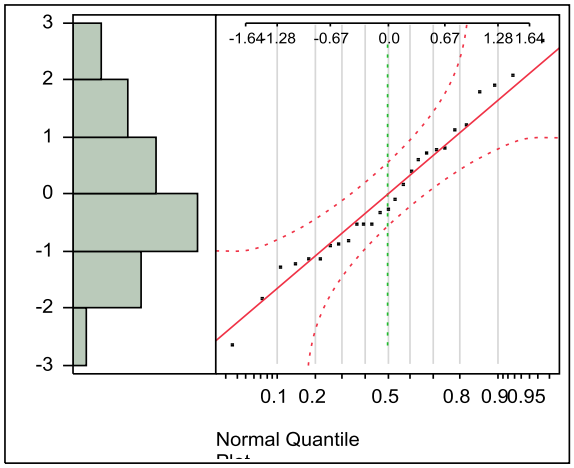

Figure 77. Raw Bio-oil TAN Normality Plot.

Table 60. Raw Bio-oil TAN Student t-Test Results

Level		Least Squares Mean
400	A	27.752
500	B	19.878
600	B	19.254

Levels not connected by the same letter are not significantly different.

A12. Bio-oil Distillate MC Statistical Analysis

Table 61. Bio-oil Distillate %MC ANOVA

Source	DF	Sum of Squares	Mean Square	F Ratio	Prob > F
Model	7	33.719	4.817	8.469	<.0001*
Error	31	17.630	0.568		
C. Total	38	51.350			

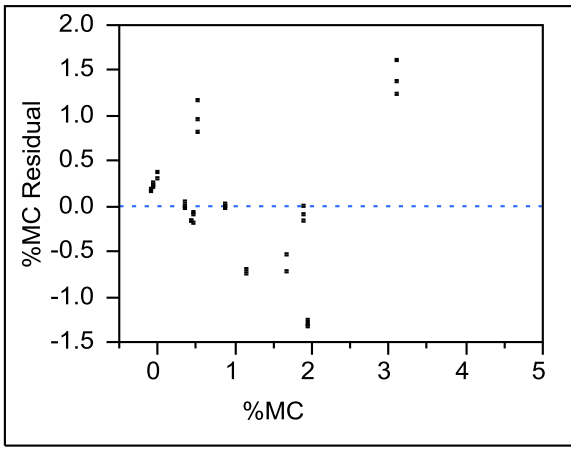

Figure 78.Bio-oil Distillate MC Variance Verification.

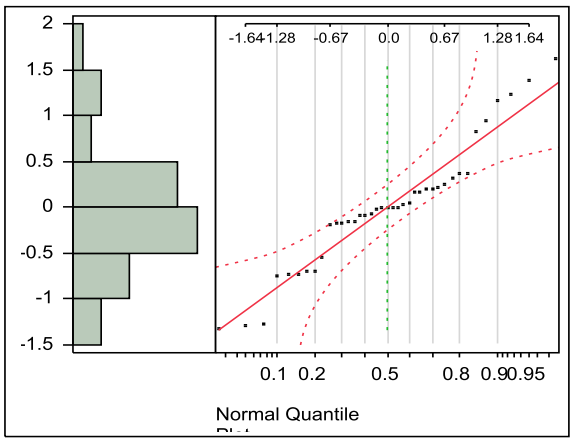

Figure 79. Bio-oil Distillate MC Normality Plot.

Table 62. Bio-oil Distillate %MC Student t-Test Results for Pyrolysis Temperature

Pyrolysis Temperature			
Level			**Least Squares Mean**
500	A		2.337
600		B	0.898
400		B	0.370
Among Bio-oil Distillates			
Level			**Least Squares Mean**
2	A		1.980
7	A	B	1.705
6	A	B	1.190
3		B	0.823
4		B	0.769
5		B	0.744

t-test results of bio-oil distillates blocked by pyrolysis temperature and distillate fraction. Levels not connected by the same letter are not significantly different.

A13. Bio-oil Distillate Density Statistical Analysis

Table 63. Bio-oil Distillate Density ANOVA

Source	DF	Sum of Squares	Mean Square	F Ratio	Prob > F
Model	7	0.231	0.033	4.590	0.0013*
Error	31	0.223	0.007		
C. Total	38	0.454			

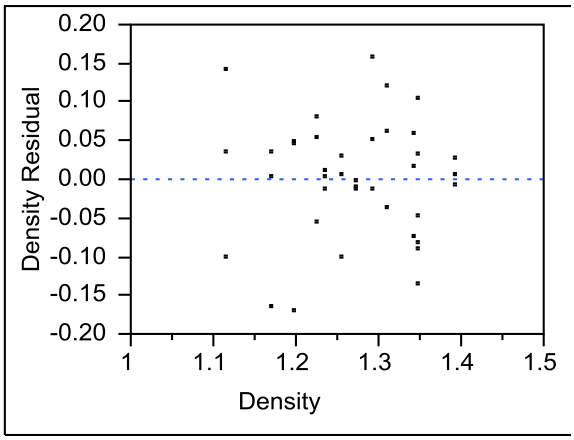

Figure 80. Bio-oil Distillate Density Normality Plot.

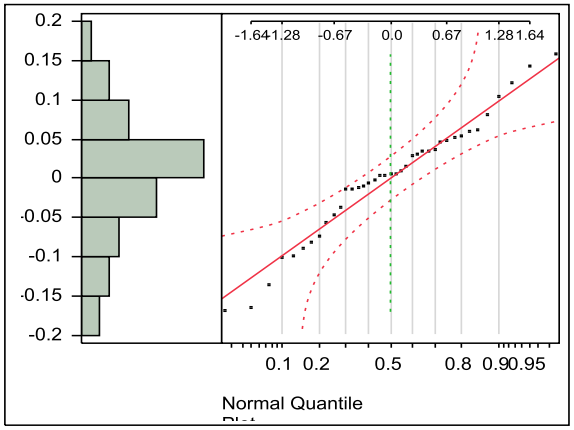

Figure 81. Bio-oil Distillate Density Normality Plot.

Table 64. Bio-oil Distillate Density Student t-Test Results

Pyrolysis Temperature

Level				Least Squares Mean
400	A			1.326
500	A			1.289
600		B		1.204

t-Test Results for MC Among Bio-oil Distillate MC

Level				Least Squares Mean
5	A			1.340
7	A	B	C	1.294
3	A	B		1.294
6	A	B	C	1.289
2		B	C	1.239
4			C	1.182

t-test results of bio-oil distillate mean density blocked by pyrolysis temperature and distillate fraction. Levels not connected by the same letter are not significantly different.

A14. Bio-oil Distillate TAN Statistical Analysis

Table 65. Bio-oil Distillate TAN ANOVA

Source	DF	Sum of Squares	Mean Square	F Ratio	Prob > F
Model	7	42.075	6.010	1.778	0.127
Error	31	104.752	3.379		
C. Total	38	146.828			

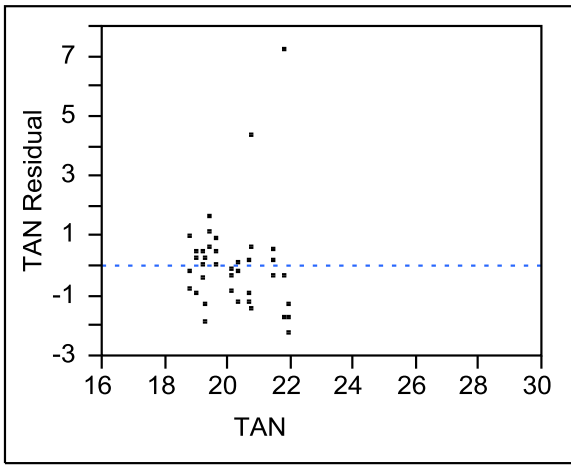

Figure 82. Bio-oil Distillate TAN Variance Verification.

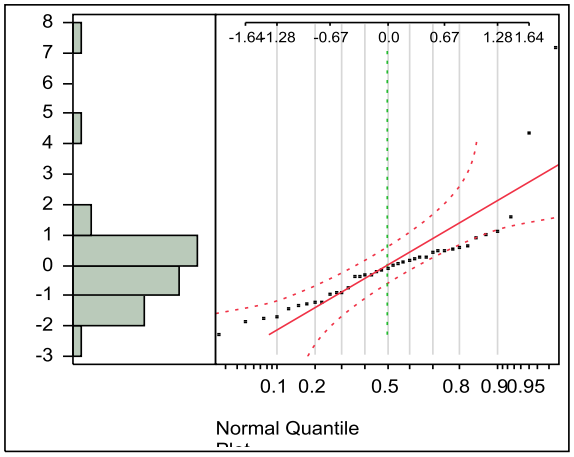

Figure 83. Bio-oil Distillate TAN Normality Plot.

Table 66. Bio-oil Distillate TAN Student t-Test Results

Pyrolysis Temperature			
Level			**Least Squares Mean**
400	A		20.054
500	A		19.931
600	A		19.597
Among Bio-oil Distillate			
Level			**Least Squares Mean**
3	A		21.756
4	A	B	20.601
5	A	B	19.935
2		B	19.247
6		B	19.020
7		B	18.606

Levels not connected by the same letter are significantly different.

A15. Bio-oil Distillate GCMS Statistical Analysis

Table 67. Bio-oil Distillate GCMS Results ANOVA

Bio-oil Distillate Paraffins ANOVA					
Source	DF	Sum of Squares	Mean Square	F Ratio	Prob > F
Model	7	1906.857	272.408	2.076	0.219
Error	5	655.984	131.197		
C. Total	12	2562.841			
Bio-oil Distillate Isoparaffins ANOVA					
Source	DF	Sum of Squares	Mean Square	F Ratio	Prob > F
Model	7	2208.485	315.498	0.983	0.526
Error	5	1603.366	320.673		
C. Total	12	3811.852			
Bio-oil Distillate Aromatics ANOVA					
Source	DF	Sum of Squares	Mean Square	F Ratio	Prob > F
Model	7	6.552	0.936	4.525	0.057
Error	5	1.034	0.206		
C. Total	12	7.586			
Bio-oil Distillate Naphthenics ANOVA					
Source	DF	Sum of Squares	Mean Square	F Ratio	Prob > F
Model	7	1.255	0.179	5.957	0.033*
Error	5	0.150	0.030		
C. Total	12	1.406			
Bio-oil Distillate Olefins ANOVA					
Source	DF	Sum of Squares	Mean Square	F Ratio	Prob > F
Model	7	0.444	0.063	1.416	0.362
Error	5	0.223	0.044		
C. Total	12	0.668			
Bio-oil Distillate Oxygenates ANOVA					
Source	DF	Sum of Squares	Mean Square	F Ratio	Prob > F
Model	7	2626.217	375.174	3.915	0.076
Error	5	479.140	95.828		
C. Total	12	3105.358			
Bio-oil Distillate Halogenates ANOVA					
Source	DF	Sum of Squares	Mean Square	F Ratio	Prob > F
Model	7	0.949	0.135	13.852	0.005*
Error	5	0.048	0.009		
C. Total	12	0.997			

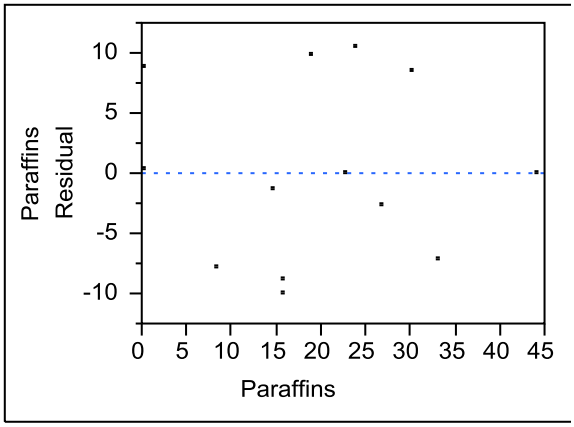

Figure 84. Bio-oil Distillate Paraffin Variance Verification.

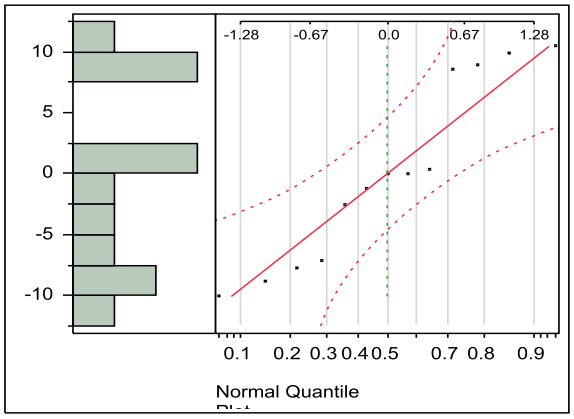

Figure 85. Bio-oil Distillate Paraffin Normality Plot.

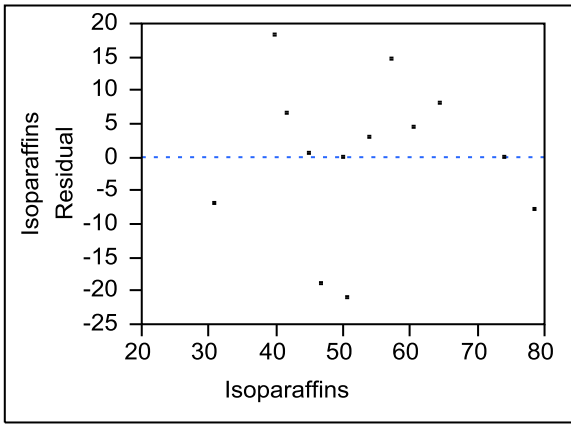

Figure 86. Bio-oil Distillate Isoparaffin Variance Verification.

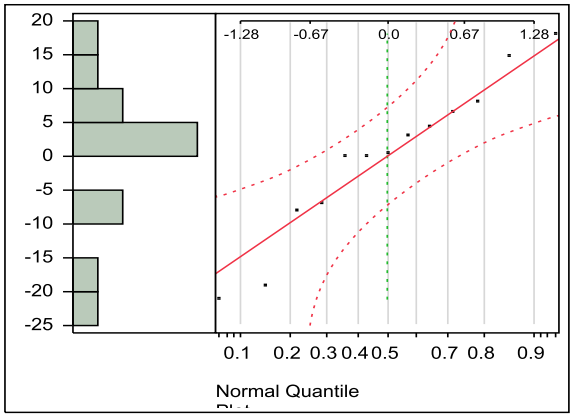

Figure 87. Bio-oil Distillate Isoparaffin Normality Plot.

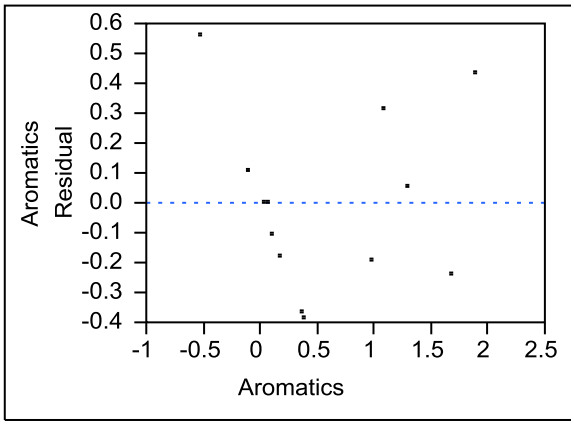

Figure 88. Bio-oil Distillate Aromatic Variance Verification.

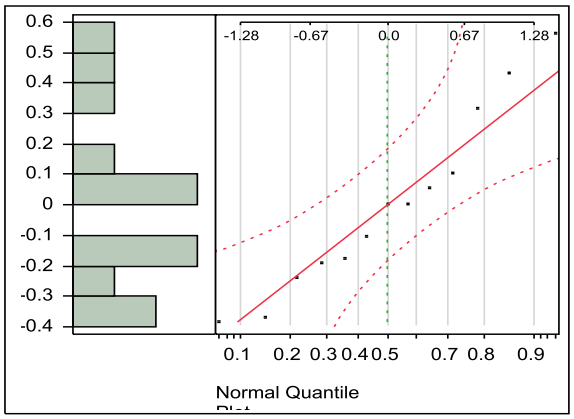

Figure 89. Bio-oil Distillate Aromatic Normality Plot.

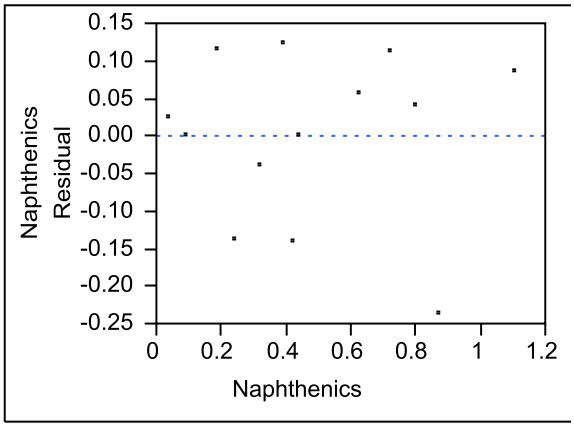

Figure 90. Bio-oil Distillate Naphthenic Variance Verification.

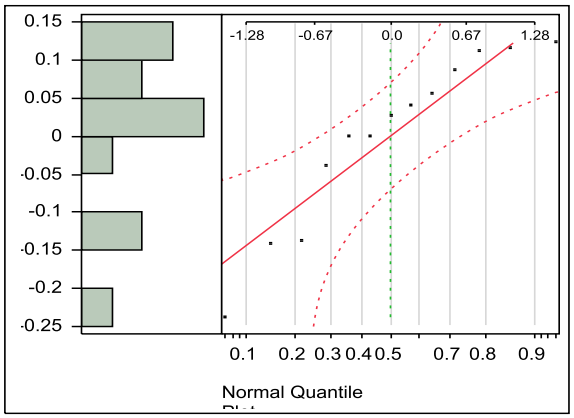

Figure 91. Bio-oil Distillate Naphthenic Normality Plot.

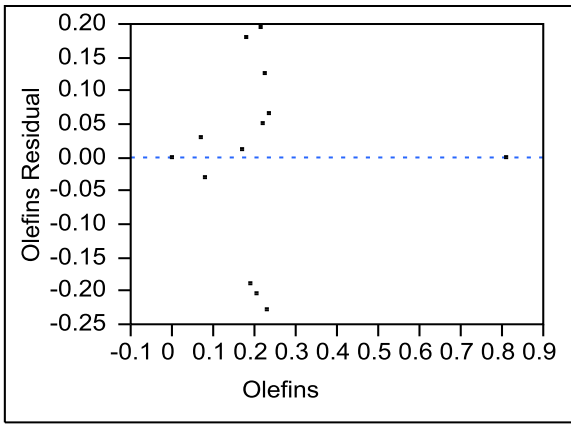

Figure 92. Bio-oil Distillate Olefin Variance Verification.

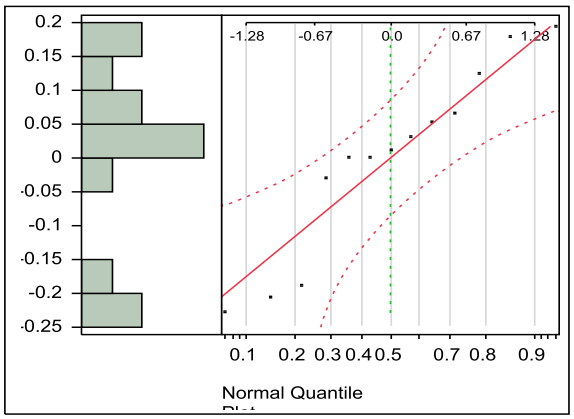

Figure 93. Bio-oil Distillate Olefin Normality Plot.

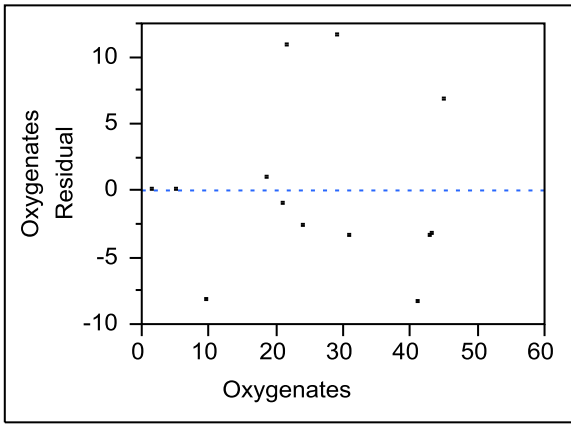

Figure 94. Bio-oil Distillate Oxygenate Variance Vereification.

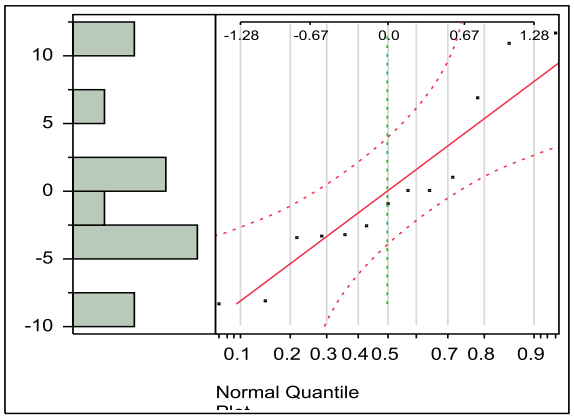

Figure 95. Bio-oil Distillate Oxygenate Normality Plot.

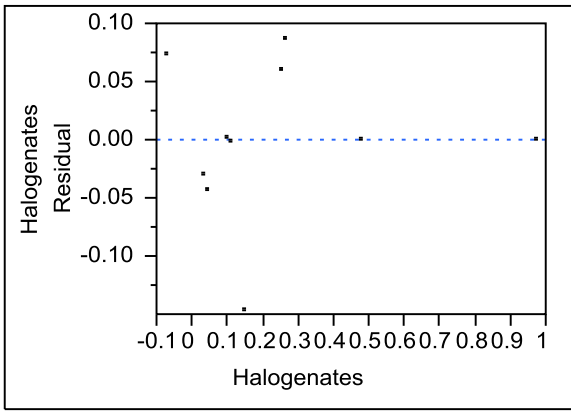

Figure 96. Bio-oil Distillate Halogenate Variance Verification.

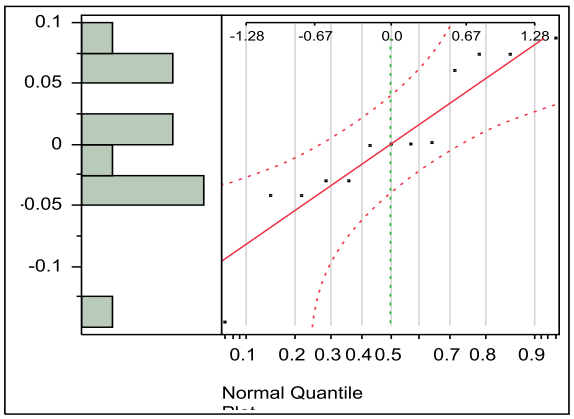

Figure 97. Bio-oil Distillate Halogenate Normality Plot.

Table 68. t-Test Results for Bio-oil Distillate Naphthenics Analysis

Naphthenics Pyrolysis Temperature			
Level			**Least Squares Mean**
600	A		0.830
400		B	0.350
500		B	0.146

Levels not connected by the same level are not significantly different.

Table 69. t-Test Results for Bio-oil Distillate PIANO, Oxygenate and Halogenate Among Distillate Fractions

Paraffins Analysis					
Level					**Least Squares Mean**
6	A				55.568
7	A	B			33.978
4	A	B			25.953
3	A	B			19.640
2		B			11.653
5		B			11.668

Aromatics Analysis					
Level					**Least Squares Mean**
2	A				1.513
3	A	B			0.910
4		B	C		0.010
7		B	C		-0.096
6		B	C		-0.136
5			C		-0.270

Naphthenics Analysis					
Level					**Least Squares Mean**
2	A				0.716
6	A	B			0.532
3	A	B			0.480
5	A	B			0.412
4		B			0.330
7	A	B			0.182

Olefins Analysis					
Level					**Least Squares Mean**
7	A				0.791
3	A	B			0.216
4	A	B			0.210
2	A	B			0.196
5		B			0.061
6		B			-0.018

Oxygenate Analysis					
Level					**Least Squares Mean**
3	A				39.626
2	A	B			37.856
4		B	C		18.440
5		B	C		15.431
6			C		-0.498
7			C		-4.058

Halogenate Analysis					
Level					**Least Squares Mean**
7	A				0.927
6		B			0.437
4		B	C		0.220
5			C	D	0.068
3				D	1.110e-16
2				D	5.551e-17

Levels not connected by the same letter are significantly different.

A16. Catalyst Deoxygenation Statistical Analysis

Table 70. Catalyst Deoxygenation/Hydrogenation Capability ANOVA

Source	DF	Sum of Squares	Mean Square	F Ratio	Prob > F
Model	2	7294.839	3647.420	87.614	<.0001*
Error	6	249.781	41.630		
C. Total	8	7544.621			

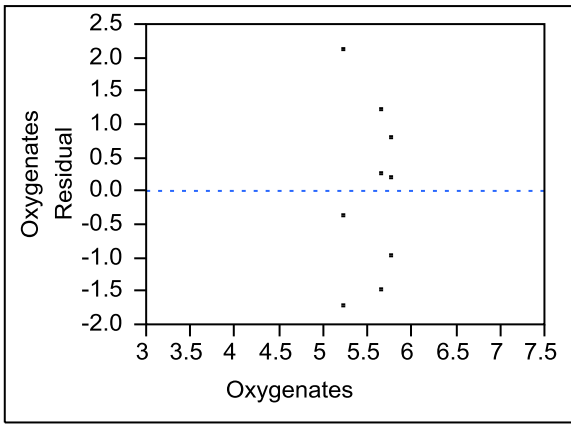

Figure 98. Hydrogenated Product Oxygenate Variance Vereification.

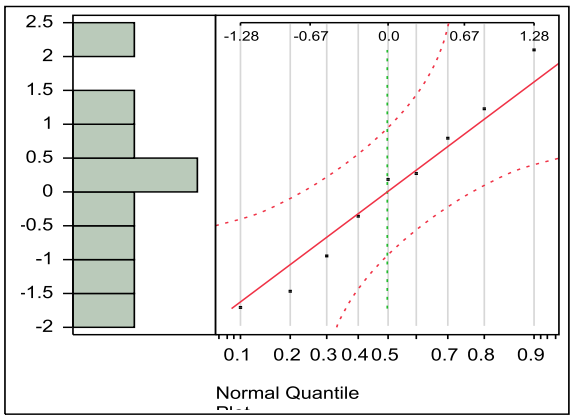

Figure 99. Hydrogenated Product Oxygenate Normality Plot.

A17. Hydrogenated Product Statistical Analysis

Table 71. Hydrogenated Product PIANO Results ANOVA

Hydrogenated Product Paraffins ANOVA					
Source	**DF**	**Sum of Squares**	**Mean Square**	**F Ratio**	**Prob > F**
Model	2	132.239	66.119	4.083	0.076
Error	6	97.149	16.191		
C. Total	8	229.389			
Hydrogenated Product Isoparaffins ANOVA					
Source	DF	Sum of Squares	Mean Square	F Ratio	Prob > F
Model	2	98.702	49.351	7.327	0.024*
Error	6	40.408	6.734		
C. Total	8	139.110			
Hydrogenated Product Aromatics ANOVA					
Source	DF	Sum of Squares	Mean Square	F Ratio	Prob > F
Model	2	1937.738	968.869	23.678	0.001*
Error	6	245.505	40.918		
C. Total	8	2183.244			
Hydrogenated Product Naphthenics ANOVA					
Source	DF	Sum of Squares	Mean Square	F Ratio	Prob > F
Model	2	4471.088	2235.540	15.060	0.004*
Error	6	890.646	148.440		
C. Total	8	5361.735			
Hydrogenated Product Olefins ANOVA					
Source	DF	Sum of Squares	Mean Square	F Ratio	Prob > F
Model	2	7294.839	3647.420	87.614	<.0001*
Error	6	249.781	41.630		
C. Total	8	7544.621			

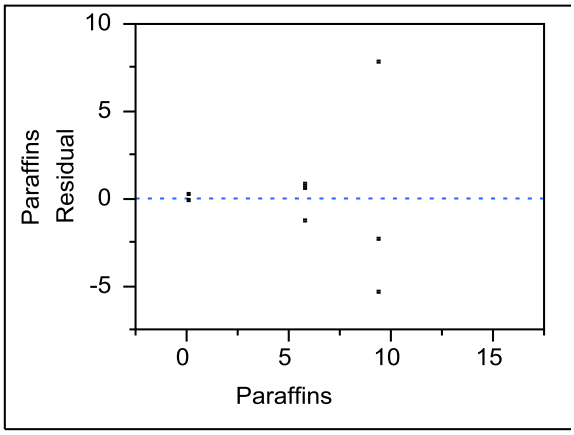

Figure 100. Hydrogenated Product Paraffin Variance Verification.

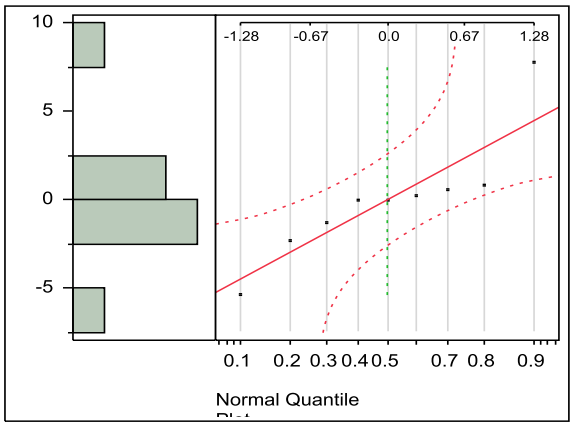

Figure 102. Hydrogenated Product Paraffin Normality Plot.

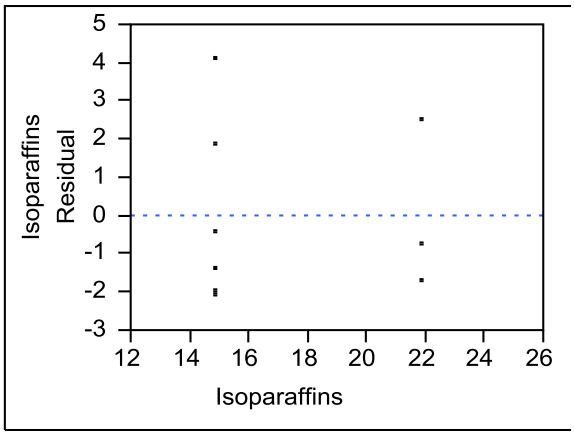

Figure 101. Hydrogenated Product Isoparaffin Variance Verification.

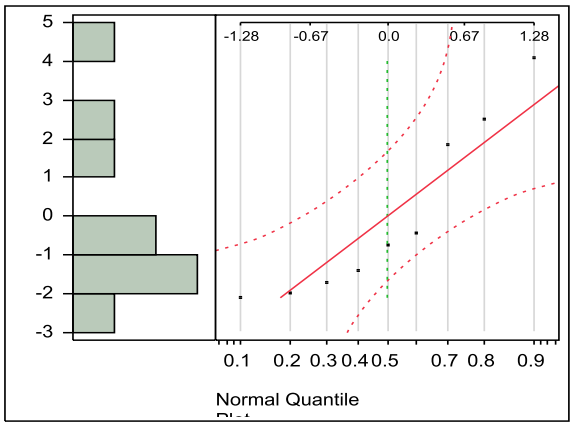

Figure 103. Hydrogenated Product Isoparaffin Normality Plot.

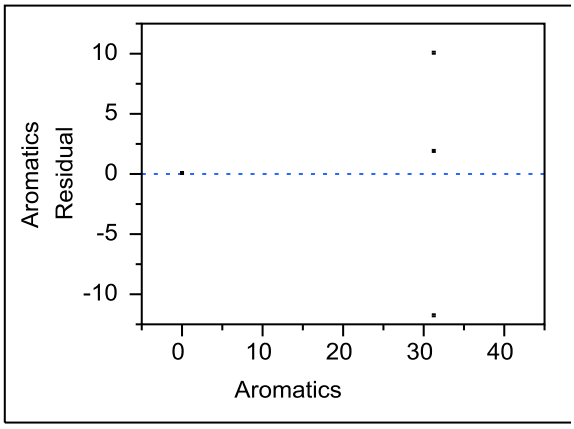

Figure 104. Hydrogenated Product Aromatic Variance Verification.

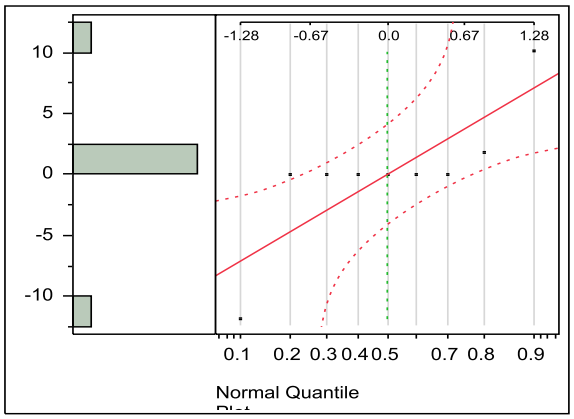

Figure 105. Hydrogenated Product Aromatic Normality Plot.

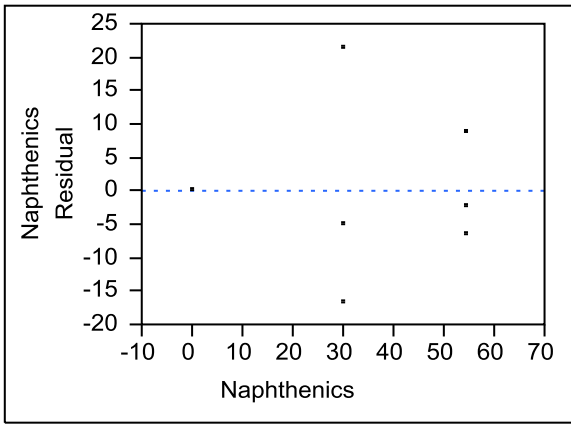

Figure 106. Hydrogenated Product Naphthenic Variance Verification.

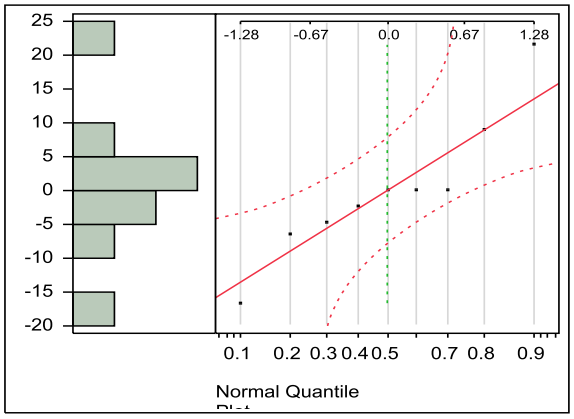

Figure 107. Hydrogenated Product Naphthenic Normality Plot.

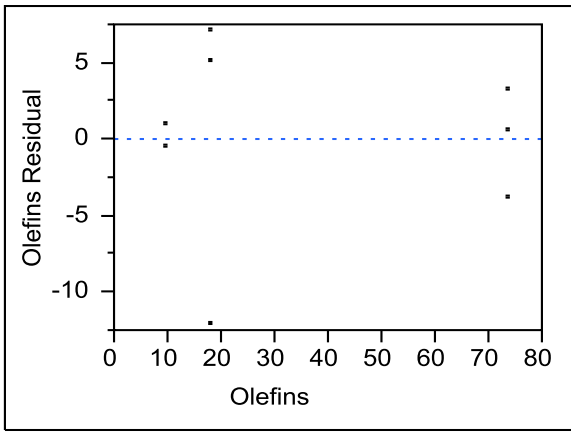

Figure 108. Hydrogenated Product Olefin Variance Verification.

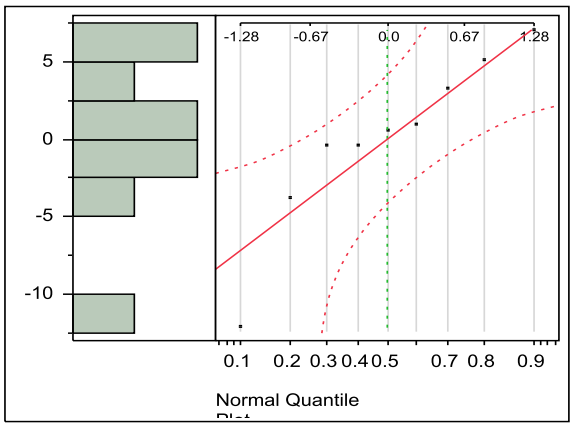

Figure 109. Hydrogenated Product Olefin Normality Plot.

Table 72. t-Test Results for Model Mixture Hydrogenation Products

Paraffins			
Level			**Least Squares Mean**
Pd/C	A		9.403
Shvo's	A	B	5.826
Fluorous Pd		B	0.096
Isoparaffins			
Level			**Least Squares Mean**
Fluorous Pd	A		21.900
Pd/C		B	14.890
Shvo's		B	14.860
Aromatics			
Level			Least Squares Mean
Pd/C	A		31.126
Shvo's		B	0.000
Fluorous Pd		B	-1.776e-15
Naphthenics			
Level			**Least Squares Mean**
Pd/C	A		54.516
Shvo's		B	29.806
Fluorous Pd		B	3.552e-15
Olefins			
Level			**Least Squares Mean**
Pd/C	A		73.653
Shvo's		B	17.826
Fluorous Pd		B	9.546

Levels not connected by the same letter are significantly different.

A18. Raw Bio-oil and Distillate TAN Statistical Analysis

Table 73. TAN ANOVA for Raw Bio-oil and Bio-oil Distilled Fractions

Source	DF	Sum of Squares	Mean Square	F Ratio	Prob > F
Model	15	503.816	33.587	15.346	<.0001*
Error	50	109.433	2.188		
C. Total	65	613.250			

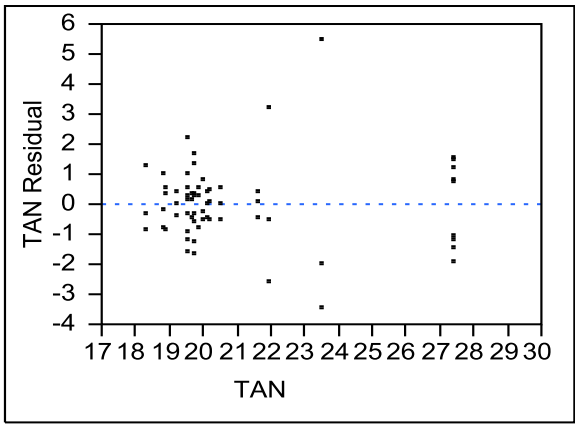

Figure 110. Raw Bio-oil and Bio-oil Distillate Combined TAN Variance Verification.

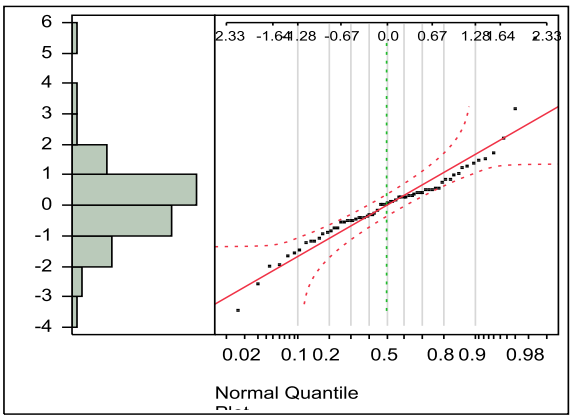

Figure 111. Raw Bio-oil and Bio-oil Distillate Combined TAN Normality Plot.

Table 74. t-Test Results of the TAN Data Analyzed According To Distillate Fraction

Level				Least Squares Mean
0	A			22.221
3	A	B		21.756
4		B	C	20.601
5	A	B	C	.
6	A	B	C	.
7	A	B	C	.
2			C	19.247

Levels not connected by the same letter are significantly different. Level 0 represents the raw bio-oil. There is no level 1 because it was determined that the first distillate fraction was the water fraction and therefor was not analyzed.

Table 75. t-Test Results of the TAN Data Analyzed According To Distillate Fraction and Pyrolysis Temperature

Level						Least Squares Mean
400,0	A					27.418
500,3		B				23.513
400,4		B	C			21.950
600,3		B	C	D		21.583
400,2			C	D	E	20.523
400,3			C	D	E	20.173
600,5			C	D	E	20.133
600,6	A	B	C	D	E	.
600,7	A	B	C	D	E	.
500,4			C	D	E	19.976
500,5	A	B	C	D	E	.
500,6	A	B	C	D	E	.
500,7	A	B	C	D	E	.
600,4			C	D	E	19.876
600,0				D	E	19.698
400,5			C	D	E	19.667
500,0					E	19.545
400,6				D	E	19.213
600,2					E	18.893
400,7					E	18.800
500,2					E	18.326

Levels not connected by the same letter are significantly different. Level 0 represents the raw bio-oil. There is no level 1 because it was determined that the first distillate fraction was the water fraction and therefor was not analyzed.

A19. Raw Bio-oil and Distillate MC Statistical Analysis

Table 76. MC ANOVA for Raw Bio-oil and Bio-oil Distilled Fractions

Source	DF	Sum of Squares	Mean Square	F Ratio	Prob > F
Model	15	6334.7575	422.317	531.7904	<.0001*
Error	50	39.7071	0.794		
C. Total	65	6374.4646			

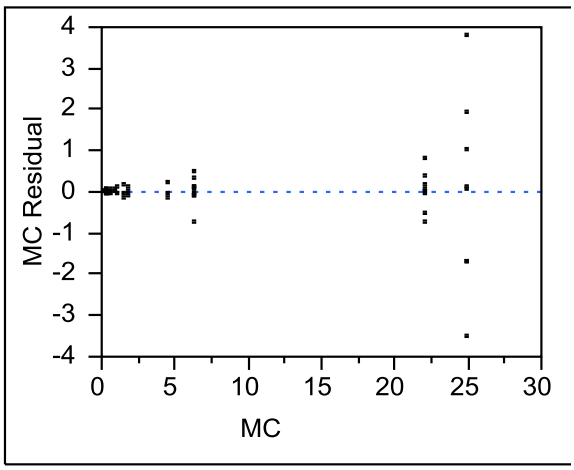

Figure 112. Raw Bio-oil and Bio-oil Distillate Combined MC Variaance Verification.

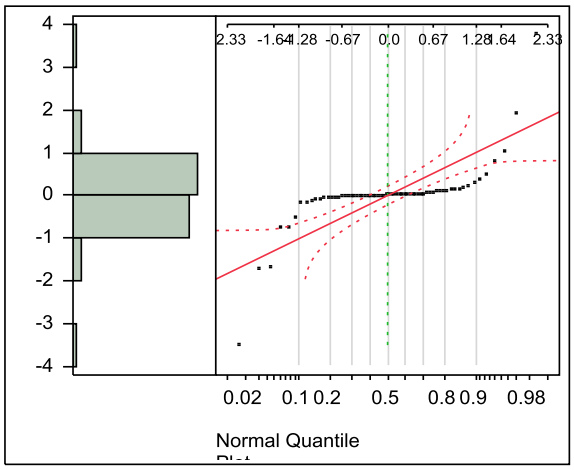

Figure 113. Raw Bio-oil and Bio-oil Distillate Combined MC Normality Plot.

Table 77. Transformed MC ANOVA for Raw Bio-oil and Bio-oil Distilled Fractions

Source	DF	Sum of Squares	Mean Square	F Ratio	Prob > F
Model	15	1129.901	75.326	2372.128	<.0001*
Error	50	1.587	0.031		
C. Total	65	1131.489			

The results of the statistical analysis of the transformed MC data suggests that there is evidence to reject H_0 and suggest that distillation does affect the MC of the raw bio-oil.

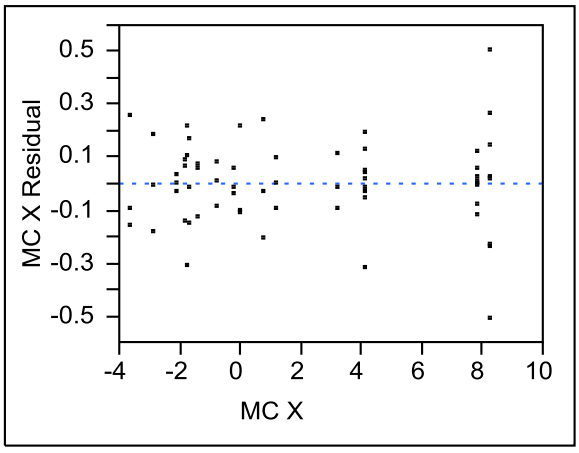

Figure 114. Raw Bio-oil and Bio-oil Distillate Combined Transformed MC Normality Plot.

Table 78. t-Test Results of the MC Data Analyzed According To Distillate Fraction

Level					Least Squares Mean
0	A				6.713
2		B			0.590
3			C		-0.604
4				D	-1.160
5	A	B	C	D	.
6	A	B	C	D	.
7	A	B	C	D	.

Levels not connected by the same letter are significantly different. Level 0 represents the raw bio-oil. There is no level 1 because it was determined that the first distillate fraction was the water fraction and therefor was not analyzed.

Table 79. t-Test Results of the TAN Data Analyzed According To Distillate Fraction and Pyrolysis Temperature

Level														Least Squares Mean
500,0	A													8.235
600,0		B												7.818
400,0			C											4.086
500,2				D										3.215
500,4					E									1.151
500,5	A	B	C	D	E	F	G	H	I	J	K	L	M	.
500,6	A	B	C	D	E	F	G	H	I	J	K	L	M	.
500,7	A	B	C	D	E	F	G	H	I	J	K	L	M	.
600,3						F								0.745
600,2							G							0.0008
400,7							G							-0.243
500,3								H						-0.746
400,2									I					-1.443
400,6									I	J				-1.697
600,4										J				-1.777
400,3										J	K			-1.813
600,5											K			-2.099
600,6	A	B	C	D	E	F	G	H	I	J	K	L	M	.
600,7	A	B	C	D	E	F	G	H	I	J	K	L	M	.
400,4												L		-2.855
400,5													M	-3.615

Levels not connected by the same letter are significantly different. Level 0 represents the raw bio-oil. There is no level 1 because it was determined that the first distillate fraction was the water fraction and therefor was not analyzed.

APPENDIX B

GCMS ANALYSIS DATA FOR ALL BIO-OIL DISTILLATES

B1. 400°C Bio-oil Distillate Data Analysis

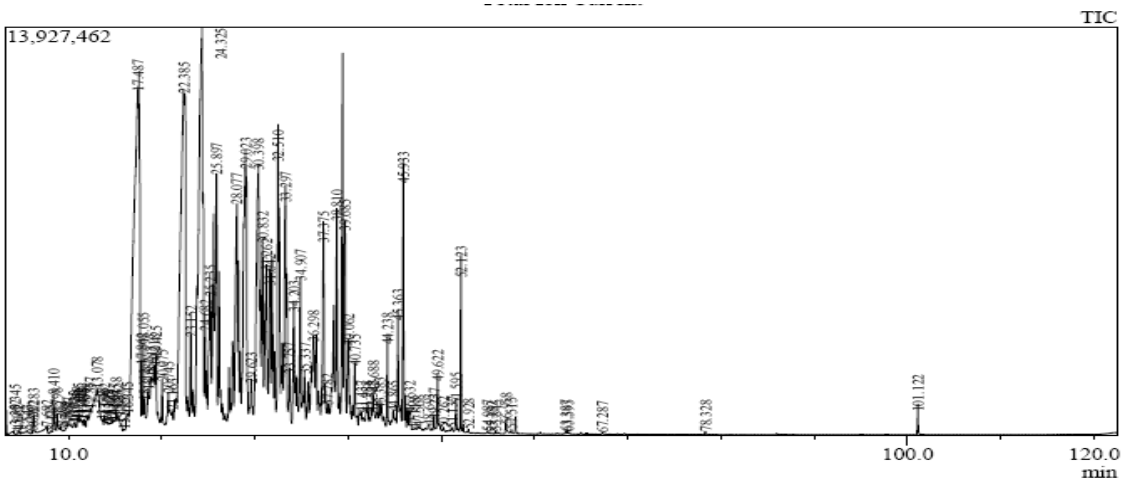

Figure 115. 400°C Bio-oil Distillate #2 GCMS Chromatogram and Spectrum Process Data

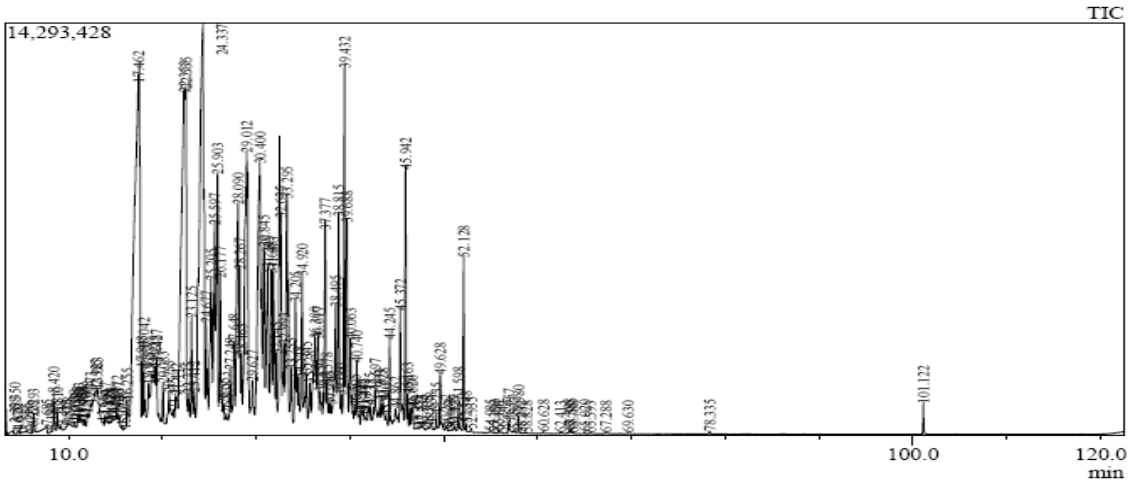

Figure 116. 400°C Bio-oil Distillate #3 GCMS Chromatogram and Spectrum Process Data .

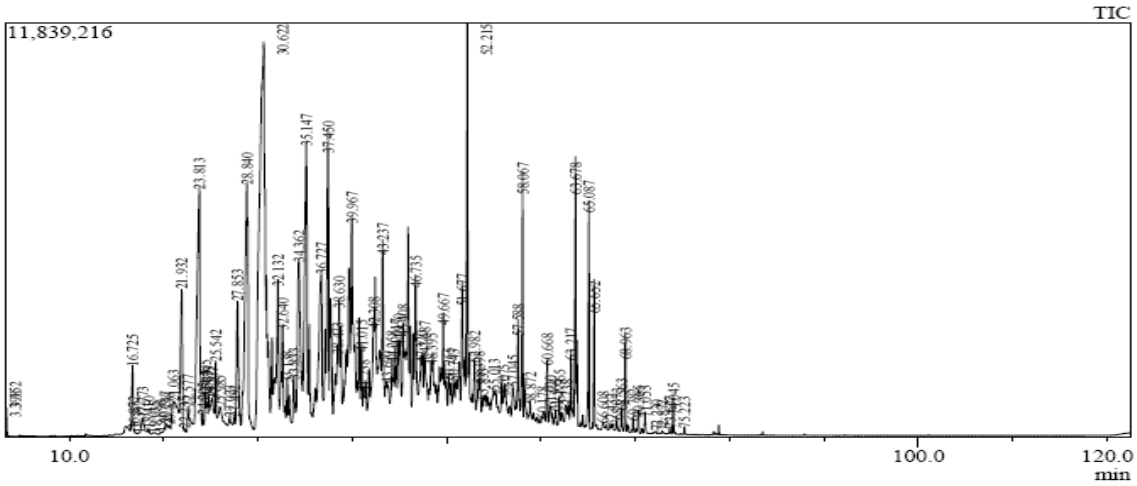

Figure 117. 400°C Bio-oil Distillate #3 GCMS Chromatogram and Spectrum Process Data.

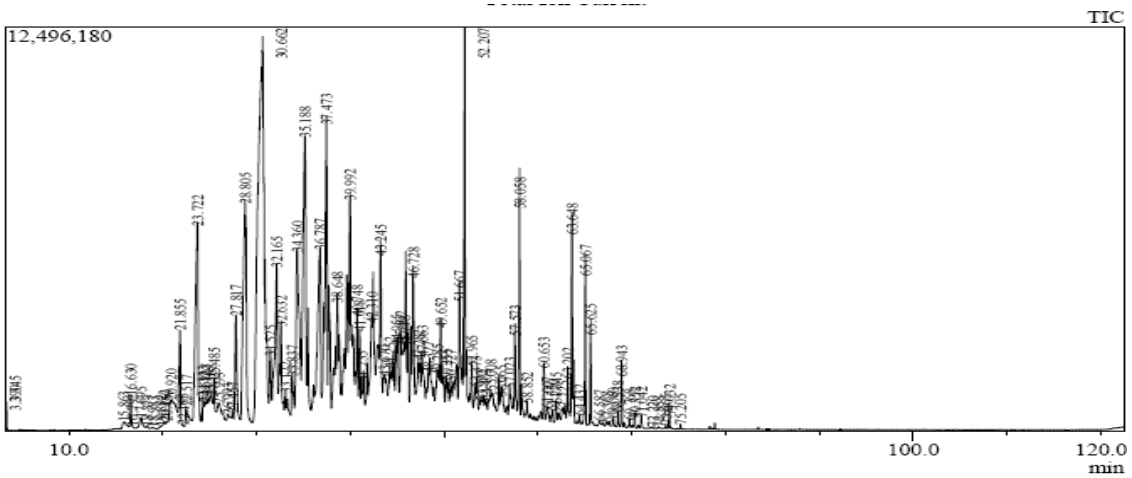

Figure 118. 400°C Bio-oil Distillate #4 GCMS Chromatogram and Spectrum Process Data .

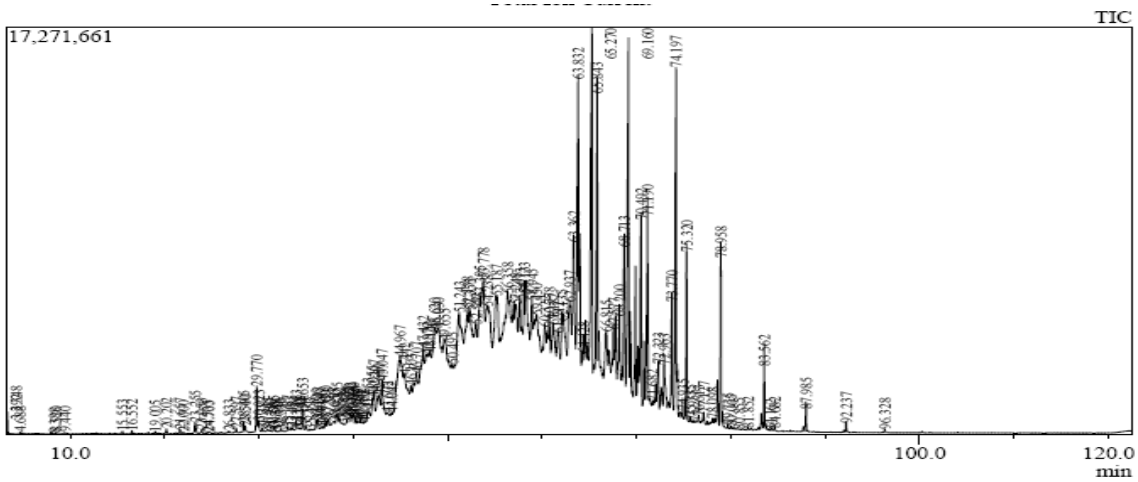

Figure 119. 400°C Bio-oil Distillate #6 GCMS Chromatogram and Spectrum Process Data.

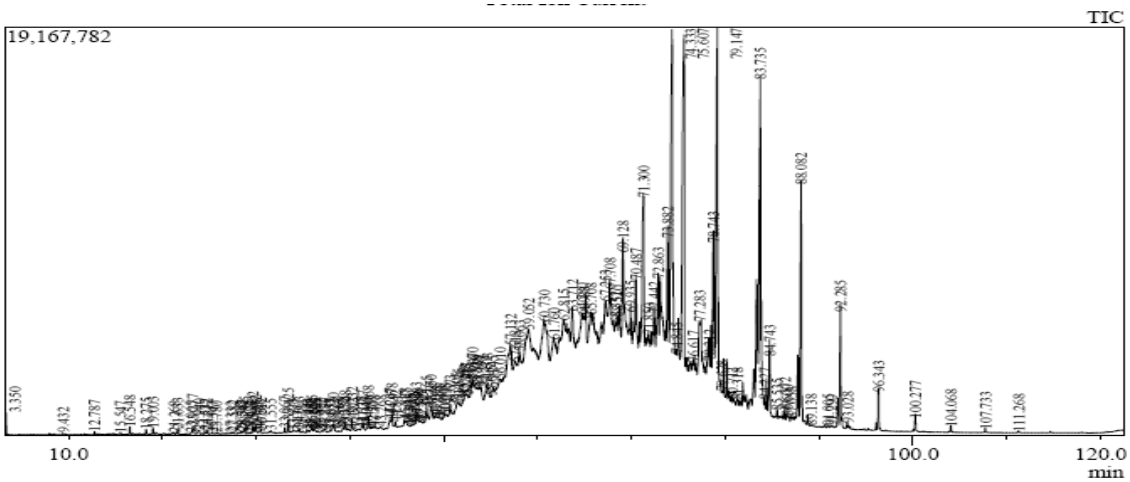

Figure 120. 400°C Bio-oil Distillate #7 GCMS Chromatogram and Spectrum Process Data.

Table 80. Spectrum Process Table For 400°C Distillates #2, 3, and 4

Distillate #2 400°C		Distillate #3 400°C		Distillate #4 400°C	
Retention Time	**Compound Name**	**Retention Time**	**Compound Name**	**Retention Time**	**Compound Name**
3.305	Cyclohexene	3.35	Cyclohexene	3.352	Cyclohexene
3.378	Cyclohexene	3.398	Cyclohexene	3.398	Cyclohexene
4.555	1-Butanol, 3-methyl-	4.605	1-Butanol, 3-methyl-	16.725	Phenol
4.625	3-Penten-2-one, (E)-	4.67	3-Penten-2-one, (E)-	16.872	3-Pentenoic acid, 4-methyl-
5.482	1-Butanol, 3-methyl-	5.555	1-Butanol, 3-methyl-	17.773	2-Cyclopenten-1-one, 2,3-dimethyl-
6.012	3-Hexanone	6.073	3-Hexanone	21.063	2-Cyclopenten-1-one, 2,3-dimethyl-
6.158	2-Hexanone	6.228	2-Hexanone	21.932	Phenol, 2-methyl-
6.235	Cyclopentanone	6.293	Cyclopentanone	22.235	Cycloheptanone, 4-methyl-, (R)-
7.602	Hexanoic acid	7.685	Hexanoic acid	22.577	Acetophenone
8.098	2-Pentanone, 3-methylene-	8.188	2-Pentanone, 3-methylene-	23.813	Phenol, 2-methyl-
8.312	Cyclopentanone, 2-methyl-	8.42	Cyclopentanone, 2-methyl-	24.205	3-Acetyl-2,5-dimethyl furan
8.715	Cyclopentanone, 3-methyl-	8.81	Cyclopentanone, 3-methyl-	24.405	1-Methylcyclooctene
9.132	2-Hexanone, 5-methyl-	9.218	2-Hexanone, 5-methyl-	24.773	2-Nonanone
9.915	4-Heptanone	9.998	Vinyl butyrate	25.542	Phenol, 2,6-dimethyl-
10.518	Cyclopentanone, 2,5-dimethyl-	10.752	3-Heptanone	25.985	Cyclohexane, (1-methylethylidene)-
10.685	3-Heptanone	10.993	2-Heptanone	27.492	Ethanone, 1-(3-methylphenyl)-
10.892	2-Heptanone	11.133	Cyclopentanone, 2,4-dimethyl-	27.853	Phenol, 2-ethyl-
11.255	Cyclopentanone, 2,3-dimethyl-	11.333	Cyclopentanone, 2,3-dimethyl-	28.84	Phenol, 2,6-dimethyl-
11.388	Cyclopentanone, 2,4-dimethyl-	11.458	Cyclopentanone, 2,4-dimethyl-	30.622	Phenol, 3-ethyl-
11.612	2-Cyclopenten-1-one, 2-methyl-	11.708	2-Cyclopenten-1-one, 2-methyl-	32.132	Phenol, 2,3-dimethyl-
11.878	Ethanone, 1-(2-furanyl)-	12.008	Ethanone, 1-(2-furanyl)-	32.64	Phenol, 2,4,6-trimethyl-
12.102	Benzene, methoxy-	13.917	Cyclopentanone, 2-ethyl-	33.138	Benzofuran, 4,7-dimethyl-
12.435	2-Cyclopenten-1-one, 2-methyl-	14.665	Benzene, propyl-	33.833	Phenol, 2-propyl-
13.795	Cyclopentanone, 2-ethyl-	15.728	Benzene, 1,2,4-trimethyl-	34.362	Phenol, 4-(1-methylethyl)-
14.315	Cycloheptanone	17.462	Phenol	35.147	Phenol, 2-ethyl-5-methyl-
14.555	Benzene, propyl-	17.843	3-Octanone	36.727	Phenol, 2-ethyl-4-methyl-

Table 80 Continued

Distillate #2 400°C		Distillate #3 400°C		Distillate #4 400°C	
Retention Time	**Compound Name**	**Retention Time**	**Compound Name**	**Retention Time**	**Compound Name**
15.008	1,3,5-Cycloheptatriene, 7,7-dimethyl-	18.042	2-Octanone	37.45	Phenol, 4-ethyl-2-methoxy-
15.275	Benzene, 1,2,3-trimethyl-	19.228	Benzene, 1,2,3-trimethyl-	38.473	Naphthalene, 1-methyl-
15.635	Benzene, 1,2,4-trimethyl-	19.427	Benzene, 1-methoxy-4-methyl-	38.63	Phenol, 2-ethyl-4,5-dimethyl-
16.062	Cyclopropene, 1-butyl-2-ethyl-	20.083	Indane	39.32	3-Tetradecene, (Z)-
16.502	Phenol	21.175	Benzene, 1,4-diethyl-	45.372	Pentadecane
17.835	3-Octanone	22.535	Phenol, 2-methyl-	45.408	1-Tridecene
17.856	Nonane, 4-ethyl-5-methyl-	22.775	4H-Cyclopentacyclooctene,	46.746	Pentadecane
17.915	2-Octanone	23.125	Acetophenone	46.756	Benzene, nonyl-
19.115	Benzene, 1,2,3-trimethyl-	24.337	Phenol, 2-methyl-	48.652	9-Octadecene, (E)-
19.328	Benzene, 1-methoxy-4-methyl-	25.597	Benzofuran, 2-methyl-	49.648	Hexadecane
19.835	Indane	25.903	Phenol, 2,6-dimethyl-	49.667	7-Hexadecene, (Z)-
20.956	Octane, 2,3-dimethyl-	26.177	Phenol, 2-ethyl-5-methyl-	50.455	Pentadecane, 2,6,10-trimethyl-
21.062	Benzene, 1,4-diethyl-	27.248	Octanoic acid, methyl ester	51.227	5-Octadecene, (E)-
21.275	Phenol, 2-methyl-	27.648	1H-Indene, 2,3-dihydro-4-methyl-	51.677	Nonadecane
22.531	Benzene, propyl-	28.09	Phenol, 2-ethyl-	52.204	9-Octadecene, (E)-
23.008	Acetophenone	28.267	Benzene, 2-ethenyl-1,4-dimethyl-	52.204	Hexadecane
23.595	Phenol, 3-methyl-	28.463	1,3-Cyclopentadiene, 1,2,3,4-tetramethyl-5-methylene-	52.215	1-Dodecanol, 3,7,11-trimethyl-
25.293	Nonane, 3-methyl-	29.012	Phenol, 2,6-dimethyl-	52.409	1-Nonanol, 4,8-dimethyl-
25.408	Phenol, 2,6-dimethyl-	29.627	Benzene, 1-methyl-4-(2-methylpropyl)-	54.53	7-Heptadecene, 1-chloro-
26.839	Cyclopentane, 1-methyl-3-(2-methylpropyl)-	30.4	Phenol, 4-ethyl-	55.399	1-Decanol, 2-hexyl-
26.952	Cyclohexane, 1,2-dimethyl-, cis-	31.265	Phenol, 2-ethyl-6-methyl-	55.399	9-Octadecene, (E)-
27.008	Phenol, 2-ethyl-	32.993	Benzofuran, 4,7-dimethyl-	55.867	Hexadecane
28.608	Phenol, 2,6-dimethyl-	34.92	Phenol, 2-ethyl-5-methyl-	56.075	5-Octadecene, (E)-

Table 80 Continued

Distillate #2 400°C		Distillate #3 400°C		Distillate #4 400°C	
Retention Time	**Compound Name**	**Retention Time**	**Compound Name**	**Retention Time**	**Compound Name**
29.355	Benzene, (1-methylbutyl)-	35.345	1H-Indene, 2,3-dihydro-1,2-dimethyl-	57.146	2-Hexadecene, 3,7,11,15-tetramethyl-, [R-[R*,R*-(E)]]-
29.888	Phenol, 4-ethyl-	37.783	Ethanone, 1-[4-(1-methylethenyl)phenyl]-	57.588	2-Hexadecene, 3,7,11,15-tetramethyl-, [R-[R*,R*-(E)]]-
31.008	Phenol, 2-ethyl-6-methyl-	38.815	1-Undecene	58.055	Cyclopropane, tetramethylpropylidene-
32.485	1-Octanol, 2-butyl-	39.432	Pentadecane	58.067	9-Octadecene, (E)-
32.823	E-11-Tetradecen-1-ol trifluoroacetate	40.063	1H-Inden-1-one, 2,3-dihydro-3,3-dimethyl-	58.848	Eicosane
33.323	Nonane, 3,7-dimethyl-	40.505	Benzene, 4-(2-butenyl)-1,2-dimethyl-, (E)-	58.851	Pentadecanoic acid, 14-methyl-, methyl ester
34.688	Phenol, 2-ethyl-5-methyl-	42.697	1-Octanol, 2,7-dimethyl-	58.872	C11
35.062	1H-Indene, 2,3-dihydro-1,2-dimethyl-	43.203	Benzene, heptyl-	60.668	Decane, 2,3,6-trimethyl-
35.574	Decane, 2-methyl-	44.245	Dodecane, 2,7,10-trimethyl-	61.02	1-Decene, 3,4-dimethyl-
36.451	Decane, 3-methyl-	45.372	3-Tetradecene, (Z)-	61.561	6,10,13-Trimethyltetradecanol
37.929	4-Decene, 3-methyl-, (E)-	45.942	Pentadecane	61.565	Undecane, 3,7-dimethyl-
38.102	1-Undecene	46.163	5-Tetradecene, (E)-	63.217	Octadecanoic acid, 2-oxo-, methyl ester
38.346	Cyclohexane, pentyl-	48.638	Octane, 2-cyclohexyl-	63.652	Hexadecane, 1-chloro-
39.024	C11	49.235	Heptadecane, 2,6,10,15-tetramethyl-	63.678	Heptane, 3-(bromomethyl)-
40.002	Undecane, 6-methyl-	49.628	Pentadecane	65.07	Undecane, 2,10-dimethyl-
40.31	Undecane, 5-methyl-	50.257	Oxirane, [(dodecyloxy)methyl]-	65.087	Dodecane, 3-methyl-
41.672	n-Amylcyclohexane	50.908	1-Nonanol, 4,8-dimethyl-	65.652	Octane, 2,3,7-trimethyl-
42.582	1-Octanol, 2,7-dimethyl-	51.127	3-Tetradecene, (Z)-	65.889	C13
44.075	Dodecane, 2,7,10-trimethyl-	51.598	3-Hexadecene, (Z)-	65.894	Tridecane, 6-methyl-
45.004	Benzene, 1-methyl-4-(1-methylpropyl)-	52.128	Pentadecane	66.608	Dodecane, 2,5-dimethyl-
45.035	3-Tetradecene, (Z)-	52.348	7-Hexadecene, (Z)-	67.361	Octadecane, 2-methyl-
45.115	Undecane, 3-methyl-	52.935	7-Hexadecene, (Z)-	68.073	Cyclopentane, hexyl-

Table 80 Continued

Distillate #2 400°C		Distillate #3 400°C		Distillate #4 400°C	
Retention Time	**Compound Name**	**Retention Time**	**Compound Name**	**Retention Time**	**Compound Name**
45.348	Decane, 2,3,6-trimethyl-	54.985	Cyclohexane, (2-methylpropyl)-	68.563	Tridecane, 6-methyl-
45.728	Pentadecane	55.842	Hexadecane	68.945	Tridecane, 4-methyl-
46.705	1-Decene, 3,4-dimethyl-	56.242	Tetradecane, 3-methyl-	68.963	Hexadecane
46.707	6,10,13-Trimethyltetradecanol	56.957	Diethyl Phthalate	69.782	C14
47.968	Cyclopentane, hexyl-	57.527	3-Hexadecene, (Z)-	70.365	Oxalic acid, isobutyl hexadecyl ester
48.928	Dodecane	57.98	Tetradecane	71.021	Hexadecane
49.408	Pentadecane	58.232	n-Tridecan-1-ol	71.021	Tetradecane, 3-methyl-
49.605	Octadecanoic acid, 2-oxo-, methyl ester	58.828	n-Tridecan-1-ol	71.053	Nonane, 3-methyl-5-propyl-
50.102	1-Decanol, 2-hexyl-	60.628	Dodecane, 2,6,10-trimethyl-	72.23	C15
50.528	3-Tetradecene, (Z)-	63.585	Eicosane	73.652	Undecane, 3,8-dimethyl-
51.328	3-Tetradecene, (Z)-	63.788	Heptadecane, 2,6,10,15-tetramethyl-	73.677	Decane, 3,6-dimethyl-
51.579	1-Octanol, 2-butyl-	65.02	1-Nonanol, 4,8-dimethyl-	74.001	Hexadecane
51.74	Undecane, 2,8-dimethyl-	65.593	1-Nonanol, 4,8-dimethyl-	74.001	C16
51.915	Pentadecane	67.288	1-Chloro-2-methyl-2-phenylpropane	74.045	Nonadecane
52.11	Dodecane, 3-methyl-	101.122	Di-n-octyl phthalate	75.223	Dodecane
52.333	Undecane, 2,10-dimethyl-			78.847	C17
52.608	3-Tetradecene, (Z)-			78.847	Dodecane, 2,6,11-trimethyl-
54.635	Cyclopentane, (2-methylpropyl)-				
55.702	Hexadecane				
55.815	Octadecane, 2-methyl-				
56.768	Diethyl Phthalate				
57.355	3-Hexadecene, (Z)-				
57.949	Tridecane, 6-methyl-				
63.488	Hexadecane				
63.563	Oxalic acid, isobutyl hexadecyl ester				

Table 80 Continued

Distillate #2 400°C		Distillate #3 400°C		Distillate #4 400°C	
Retention Time	**Compound Name**	**Retention Time**	**Compound Name**	**Retention Time**	**Compound Name**
67.062	1-Chloro-2-methyl-2-phenylpropane				
77.995	Bicyclo[6.1.0]nonane, 9-(1-methylethylidene)-				
100.928	Di-n-octyl phthalate				

Table 81. Spectrum Process Table For 400°C Distillates #5, 6, and 7

Distillate #5 400°C		Distillate #6 400°C		Distillate #7 400°C	
Retention Time	**Compound Name**	**Retention Time**	**Compound Name**	**Retention Time**	**Compound Name**
3.345	Cyclohexene	3.348	Cyclohexene	3.35	Cyclohexene
3.39	Cyclohexene	3.392	Cyclohexene	12.787	1H-Pyrrole, 2,4-dimethyl-
15.863	2-Cyclopenten-1-one, 3-methyl-	8.388	3-Penten-2-one, 4-methyl-	16.548	Carbamic acid, phenyl ester
16.63	Phenol	8.52	1,5-Dimethyl-1,4-cyclohexadiene	18.275	1H-Pyrrole, 2-ethyl-4-methyl-
16.792	3-Pentenoic acid, 4-methyl-	9.44	(E,E,E)-2,4,6-Octatriene	19.003	1H-Pyrrole, 2,3,5-trimethyl-
17.695	2-Cyclopenten-1-one, 2,3-dimethyl-	15.553	3,5-Heptadien-2-ol, 2,6-dimethyl-	21.633	Phenol, 2-methyl-
20.182	11-Hexadecyn-1-ol	16.552	Carbamic acid, phenyl ester	23.277	Phenol, 2-methyl-
20.45	2-Acetyl-5-methylfuran	20.202	2-Cyclopenten-1-one, 2,3-dimethyl-	24.532	1H-Pyrrole, 3-ethyl-2,4-dimethyl-
20.92	2-Cyclopenten-1-one, 2,3-dimethyl-	21.657	Phenol, 2-methyl-	24.812	1H-Pyrrole, 3-ethyl-2,4-dimethyl-
21.855	Phenol, 2-methyl-	23.255	Phenol, 2-methyl-	27.582	Phenol, 2,3-dimethyl-
22.165	Cyclopentane, 1-methyl-2-propyl-	24.703	Cyclohexane, (1-methylethylidene)-	28.383	Phenol, 2,6-dimethyl-
23.722	Phenol, 2-methyl-	27.597	Phenol, 2-ethyl-	28.542	Phenol, 2,6-dimethyl-
24.333	1-Methylcyclooctene	28.405	Phenol, 2,3-dimethyl-	29.692	Phenol, 3-ethyl-
24.512	1-(2,4-Dimethyl-furan-3-yl)-ethanone	28.56	Phenol, 2,6-dimethyl-	29.972	Phenol, 2,3-dimethyl-
24.707	2-Nonanone	29.77	Phenol, 2-ethyl-	30.512	Furan, 2-(2-furanylmethyl)-5-methyl-
25.485	Phenol, 2,6-dimethyl-	30.023	Phenol, 2,6-dimethyl-	31.555	Phenol, 2,3-dimethyl-

Table 81 Continued

Distillate #5 400°C		Distillate #6 400°C		Distillate #7 400°C	
Retention Time	**Compound Name**	**Retention Time**	**Compound Name**	**Retention Time**	**Compound Name**
27.457	Ethanone, 1-(3-methylphenyl)-	31.21	Phenol, 2-methoxy-4-methyl-	34.603	Phenol, 2-ethyl-6-methyl-
27.817	Phenol, 2-ethyl-	31.585	Phenol, 2,3-dimethyl-	36.203	Phenol, 2,3,6-trimethyl-
28.805	Phenol, 2,5-dimethyl-	32.33	Phenol, 2,4,6-trimethyl-	36.972	Phenol, 2,4,6-trimethyl-
30.662	Phenol, 3-ethyl-	33.963	Phenol, 4-(1-methylethyl)-	38.22	5H-1-Pyrindine
32.165	Phenol, 2,3-dimethyl-	34.653	Phenol, 2-ethyl-5-methyl-	39.227	2-Methoxy-4-vinylphenol
32.632	Phenol, 2,4,6-trimethyl-	35.017	Phenol, 2-ethyl-6-methyl-	39.548	p-Benzoquinone, 2,3,5,6-tetramethyl-
33.122	Benzofuran, 4,7-dimethyl-	36.248	Phenol, 2-ethyl-5-methyl-	40.232	1H-Indole, 2-methyl-
33.837	Phenol, 2-propyl-	36.718	Phenol, 2,4,6-trimethyl-	44.478	1H-Indole, 1,2-dimethyl-
34.36	Phenol, 3,4,5-trimethyl-	37.09	Phenol, 4-ethyl-2-methoxy-	45.826	1,4-Benzenedicarboxaldehyde, 2,5-dimethyl-
35.188	Phenol, 2-ethyl-5-methyl-	38.05	Nonanoic acid	46.017	1,4-Benzenedicarboxaldehyde, 2,5-dimethyl-
36.787	Phenol, 2-ethyl-4-methyl-	39.672	Thymol	47.063	Benzonitrile, 2,4,6-trimethyl-
38.648	Phenol, 2-ethyl-4,5-dimethyl-	40.02	Phenol, 2,4,6-trimethyl-	48.65	1H-Indole, 2,3-dimethyl-
39.305	Benzene, 1-methoxy-4-propyl-	40.742	(4-Methoxy-benzyl)-phenethyl-amine	50.098	Dodecanoic acid
41.018	Pentadecane	41.553	1H-Inden-5-ol, 2,3-dihydro-	50.673	2-Nonadecanone
44.617	9-Octadecene, (E)-	52.138	Tridecane	52.062	2-Hexadecene, 3,7,11,15-tetramethyl-, [R-[R*,R*-(E)]]-
45.369	Pentadecane	63.362	9-Eicosene, (E)-	52.062	2-Pentadecanone, 6,10,14-trimethyl-
46.734	Naphthalene, 1,4,6-trimethyl-	63.832	Heptadecane	53.248	9-Octadecanone
48.631	Benzene, nonyl-	65.27	1-Dodecanol, 3,7,11-trimethyl-	57.132	1-Heptadecene
49.638	9-Octadecene, (E)-	65.843	2-Hexadecene, 3,7,11,15-tetramethyl-, [R-[R*,R*-(E)]]-	58.014	2-Pentadecanone, 6,10,14-trimethyl-
49.652	Hexadecane	68.2	Acetic acid, 3,7,11,15-tetramethyl-hexadecyl ester	60.044	Hexadecanoic acid, methyl ester
50.443	7-Hexadecene, (Z)-	68.713	9-Eicosene, (E)-	61.716	Eicosanoic acid
50.949	Tridecane, 6-methyl-	69.16	Octadecane	62.193	n-Nonadecanol-1

Table 81 Continued

Distillate #5 400°C		Distillate #6 400°C		Distillate #7 400°C	
Retention Time	**Compound Name**	**Retention Time**	**Compound Name**	**Retention Time**	**Compound Name**
51.667	5-Eicosene, (E)-	70.492	2-Hexadecene, 3,7,11,15-tetramethyl-, [R-[R*,R*-(E)]]-	62.214	Heneicosane
51.809	Nonadecane	71.19	2-Hexadecene, 3,7,11,15-tetramethyl-, [R-[R*,R*-(E)]]-	65.718	Heneicosane
52.201	9-Octadecene, (E)-	72.323	Cyclopentane, 1,3-dimethyl-2-(1-methylethylidene)-, trans-	66.725	Oxirane, tetradecyl-
52.201	Hexadecane	73.77	9-Eicosene, (E)-	67.674	Heptadecanoic acid, methyl ester
52.207	5-Eicosene, (E)-	74.197	Heptadecane, 2,6,10,15-tetramethyl-	69.09	Octacosyl trifluoroacetate
52.392	1-Dodecanol, 3,7,11-trimethyl-	74.935	Cycloeicosane	69.128	Tetracosane
54.403	1-Nonanol, 4,8-dimethyl-	75.32	Hexadecanoic acid, 15-methyl-, methyl ester	70.189	1-Octacosanol
54.511	7-Heptadecene, 1-chloro-	77.127	Tetracosane, 11-decyl-	70.487	9-Eicosene, (E)-
55.134	1-Decanol, 2-hexyl-	78.958	Nonadecane	70.861	Heneicosane
55.39	3-Eicosene, (E)-	79.735	5-Eicosene, (E)-	71.3	Triacontane, 11,20-didecyl-
55.39	Hexadecane	80.065	Heneicosanoic acid, methyl ester	71.648	n-Heptadecanol-1
55.852	5-Octadecene, (E)-	81.852	Triacontane, 11,20-didecyl-	71.651	Heneicosane
56.065	2-Hexadecene, 3,7,11,15-tetramethyl-, [R-[R*,R*-(E)]]-	83.562	Nonadecane	72.863	Heneicosane
57.573	2-Hexadecene, 3,7,11,15-tetramethyl-, [R-[R*,R*-(E)]]-	84.682	Hexadecanoic acid, 15-methyl-, methyl ester	73.227	Heptadecane, 2,6,10,15-tetramethyl-
57.68	2,5,9-Tetradecatriene, 3,12-diethyl-	87.985	Tetracosane	73.62	Heptadecane, 2,6,10,15-tetramethyl-
58.041	9-Octadecene, (E)-	92.237	Tetracosane	73.851	Heptadecane, 2,6,10,15-tetramethyl-
58.058	2-Bromo dodecane	96.328	2-Bromo dodecane	73.882	Heptadecane, 2,6,10,15-tetramethyl-
58.829	Hexadecanoic acid, 15-methyl-, methyl ester			74.333	C11

Table 81 Continued

Distillate #5 400°C		Distillate #6 400°C		Distillate #7 400°C	
Retention Time	**Compound Name**	**Retention Time**	**Compound Name**	**Retention Time**	**Compound Name**
58.832	C11			74.443	Decane, 2,3,6-trimethyl-
58.852	Undecane, 3-methyl-			74.994	Undecane, 2,8-dimethyl-
59.852	Decane, 2,3,6-trimethyl-			75.607	Undecane, 2,10-dimethyl-
60.653	6,10,13-Trimethyltetradecanol			76.898	Decane, 3,8-dimethyl-
61.007	Undecane, 3,7-dimethyl-			77.214	Undecane, 4-ethyl-
61.542	Octadecanoic acid, 2-oxo-, methyl ester			77.214	Benzene, 4-(2-butenyl)-1,2-dimethyl-, (E)-
61.55	Hexadecane, 1-chloro-			77.283	C14
63.202	Heptane, 3-(bromomethyl)-			78.743	Octadecanoic acid, 2-oxo-, methyl ester
63.636	Undecane, 2,8-dimethyl-			79.147	Decane, 3,7-dimethyl-
63.648	Undecane, 2,10-dimethyl-			79.152	Tetradecane, 3-methyl-
64.432	Dodecane, 3-methyl-			79.251	Cyclopentane, 1-hexyl-3-methyl-
65.067	Octane, 2,3,7-trimethyl-			82.239	C15
65.602	C13			83.735	Undecane, 3,8-dimethyl-
65.602	Heneicosane, 11-(1-ethylpropyl)-			84.227	Sulfurous acid, decyl pentyl ester
65.625	Tridecane, 6-methyl-			84.395	Decane, 3,6-dimethyl-
65.865	Dodecane, 2,5-dimethyl-			84.395	Hexadecane
66.587	Octadecane, 2-methyl-			84.743	Tetradecane, 3-methyl-
68.035	Cyclopentane, hexyl-			85.535	5-Octadecene, (E)-
68.06	Tridecane, 6-methyl-			86.372	C16
68.538	Tridecane, 4-methyl-			86.6	Nonadecane
68.943	Hexadecane			87.058	Dodecane
69.239	5-Octadecene, (E)-			88.082	Nonadecane
69.768	C14			91.005	Decane, 3,7-dimethyl-
70.352	Oxalic acid, isobutyl hexadecyl ester			91.29	Hexadecane
71.015	Pentadecane			92.285	Heptadecane, 3-methyl-
71.015	Hexadecane			96.343	C17

Table 81 Continued

Distillate #5 400°C		Distillate #6 400°C		Distillate #7 400°C	
Retention Time	**Compound Name**	**Retention Time**	**Compound Name**	**Retention Time**	**Compound Name**
71.042	Tetradecane, 3-methyl-			100.277	Dodecane, 2,6,11-trimethyl-
72.22	C15			104.068	2-Bromo dodecane
73.642	Undecane, 3,8-dimethyl-			107.733	C18
73.665	Decane, 3,6-dimethyl-			111.268	Heptadecane, 2,6,10,15-tetramethyl-
73.987	Hexadecane				
73.987	C16				
74.032	Nonadecane				
75.205	Dodecane				
78.847	C17				
78.847	Dodecane, 2,6,11-trimethyl-				

B2. 500°C Bio-oil Distillate Data Analysis

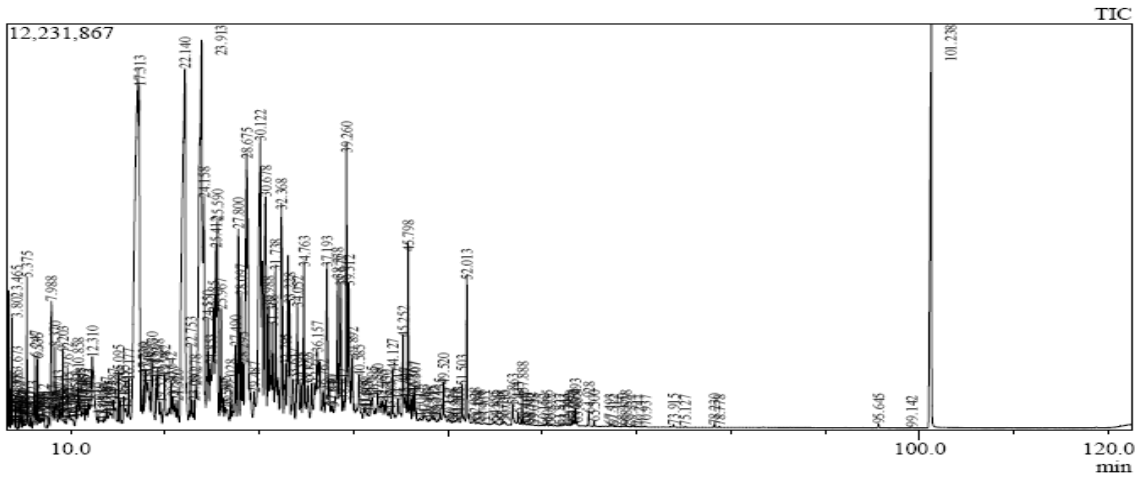

Figure 121. 500°C Bio-oil Distillate #2 GCMS Chromatogram and Spectrum Process Data.

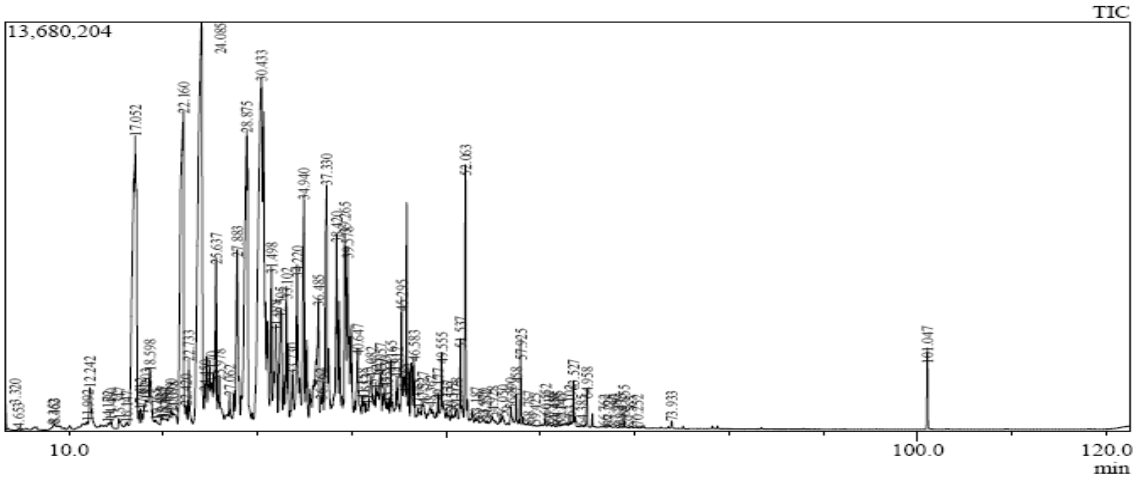

Figure 122. 500°C Bio-oil Distillate #3 GCMS Chromatogram and Spectrum Process Data.

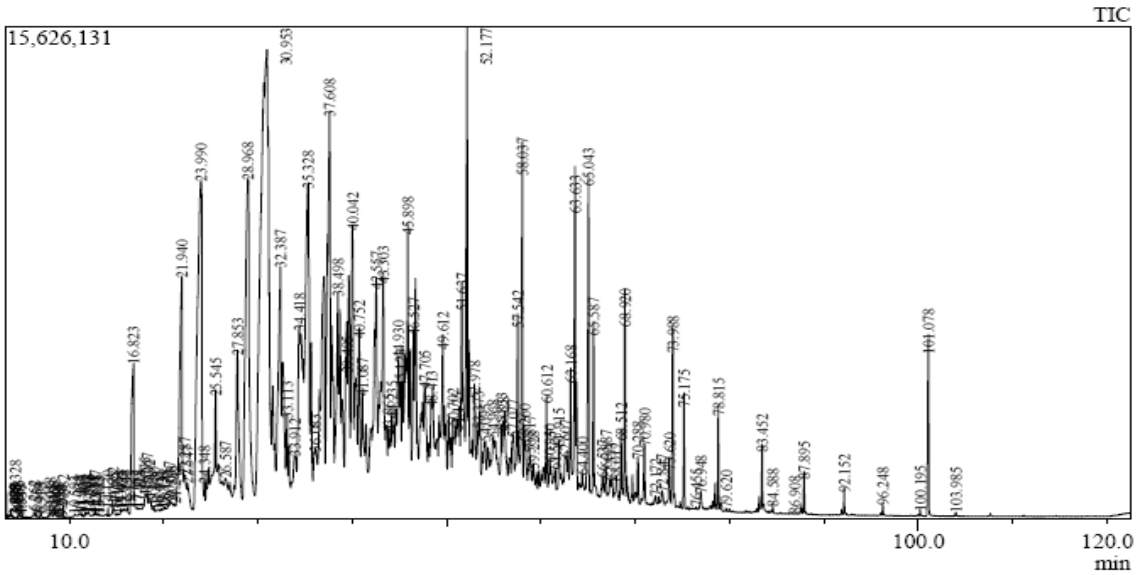

Figure 123. 500°C Bio-oil Distillate #4 GCMS Chromatogram and Spectrum Process Data.

Table 82. Spectrum Process Table For 500°C Distillates #2, 3, and 4

Distillate #2 500°C		Distillate #3 500°C		Distillate #4 500°C	
Retention Time	**Compound Name**	**Retention Time**	**Compound Name**	**Retention Time**	**Compound Name**
3.318	Cyclohexene	3.32	Cyclohexene	3.328	Cyclohexene
3.37	Cyclohexene	8.352	Cyclopentanone, 2-methyl-	3.488	2-Pentanone
3.465	2-Pentanone	11.992	Pentanoic acid	3.808	Furan, 2,5-dimethyl-
3.802	Furan, 2,5-dimethyl-	12.242	2-Cyclopenten-1-one, 2-methyl-	3.885	Propanoic acid
4.025	n-Propyl acetate	14.48	Cyclopropene, 1-butyl-2-ethyl-	3.978	Furan, 2,4-dimethyl-
4.128	Propanoic acid	15.347	Cyclopropene, 1-butyl-2-ethyl-	4.573	1H-Pyrrole, 1-methyl-
4.205	Butanoic acid, methyl ester	16.147	Cyclopentanone, 2,3-dimethyl-	4.848	1,3,5-Hexatriene, 3-methyl-, (E)-
4.462	4-Hexen-2-one, 3-methyl-	17.052	Phenol	4.937	Pyrrole
4.627	Ethanone, 1-cyclopropyl-	17.612	2-Octanone	6.262	Cyclopentanone
4.84	1,3,5-Hexatriene, 3-methyl-, (E)-	18.203	2-Cyclopenten-1-one, 2,3-dimethyl-	6.535	trans,trans-3,5-Heptadien-2-one
4.98	2-Pentanone, 3-methyl-	22.16	Phenol, 2-methyl-	6.918	trans,trans-3,5-Heptadien-2-one
5.375	1,3,5-Cycloheptatriene	22.733	Acetophenone	6.995	1H-Pyrrole, 1-ethyl-
5.777	Butanoic acid, 3-methyl-, methyl ester	24.085	Phenol, 2-methyl-	8.468	1,5-Dimethyl-1,4-cyclohexadiene
6.023	3-Hexanone	25.17	cis-Decalin, 2-syn-methyl-	9.382	Toluene-D3
6.247	Cyclopentanone	25.637	Phenol, 2,6-dimethyl-	11.465	(E,E,E)-2,4,6-Octatriene
6.535	trans,trans-3,5-Heptadien-2-one	25.978	Phenol, 2-ethyl-5-methyl-	11.742	Ethanone, 1-(2-methyl-1-cyclopenten-1-yl)-
6.632	4-Penten-2-one, 3-methyl-	27.062	Octanoic acid, methyl ester	12.068	Ethanone, 1-(2-methyl-1-cyclopenten-1-yl)-
6.738	Propanoic acid, anhydride	27.883	Phenol, 2-ethyl-	12.747	1H-Pyrrole, 2,4-dimethyl-
6.8	1,4-Pentadiene, 2,3,3-trimethyl-	28.875	Phenol, 2,5-dimethyl-	14.13	4-Oxatricyclo[4.3.1.1(3,8)]undecan-5-one
6.917	1-Propen-2-ol, acetate	30.433	Phenol, 3-ethyl-	15.495	1-Hexen-3-yne, 2,5,5-trimethyl-
7.003	4-Pentenoic acid, methyl ester	31.498	Phenol, 2-methoxy-4-methyl-	16.823	Phenol
7.112	Furan, 2,3,5-trimethyl-	31.978	Phenol, 2,3-dimethyl-	18.267	1H-Pyrrole, 2-ethyl-4-methyl-
7.632	Pentanoic acid, methyl ester	32.505	Phenol, 2,3,6-trimethyl-	18.98	1H-Pyrrole, 2,3,5-trimethyl-
7.988	Furfural	33.102	Benzofuran, 4,7-dimethyl-	19.737	Heptanoic acid, methyl ester
8.137	2-Pentanone, 3-methylene-	33.73	Phenol, 2-propyl-	20.868	2-Acetyl-5-methylfuran

Table 82 Continued

Distillate #2 500°C		Distillate #3 500°C		Distillate #4 500°C	
Retention Time	**Compound Name**	**Retention Time**	**Compound Name**	**Retention Time**	**Compound Name**
8.37	Cyclopentanone, 2-methyl-	34.94	Phenol, 2-ethyl-5-methyl-	22.547	Acetophenone
8.743	Cyclopentanone, 3-methyl-	37.33	Phenol, 4-ethyl-2-methoxy-	23.99	Phenol, 3-methyl-
9.008	2-Furanmethanol	39.265	Tridecane	24.348	3-Acetyl-2,5-dimethyl furan
9.203	Ethylbenzene	39.578	1H-Inden-1-one, 2,3-dihydro-3,3-dimethyl-	25.545	Phenol, 2,6-dimethyl-
9.557	Butanoic acid, 3-methyl-	43.755	1,2,3-Trimethylindene	27.853	Phenol, 2-ethyl-
9.672	o-Xylene	45.295	3-Tetradecene, (Z)-	28.968	Phenol, 2,5-dimethyl-
9.927	Butanoic acid, 2-propenyl ester	47.527	Naphthalene, 2,3-dimethyl-	30.953	Phenol, 3-ethyl-
10.687	3-Heptanone	49.555	Pentadecane	32.387	Phenol, 3,4-dimethyl-
10.858	o-Xylene	51.537	9-Octadecene, (E)-	33.113	Benzofuran, 4,7-dimethyl-
11.257	Cyclopentanone, 2,3-dimethyl-	52.063	Pentadecane	33.912	Phenol, 2-propyl-
11.453	Decane	53.187	Naphthalene, 1,4,5-trimethyl-	34.418	Phenol, 2,3,6-trimethyl-
11.625	2-Cyclopenten-1-one, 2-methyl-	53.97	Naphthalene, 1,4,5-trimethyl-	35.328	Phenol, 2-ethyl-5-methyl-
11.745	2,5-Dimethylhex-5-en-3-yn-2-ol	54.252	Naphthalene, 1,4,6-trimethyl-	38.498	Naphthalene, 1-methyl-
11.923	Ethanone, 1-(2-furanyl)-	56.89	Diethyl Phthalate	41.087	Benzene, 1-methoxy-4-propyl-
13.01	Hexanoic acid, methyl ester	57.458	9-Octadecene, (E)-	45.898	Tridecane
13.807	1-Octanol	57.925	Pentadecane	46.527	Naphthalene, 2,3-dimethyl-
14.587	Benzene, propyl-	58.757	7-Hexadecene, (Z)-	49.612	Dodecane, 4,6-dimethyl-
15.095	Benzene, 1-ethyl-2-methyl-	60.552	Dodecane, 2,6,10-trimethyl-	51.637	1-Tridecene
15.29	Benzene, 1-ethyl-2-methyl-	60.91	5-Eicosene, (E)-	52.177	Pentadecane
15.655	Benzene, 1,2,3-trimethyl-	61.458	Nonadecane	54.095	Naphthalene, 1,4,6-trimethyl-
16.177	Benzene, 1-ethyl-2-methyl-	62.145	Cyclododecane	55.833	Pentadecane
17.313	Phenol	63.102	9-Octadecene, (E)-	57.542	1-Pentadecene
17.525	Nonane, 4-ethyl-5-methyl-	63.527	Hexadecane	58.037	Hexadecane
17.73	2-Octanone	64.958	1-Dodecanol, 3,7,11-trimethyl-	60.612	Pentadecane, 2,6,10-trimethyl-
17.998	Decane	68.475	9-Octadecene, (E)-	60.95	Cyclotetracosane
19.122	Benzene, 1,2,3-trimethyl-	68.855	Eicosane	61.507	Nonadecane

Table 82 Continued

Distillate #2 500°C		Distillate #3 500°C		Distillate #4 500°C	
Retention Time	**Compound Name**	**Retention Time**	**Compound Name**	**Retention Time**	**Compound Name**
19.298	Benzene, 1-methoxy-4-methyl-	70.252	2-Hexadecene, 3,7,11,15-tetramethyl-, [R-[R*,R*-(E)]]-	63.168	1-Pentadecene
19.982	Indane	73.933	2-Bromo dodecane	63.633	Heptadecane
21.32	Benzene, 1-methyl-3-propyl-			65.043	1-Dodecanol, 3,7,11-trimethyl-
22.14	Phenol, 2-methyl-			65.587	1-Nonanol, 4,8-dimethyl-
22.753	Acetophenone			68.012	Acetic acid, 3,7,11,15-tetramethyl-hexadecyl ester
23.073	Benzene, propyl-			68.512	9-Eicosene, (E)-
23.288	Cyclohexane, 1,1,2,3-tetramethyl-			68.92	Hexadecane
23.913	Phenol, 3-methyl-			70.288	2-Hexadecene, 3,7,11,15-tetramethyl-, [R-[R*,R*-(E)]]-
24.158	Phenol, 2-methoxy-			70.98	2-Hexadecene, 3,7,11,15-tetramethyl-, [R-[R*,R*-(E)]]-
24.853	2-Nonanone			72.172	Zinc, bis(2,2-dimethyl-3(cis)-(1-methylprop-2-enyl)-cyclopropyl)-
25.173	Nonane, 3-methyl-			73.62	9-Eicosene, (E)-
25.185	Tridecane			73.988	Tetracosane
25.412	Benzofuran, 2-methyl-			75.175	Hexadecanoic acid, 15-methyl-, methyl ester
25.59	Phenol, 2,6-dimethyl-			76.948	Eicosanoic acid
25.967	Phenol, 2-ethyl-5-methyl-			78.815	Tetracosane
27.028	Octanoic acid, methyl ester			79.62	5-Eicosene, (E)-
27.49	1H-Indene, 2,3-dihydro-4-methyl-			83.452	Heptadecane, 2,6,10,15-tetramethyl-
27.8	Phenol, 2-ethyl-			84.588	Hexadecanoic acid, 15-methyl-, methyl ester
28.097	Benzene, 1-methyl-2-(2-propenyl)-			87.895	Heptadecane, 2,6,10,15-tetramethyl-
28.675	Phenol, 2,6-dimethyl-			92.152	Heptadecane, 2,6,10,15-tetramethyl-

Table 82 Continued

Distillate #2 500°C		Distillate #3 500°C		Distillate #4 500°C	
Retention Time	**Compound Name**	**Retention Time**	**Compound Name**	**Retention Time**	**Compound Name**
30.122	Phenol, 4-ethyl-			96.248	Tetracosane
30.678	Azulene			100.195	Heptadecane, 2,6,10,15-tetramethyl-
31.368	Phenol, 2-methoxy-4-methyl-			101.078	Di-n-octyl phthalate
32.338	1-Pentanol, 4-methyl-2-propyl-			103.985	Heptadecane, 2,6,10,15-tetramethyl-
32.678	E-11-Tetradecen-1-ol trifluoroacetate				
32.795	Benzofuran, 4,7-dimethyl-				
33.193	Nonane, 3,7-dimethyl-				
33.406	Benzene, 1-methyl-3-propyl-				
34.052	Phenol, 2,3,6-trimethyl-				
34.396	6-Dodecenol				
34.763	Phenol, 2-ethyl-5-methyl-				
36.718	Decane, 3-methyl-				
36.762	Phenol, 2,4,6-trimethyl-				
37.193	Phenol, 4-ethyl-2-methoxy-				
37.64	Ethanone, 1-[4-(1-methylethenyl)phenyl]-				
37.818	4-Decene, 3-methyl-, (E)-				
38.228	Cyclohexane, pentyl-				
38.338	1,4-Methanonaphthalene, 1,4-dihydro-				
38.672	3-Tetradecene, (Z)-				
39.247	C11				
39.26	Pentadecane				
39.892	1H-Inden-1-one, 2,3-dihydro-3,3-dimethyl-				
40.195	Undecane, 5-methyl-				
42.58	1-Dodecanol, 3,7,11-trimethyl-				
43.133	Cyclopentane, 1,2-dimethyl-3-(1-methylethyl)-				

Distillate #2 500°C		Distillate #3 500°C		Distillate #4 500°C	
Retention Time	**Compound Name**	**Retention Time**	**Compound Name**	**Retention Time**	**Compound Name**
43.865	Biphenyl				
44.127	Dodecane, 2,7,10-trimethyl-				
44.912	Benzene, 1-methyl-4-(1-methylpropyl)-				
45.252	3-Tetradecene, (Z)-				
45.798	Pentadecane				
46.037	5-Tetradecene, (E)-				
46.047	Decane, 2,3,6-trimethyl-				
46.267	Naphthalene, 2,3-dimethyl-				
46.619	6,10,13-Trimethyltetradecanol				
48.522	Dodecane, 3-cyclohexyl-				
49.135	Dodecane				
49.509	Octadecanoic acid, 2-oxo-, methyl ester				
49.52	Pentadecane				
50.152	Oxirane, [(dodecyloxy)methyl]-				
51.503	3-Hexadecene, (Z)-				
52.003	Dodecane, 3-methyl-				
52.013	Pentadecane				
52.249	Undecane, 2,10-dimethyl-				
52.828	7-Hexadecene, (Z)-				
53.378	Tridecanoic acid, methyl ester				
55.737	Octadecane, 2-methyl-				
55.745	Nonadecane, 2-methyl-				
56.119	Dodecane, 2,5-dimethyl-				
56.863	Diethyl Phthalate				
57.433	9-Octadecene, (E)-				
57.882	Tridecane, 6-methyl-				
57.888	Pentadecane				
58.147	7-Hexadecene, (Z)-				
58.513	Ethanol, 2-(dodecyloxy)-				
58.732	3-Tetradecene, (Z)-				

Table 82 Continued

Distillate #2 500°C		Distillate #3 500°C		Distillate #4 500°C	
Retention Time	**Compound Name**	**Retention Time**	**Compound Name**	**Retention Time**	**Compound Name**
60.535	Dodecane, 2,7,10-trimethyl-				
60.877	Cyclotetradecane				
62.792	1-Octanol, 2-butyl-				
63.078	1-Docosene				
63.485	Oxalic acid, isobutyl hexadecyl ester				
63.493	Eicosane				
63.698	Nonadecane				
64.928	1-Nonanol, 4,8-dimethyl-				
65.485	Pentadecane				
65.485	Hexadecane				
65.5	1-Nonanol, 4,8-dimethyl-				
67.193	Benzene, 1,1'-(1,1,2,2-tetramethyl-1,2-ethanediyl)bis-				
68.45	9-Octadecene, (E)-				
68.819	Undecane, 3,8-dimethyl-				
68.828	Pentadecane				
70.247	2-Hexadecene, 3,7,11,15-tetramethyl-, [R-[R*,R*-(E)]]-				
70.937	2-Hexadecene, 3,7,11,15-tetramethyl-, [R-[R*,R*-(E)]]-				
73.908	C16				
73.908	Nonadecane				
73.908	Dodecane				
73.915	Eicosane				
75.127	Tridecanoic acid, methyl ester				
78.778	Tetradecane				
95.645	Hexanedioic acid, mono(2-ethylhexyl)ester				
101.238	Di-n-octyl phthalate				

B3. GCMS Chromatograms and Spectrum Process Data for 600°C Bio-oil Distillates

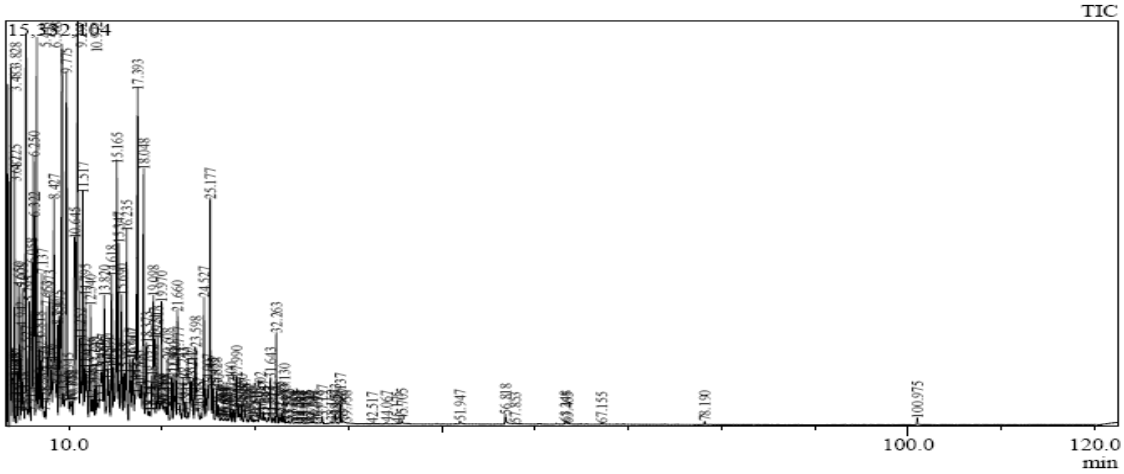

Figure 124. 600°C Bio-oil Distillate #2 GCMS Chromatogram and Spectrum Process Data.

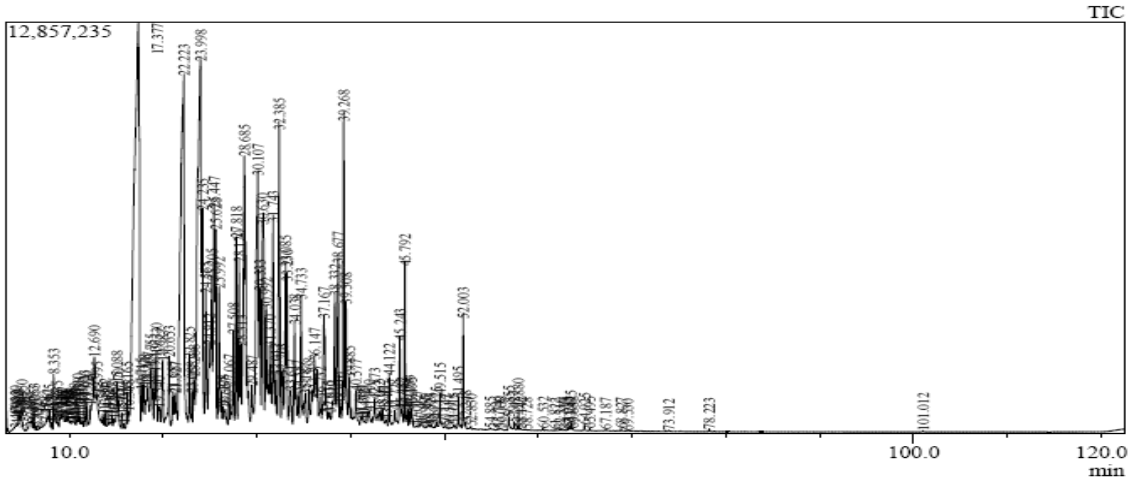

Figure 125. 600°C Bio-oil Distillate #3 GCMS Chromatogram and Spectrum Process Data.

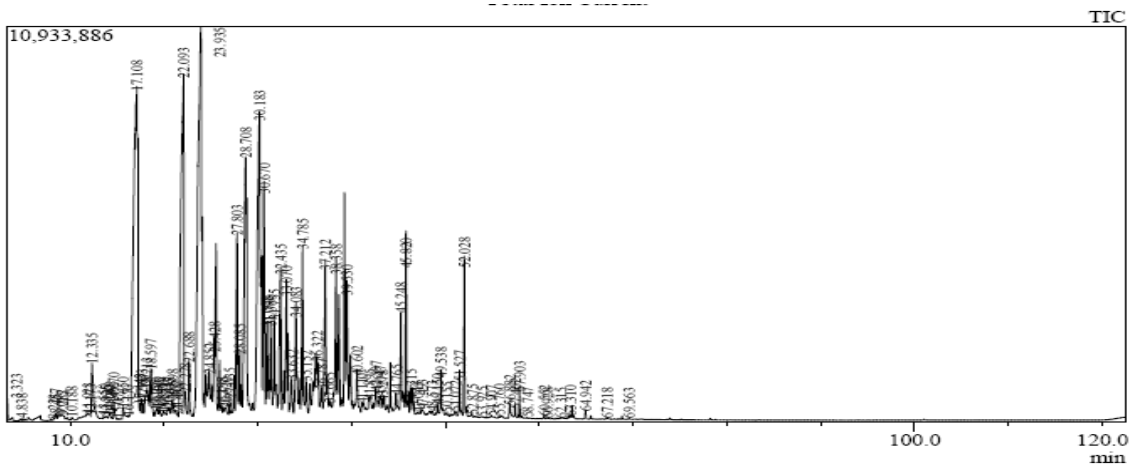

Figure 126. 600°C Bio-oil Distillate #4 GCMS Chromatogram and Spectrum Process Data.

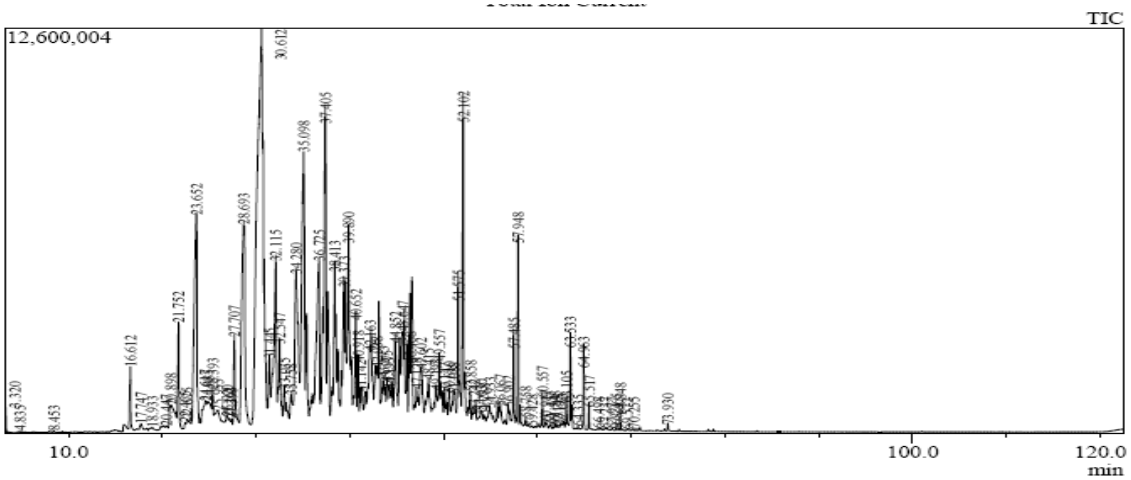

Figure 127. 600°C Bio-oil Distillate #5 GCMS Chromatogram and Spectrum Process Data.

Table 83. Spectrum Process Table For 600°C Distillates #2 and 3

Distillate #2 600°C		Distillate #3 600°C	
Retention Time	**Compound Name**	**Retention Time**	**Compound Name**
3.323	Cyclobutane, ethenyl-	3.32	Cyclohexene
3.483	2-Pentanone	3.48	2-Pentanone
3.828	Furan, 2,5-dimethyl-	4.84	1,3,5-Hexatriene, 3-methyl-, (Z)-
3.952	1,4-Pentadiene, 3,3-dimethyl-	5.538	1-Pentanol
4.013	n-Propyl acetate	6.007	Heptane
4.225	Butanoic acid, methyl ester	6.183	2-Hexanone
4.477	4-Hexen-2-one, 3-methyl-	6.253	Cyclopentanone
4.65	Methyl Isobutyl Ketone	6.492	3-Penten-2-one, 4-methyl-
5.008	2-Pentanone, 3-methyl-	7.488	Pyridine, 2-methyl-
5.443	1,3,5-Cycloheptatriene	8.112	3-Penten-2-one, 3-methyl-
5.795	Butanoic acid, 3-methyl-, methyl ester	8.353	Cyclopentanone, 2-methyl-
5.915	Furan, 2-(2-propenyl)-	8.612	2-Hexanone, 4-methyl-
6.058	3-Hexanone	8.735	Cyclopentanone, 3-methyl-
6.25	2-Hexanone	9.04	2-Furanmethanol
6.322	Cyclopentanone	9.14	2-Hexanone, 5-methyl-
6.588	trans,trans-3,5-Heptadien-2-one	9.222	Pyridine, 2-methyl-
7.137	Furan, 2,3,5-trimethyl-	9.918	2-Methylpentyl formate
7.653	Pentanoic acid, methyl ester	10.188	Butanoic acid, 3-methyl-
7.773	Phenol, 2-methyl-	10.68	3-Heptanone
8.17	2-Pentanone, 3-methylene-	10.91	2-Heptanone
8.427	Cyclopentanone, 2-methyl-	11.25	Cyclopentanone, 2,3-dimethyl-
8.79	Cyclopentanone, 3-methyl-	11.39	Cyclopentanone, 2,4-dimethyl-
9.292	Ethylbenzene	11.623	2-Cyclopenten-1-one, 2-methyl-
9.432	Thiophene, 2-ethyl-	11.92	Ethanone, 1-(2-furanyl)-
9.775	Benzene, 1,3-dimethyl-	12.295	Benzene, methoxy-
9.945	4-Heptanone	12.69	2-Cyclopenten-1-one, 2-methyl-
10.972	o-Xylene	12.995	Butanoic acid, methyl ester
11.517	Nonane	13.595	3-Nonyne
11.632	2-Cyclopenten-1-one, 2-methyl-	13.812	Cyclopentanone, 2-ethyl-
11.947	Ethanone, 1-(2-furanyl)-	14.312	Cycloheptanone
12.34	Benzene, methoxy-	14.567	Benzene, propyl-
12.728	Benzene, (1-methylethyl)-	15.088	Benzene, (1-methylethyl)-
13.012	Hexanoic acid, methyl ester	15.27	Benzene, 1-ethyl-2-methyl-
13.82	Heptane, 3-ethyl-2-methyl-	15.64	Benzene, 1,2,4-trimethyl-
14.305	1-Octene, 3,4-dimethyl-	16.165	Benzene, 1-ethyl-2-methyl-
14.618	Benzene, propyl-	16.318	Pentalene, octahydro-, cis-

Table 83 Continued

Distillate #2 600°C		Distillate #3 600°C	
Retention Time	**Compound Name**	**Retention Time**	**Compound Name**
14.822	2-Nonen-4-yne, (E)-	17.377	Phenol
15.165	Benzene, 1,2,4-trimethyl-	19.133	Benzene, 1,2,3-trimethyl-
15.347	Benzene, 1-ethyl-3-methyl-	19.33	Benzene, 1-methoxy-4-methyl-
15.69	Benzene, 1,2,4-trimethyl-	19.54	1,3,5-Cycloheptatriene, 3,7,7-trimethyl-
15.968	2-(5-Methyl-furan-2-yl)-propionaldehyde	19.987	Indane
16.235	Benzene, 1-ethyl-2-methyl-	20.653	Indene
16.617	Phenol	21.327	Benzene, 1-methyl-3-propyl-
16.907	Cyclopentene, 1,4-dimethyl-5-(1-methylethyl)-	22.223	Phenol, 2-methyl-
17.555	2-Tridecene, (E)-	22.825	Acetophenone
17.765	3-Decene	23.088	Benzene, 4-ethyl-1,2-dimethyl-
18.048	Undecane	23.288	Benzene, 1-methyl-2-(1-methylethyl)-
18.547	Cyclopentane, 1-butyl-2-ethyl-	23.998	Phenol, 3-methyl-
18.717	Octane, 3,3-dimethyl-	24.235	Phenol, 2-methoxy-
18.932	1-Octanol, 2-butyl-	25.205	Tridecane
19.098	Benzene, 1-ethyl-2-methyl-	25.447	Benzofuran, 2-methyl-
19.217	Benzene, 1-methoxy-4-methyl-	25.628	Phenol, 2,6-dimethyl-
19.707	Heptanoic acid, methyl ester	25.992	Phenol, 2-ethyl-5-methyl-
19.803	Cyclobutane, 1,3-diisopropenyl-, trans	27.067	Octanoic acid, methyl ester
19.97	Indane	27.508	1H-Indene, 2,3-dihydro-4-methyl-
20.31	Cyclopentane, butyl-	27.818	Phenol, 2-ethyl-
20.608	Benzene, 1-propynyl-	28.12	Benzene, 1-methyl-2-(2-propenyl)-
21.3	Benzene, 1-methyl-3-propyl-	28.685	Phenol, 2,6-dimethyl-
21.777	Benzene, 1-ethyl-2,4-dimethyl-	29.487	Benzene, 1-methyl-4-(2-methylpropyl)-
22.243	Benzene, 1-methyl-4-propyl-	30.107	Phenol, 4-ethyl-
23.212	Benzene, 4-ethyl-1,2-dimethyl-	31.37	Phenol, 2-methoxy-4-methyl-
23.598	3-Phenylbut-1-ene	32.703	2-Dodecene, (E)-
24.527	Cyclopropane, octyl-	33.085	Benzofuran, 4,7-dimethyl-
25.177	Undecane	34.733	Phenol, 2-ethyl-5-methyl-
25.485	2-Undecene, (E)-	35.187	1H-Indene, 2,3-dihydro-1,2-dimethyl-
25.828	Phenol, 2-ethyl-5-methyl-	35.568	(1-Methylbuta-1,3-dienyl)benzene
26.03	2-Undecene, (E)-	37.167	Phenol, 4-ethyl-2-methoxy-
26.36	2-Undecanethiol, 2-methyl-	38.332	1,4-Methanonaphthalene, 1,4-dihydro-
26.835	Octanoic acid, methyl ester	38.677	3-Tetradecene, (Z)-
27.4	1H-Indene, 2,3-dihydro-4-methyl-	38.91	6-Tridecene, (Z)-
27.99	2,4-Dimethylstyrene	39.268	Tridecane

Table 83 Continued

Distillate #2 600°C		Distillate #3 600°C	
Retention Time	**Compound Name**	**Retention Time**	**Compound Name**
28.197	Benzene, 1-ethyl-2,3-dimethyl-	39.885	1H-Inden-1-one, 2,3-dihydro-3,3-dimethyl-
28.36	Benzene,1-methyl-1,2-propadienyl-	42.573	1-Octanol, 3,7-dimethyl-
28.857	Benzene, pentyl-	43.062	Benzene, heptyl-
29.392	Benzene, 1-methyl-4-(2-methylpropyl)-	44.122	Dodecane, 2,7,10-trimethyl-
29.685	Tridecane	45.243	3-Tetradecene, (Z)-
29.87	Cyclopentane, 1-butyl-2-propyl-	45.792	Pentadecane
30.502	Azulene	46.038	5-Tetradecene, (E)-
31.392	Benzene, 1-methyl-3-(1-methyl-2-propenyl)-	48.525	Undecane, 3-cyclohexyl-
31.643	3-Tetradecene, (Z)-	49.125	Dodecane
31.913	3-Dodecene, (Z)-	49.515	Decane, 5-propyl-
32.263	Tridecane	50.142	1-Octanol, 2-butyl-
32.595	2-Dodecene, (E)-	51.495	3-Hexadecene, (Z)-
32.888	Benzofuran, 4,7-dimethyl-	52.003	Pentadecane
33.13	Undecane, 2,6-dimethyl-	52.248	5-Tetradecene, (E)-
33.582	1-Octanol, 3,7-dimethyl-	52.83	3-Tetradecene, (Z)-
34.955	3-Tetradecene, (E)-	55.74	Hexadecane
35.087	Benzene, 2-ethenyl-1,3,5-trimethyl-	56.855	Diethyl Phthalate
36.658	Undecane, 2,10-dimethyl-	57.427	3-Hexadecene, (Z)-
37.197	Octane, 2,3,7-trimethyl-	57.88	Pentadecane
38.573	3-Tetradecene, (Z)-	58.142	1-Tridecene
38.82	3-Dodecene, (Z)-	58.728	7-Hexadecene, (Z)-
39.137	Tridecane	60.532	Pentadecane, 2,6,10-trimethyl-
42.517	Cyclopropane, 1-ethyl-2-heptyl-	63.073	3-Hexadecene, (Z)-
44.067	Dodecane, 2,7,10-trimethyl-	63.475	Eicosane
45.175	3-Tetradecene, (Z)-	63.688	Undecane, 6-ethyl-
45.705	Dodecane	64.925	1-Nonanol, 4,8-dimethyl-
51.947	Hexadecane	65.495	1-Nonanol, 4,8-dimethyl-
56.818	Diethyl Phthalate	68.827	Pentadecane
57.853	Dodecane	73.912	2-Bromo dodecane
63.465	Hexadecane		
67.155	1-Chloro-2-methyl-2-phenylpropane		
100.975	Di-n-octyl phthalate		

Table 84. Spectrum Process Table For 600°C Distillates #4 and 5

Distillate #4 600°C		Distillate #5 600°C	
Retention Time	**Compound Name**	**Retention Time**	**Compound Name**
3.323	Cyclohexene	3.32	Cyclohexene
4.838	1,3,5-Hexatriene, 3-methyl-, (E)-	4.835	1,3,5-Hexatriene, 3-methyl-, (E)-
8.228	Pyrazine, methyl-	8.453	1,5-Dimethyl-1,4-cyclohexadiene
12.173	Pentanoic acid	16.612	Phenol
12.335	2-Cyclopenten-1-one, 2-methyl-	17.747	Cyclopentane, (1-methylethylidene)-
13.55	Pyrazine, 2,6-dimethyl-	20.447	2-Acetyl-5-methylfuran
14.268	Cyclopentanone, 2-ethyl-	20.898	2-Cyclopenten-1-one, 2,3-dimethyl-
14.67	Cyclopropene, 1-butyl-2-ethyl-	21.752	Phenol, 2-methyl-
15.077	Benzene, (1-methylethyl)-	22.465	Acetophenone
15.65	Cyclopropene, 1-butyl-2-ethyl-	23.652	Phenol, 3-methyl-
17.108	Phenol	25.393	Phenol, 2,6-dimethyl-
17.441	Pentafluoropropionic acid, hexadecyl ester	27.149	Ethanone, 1-(3-methylphenyl)-
17.443	2-Octanone	27.393	Phenol, 2-ethyl-
17.633	Benzene, 1-methoxy-4-methyl-	27.707	Phenol, 2,5-dimethyl-
19.27	Heptanoic acid, methyl ester	28.693	Phenol, 3-ethyl-
19.835	Benzene,1-ethynyl-2-methyl-	30.612	Phenol, 2-methoxy-4-methyl-
20.615	Spiro[4.5]decane	31.445	Phenol, 3,4-dimethyl-
20.898	Phenol, 2-methyl-	32.115	Phenol, 2,4,6-trimethyl-
22.093	Acetophenone	32.547	Benzofuran, 4,7-dimethyl-
22.688	Phenol, 2-methyl-	33.035	Phenol, 2-propyl-
23.935	2-Nonanone	33.758	Phenol, 3,4,5-trimethyl-
24.852	Phenol, 2,6-dimethyl-	34.28	Phenol, 2-ethyl-5-methyl-
25.428	Octanoic acid, methyl ester	35.098	Phenol, 2-ethyl-4-methyl-
26.594	Phenol, 2-ethyl-	36.725	1,4-Methanonaphthalene, 1,4-dihydro-
27.035	Phenol, 2,4-dimethyl-	38.413	1,4-Methanonaphthalene, 1,4-dihydro-
27.803	Phenol, 4-ethyl-	39.222	Biphenyl
28.708	Azulene	39.373	Naphthalene, 2,3-dimethyl-
30.183	Phenol, 2-ethyl-6-methyl-	40.929	Pentadecane
30.67	Phenol, 2-methoxy-4-methyl-	43.975	3-Hexadecene, (Z)-
31.008	Benzofuran, 4,7-dimethyl-	45.078	Pentadecane
31.38	Phenol, 2-ethyl-6-methyl-	46.085	9-Octadecene, (E)-
32.315	Phenol, 2-ethyl-5-methyl-	46.651	Naphthalene, 1,4,6-trimethyl-
32.317	Phenol, 2,4,6-trimethyl-	46.66	Naphthalene, 1,4,6-trimethyl-
33.07	Phenol, 4-ethyl-2-methoxy-	47.602	9-Octadecene, (E)-
33.183	1,4-Methanonaphthalene, 1,4-dihydro-	48.532	Hexadecane

Table 84 Continued

Distillate #4 600°C		Distillate #5 600°C	
Retention Time	**Compound Name**	**Retention Time**	**Compound Name**
34.083	1-Octanol, 3,7-dimethyl-	48.63	7-Hexadecene, (Z)-
34.407	Benzene, heptyl-	49.541	Pentadecane, 2,6,10-trimethyl-
34.785	3-Tetradecene, (Z)-	49.557	5-Eicosene, (E)-
36.717	Hexadecane	50.861	Nonadecane
36.787	Naphthalene, 2,3-dimethyl-	51.575	1-Hexadecanol
37.212	Cyclopentane, hexyl-	51.684	1-Heptafluorobutyryloxy-10-undecene
37.812	Dodecane	52.086	9-Octadecene, (E)-
38.358	Pentadecane	52.102	Hexadecane
39.239	Oxirane, [(dodecyloxy)methyl]-	52.293	5-Octadecene, (E)-
40.192	3-Hexadecene, (Z)-	52.858	1-Dodecanol, 3,7,11-trimethyl-
41.838	Pentadecane	53.242	1-Nonanol, 4,8-dimethyl-
42.597	5-Tetradecene, (E)-	54.288	n-Heptadecanol-1
43.047	Hexadecane	54.409	1-Dodecanol, 3,7,11-trimethyl-
45.248	Diethyl Phthalate	55.755	9-Octadecene, (E)-
45.82	3-Hexadecene, (Z)-	56.142	Hexadecane
46.053	Pentadecane	57.485	2-Hexadecene, 3,7,11,15-tetramethyl-, [R-[R*,R*-(E)]]-
46.315	3-Tetradecene, (Z)-	57.588	Eicosane
46.622	Pentadecane, 2,6,10-trimethyl-	57.94	Cyclohexane, 1-methyl-3-(1-methylethyl)-
48.518	1-Nonanol, 4,8-dimethyl-	57.948	C11
48.573	Nonane, 4-ethyl-5-methyl-	58.732	trans-Decalin, 2-methyl-
49.15	Cyclopentane, 1-methyl-3-(2-methylpropyl)-	58.758	Undecane, 3-methyl-
49.518	1-Octanol, 2-butyl-	60.557	Decane, 2,3,6-trimethyl-
49.538	1-Pentanol, 4-methyl-2-propyl-	60.917	1-Decene, 3,4-dimethyl-
50.155	Nonane, 3,7-dimethyl-	61.449	6,10,13-Trimethyltetradecanol
51.087	6-Dodecenol	61.457	Tridecane, 6-methyl-
51.508	Decane, 3-methyl-	62.148	Undecane, 3,7-dimethyl-
51.527	4-Decene, 3-methyl-, (E)-	62.663	Octadecanoic acid, 2-oxo-, methyl ester
51.675	C11	63.105	Hexadecane, 1-chloro-
52.011	Undecane, 5-methyl-	63.515	Undecane, 2,8-dimethyl-
52.028	n-Amylcyclohexane	63.533	Undecane, 2,10-dimethyl-
52.253	Decane, 2,3,6-trimethyl-	64.335	Dodecane, 3-methyl-
52.875	6,10,13-Trimethyltetradecanol	64.963	C13
55.74	Undecane, 3,7-dimethyl-	65.501	Dodecane, 2,5-dimethyl-
55.76	Octadecanoic acid, 2-oxo-, methyl ester	65.501	Octadecane, 2-methyl-
56.128	Hexadecane, 1-chloro-	65.501	Cyclopentane, hexyl-
56.882	Undecane, 2,8-dimethyl-	65.517	Tridecane, 6-methyl-

Table 84 Continued

Distillate #4 600°C		Distillate #5 600°C	
Retention Time	**Compound Name**	**Retention Time**	**Compound Name**
57.462	1-Octanol, 2-butyl-	66.498	Hexadecane
57.885	Undecane, 2,10-dimethyl-	67.977	C14
57.903	Dodecane, 3-methyl-	68.465	Oxalic acid, isobutyl hexadecyl ester
58.747	Dodecane, 2,5-dimethyl-	68.818	Pentadecane
60.552	Octadecane, 2-methyl-	68.848	Hexadecane
63.491	Tridecane, 6-methyl-	70.255	Tetradecane, 3-methyl-
64.942	Oxalic acid, isobutyl hexadecyl ester	73.55	Undecane, 3,8-dimethyl-
65.499	Pentadecane	73.895	5-Octadecene, (E)-
65.499	Hexadecane	73.895	C16
65.499	Tetradecane, 3-methyl-	73.895	Nonadecane
67.218	Undecane, 3,8-dimethyl-	73.93	Dodecane
68.821	C16		
69.563	Nonadecane		
73.915	Dodecane		

B4. GCMS Chromatograms and Spectrum Process Data for Fluorous Pd Hydrogenation Experiments

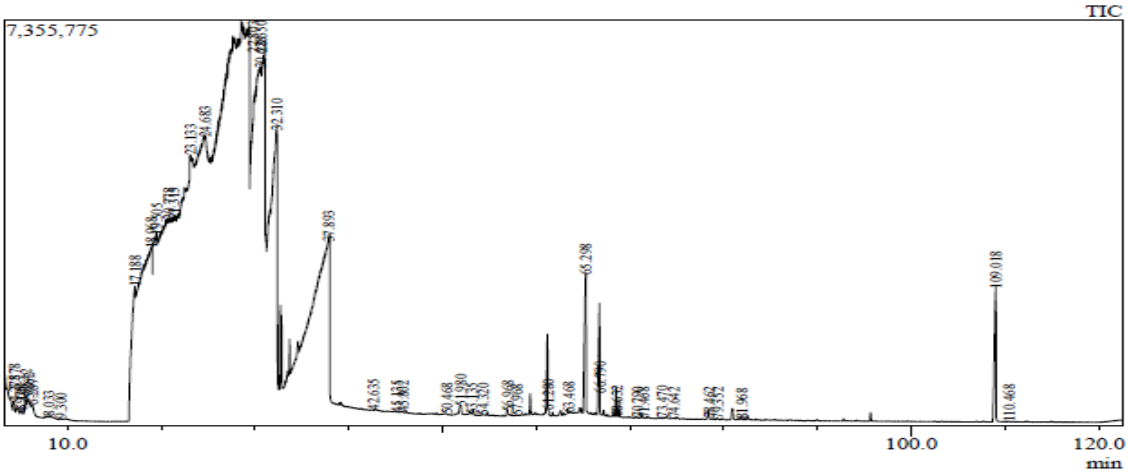

Figure 128. Trial #1 Hydrogenated Product Chromatogram and Spectrum Process Data Using Fluorous Pd.

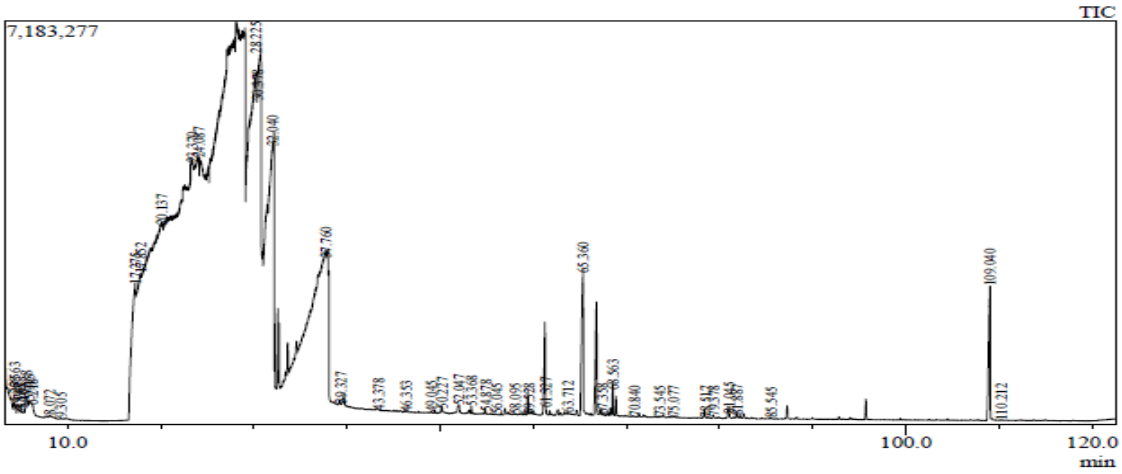

Figure 129. Trial #2 Hydrogenated Product Chromatogram and Spectrum Process Data Using Fluorous Pd.

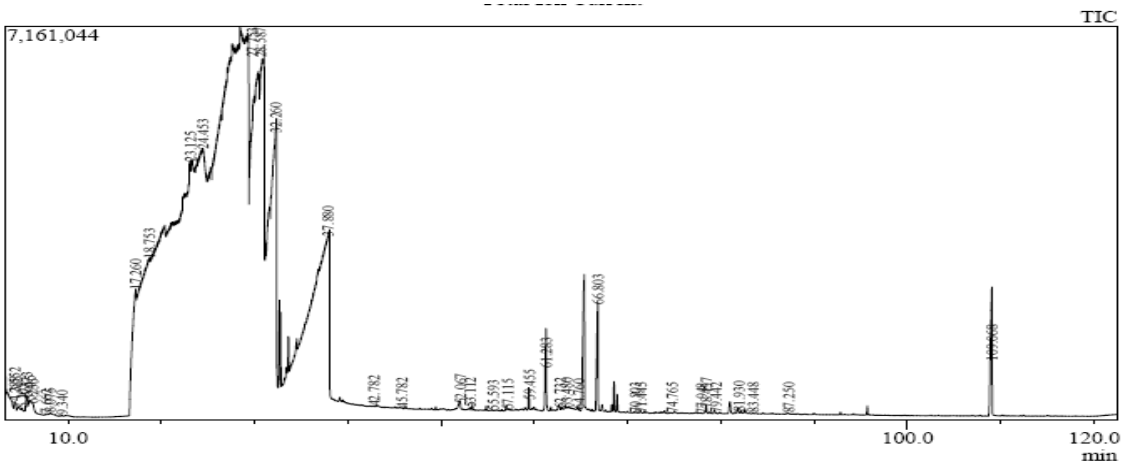

Figure 130. Trial #1 Hydrogenated Product Chromatogram and Spectrum Process Data Using Fluorous Pd.

Table 85. Spectrum Process Table For Fluorous Pd Hydrogenations

Trial #1 Fluorous Pd		Trial #2 Fluorous Pd		Trial #3 Fluorous Pd	
Retention Time	**Compound Name**	**Retention Time**	**Compound Name**	**Retention Time**	**Compound Name**
4.278	Cyclohexane, methyl-	4.298	Cyclohexane, methyl-	4.288	Cyclohexane, methyl-
4.975	Cyclohexane, methyl-	4.707	Cyclohexane, methyl-	5.105	Cyclohexane, methyl-
5.108	Cyclohexane, methyl-	5.105	Cyclohexane, methyl-	7.662	trans-3,5-Dimethylcyclohexene
8.033	Cyclohexane, ethyl-	8.072	Cyclohexane, ethyl-	8.075	Cyclohexane, ethyl-
9.3	Ethylbenzene	9.305	Ethylbenzene	9.34	Ethylbenzene
17.188	Phenol	17.275	Phenol	17.26	Phenol
19.505	Phenol	17.852	Phenol	18.753	Phenol
24.683	Phenol	20.137	Phenol	23.125	Phenol
27.643	Cyclohexane, 1,2-dimethyl-, cis-	24.087	Phenol	24.453	Phenol
30.628	Phenol, 2-methyl-	28.225	Phenol, 2-methyl-	27.58	Cyclohexane, 1,2-dimethyl-, cis-
32.31	Phenol, 2-ethyl-	30.378	Phenol, 2-methyl-	32.26	Phenol, 2-ethyl-
37.408	4-Decene, 3-methyl-, (E)-	32.04	Phenol, 2-ethyl-	33.293	Nonane, 3,7-dimethyl-
37.893	Octanoic Acid	37.76	Octanoic Acid	37.29	4-Decene, 3-methyl-, (E)-
51.98	Hexadecane	39.327	Heptadecane, 2,6-dimethyl-	37.88	Octanoic Acid
57.899	Tridecane, 6-methyl-	52.047	Hexadecane	52.022	Dodecane, 3-methyl-
63.656	Oxalic acid, isobutyl hexadecyl ester	65.36	Oxalic acid, heptyl 2-methylphenyl ester	52.067	Hexadecane
64.631	Tridecane, 2,5-dimethyl-			57.952	Tridecane, 6-methyl-
65.298	Oxalic acid, heptyl 2-methylphenyl ester			59.455	Octanoic acid, cyclohexyl ester
66.79	Oxalic acid, heptyl 2-methylphenyl ester			61.283	Octanoic acid, phenyl ester
				64.678	Tridecane, 2,5-dimethyl-
				66.803	para-Tolyl octanoate
				66.99	Oxalic acid, heptyl 2-methylphenyl ester

B5. GCMS Chromatograms and Spectrum Process Data for Pd/C Hydrogenation Experiments

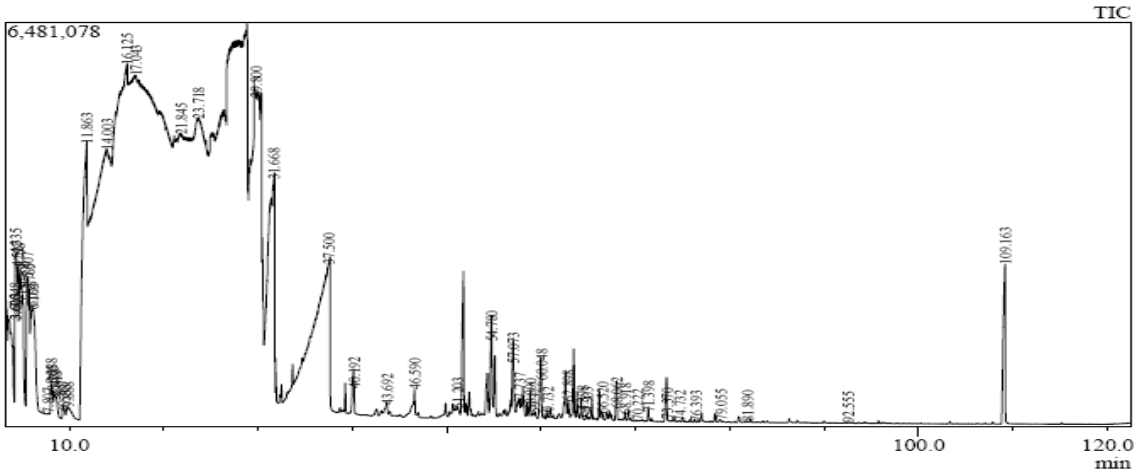

Figure 131. Trial #1 Hydrogenated Product Chromatogram and Spectrum Process Data Using Pd/C Catalyst.

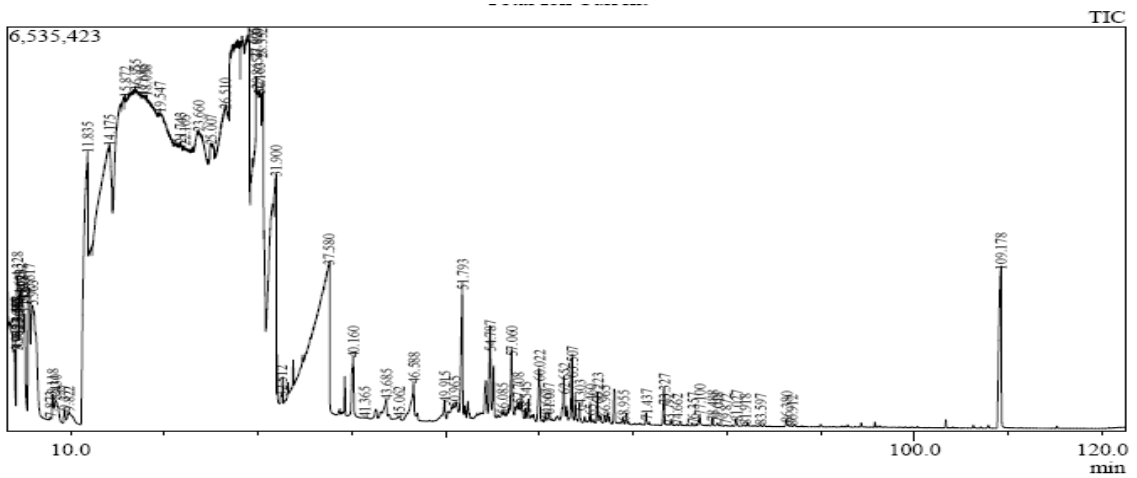

Figure 132. Trial #2 Hydrogenated Product Chromatogram and Spectrum Process Data Using Pd/C Catalyst.

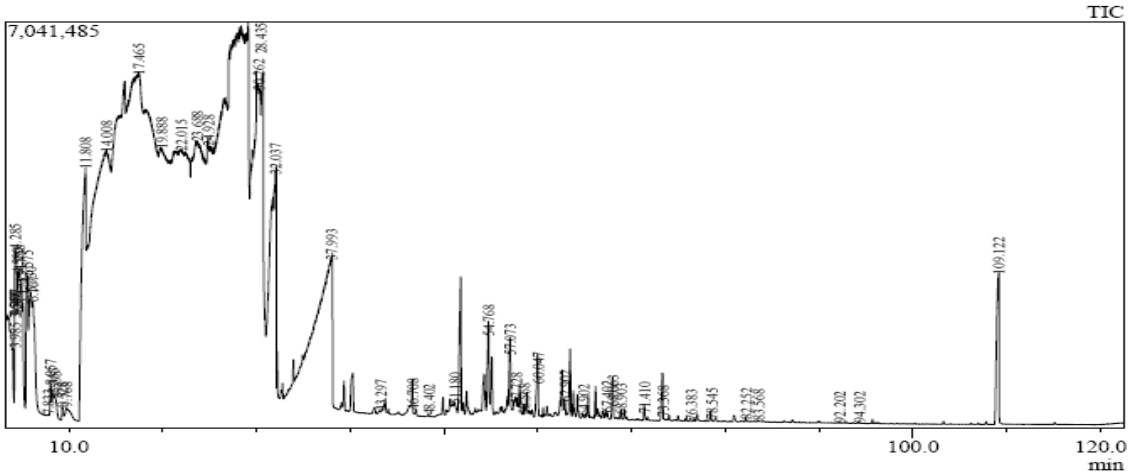

Figure 133. Trial #3 Hydrogenated Product Chromatogram and Spectrum Process Data Using Pd/C Catalyst.

Table 86. Spectrum Process Table For Pd/C Hydrogenation

Trial #1 Pd/C		Trial #2 Pd/C		Trial #3 Pd/C	
Retention Time	**Compound Name**	**Retention Time**	**Compound Name**	**Retention Time**	**Compound Name**
3.348	Benzene	3.962	Cyclohexane	3.985	Cyclohexane
4.335	Cyclohexane, methyl-	4.328	Cyclohexane, methyl-	4.285	Cyclohexane, methyl-
4.527	Cyclohexane, methyl-	4.623	Cyclohexane, methyl-	4.58	Cyclohexane, methyl-
4.758	Cyclohexane, methyl-	4.782	Cyclohexane, methyl-	4.758	Cyclohexane, methyl-
4.968	Cyclohexane, methyl-	4.898	Cyclohexane, methyl-	4.917	Cyclohexane, methyl-
5.132	Cyclohexane, methyl-	5.138	Cyclohexane, methyl-	5.125	Cyclohexane, methyl-
5.607	1,3,5-Cycloheptatriene	5.617	1,3,5-Cycloheptatriene	5.575	1,3,5-Cycloheptatriene
5.765	1,3,5-Cycloheptatriene	5.963	1,3,5-Cycloheptatriene	5.93	1,3,5-Cycloheptatriene
6.165	Toluene	7.873	Pentanoic acid, methyl ester	6.167	1,3,5-Cycloheptatriene
7.807	Pentanoic acid, methyl ester	8.118	Cyclohexane, ethyl-	7.833	Pentanoic acid, methyl ester
8.088	Cyclohexane, ethyl-	8.43	Cyclohexane, ethyl-	8.057	Cyclohexane, ethyl-
8.255	Cyclohexane, ethyl-	9.377	Ethylbenzene	8.353	Cyclohexane, ethyl-
8.473	Cyclohexane, ethyl-	9.822	o-Xylene	8.595	Cyclohexane, ethyl-
8.618	Cyclohexane, ethyl-	11.835	Cyclohexanone	9.328	Ethylbenzene

Table 86 Continued

Trial #1 Pd/C		Trial #2 Pd/C		Trial #3 Pd/C	
Retention Time	**Compound Name**	**Retention Time**	**Compound Name**	**Retention Time**	**Compound Name**
9.367	Ethylbenzene	14.175	Cyclohexanone	9.768	1,3-Cyclopentadiene, 5-(1-methylethylidene)-
9.533	Ethylbenzene	19.547	Phenol	11.808	Cyclohexanone
11.863	Cyclohexanone	26.51	Cyclohexanone, 2-methyl-	14.008	Cyclohexanone
14.003	Cyclohexanone	26.992	Cyclohexane, 1-methyl-3-(1-methylethyl)-	19.888	Phenol
17.043	Cyclohexanone, 2-methyl-	26.992	Cyclohexane, 1,2-dimethyl-, cis-	22.015	Cyclohexanone, 2-ethyl-
23.718	Phenol, 2-methyl-	27.605	Cyclohexanone, 3-methyl-	24.928	Phenol, 2-methyl-
26.755	Cyclopentane, 1-methyl-3-(2-methylpropyl)-	29.865	Cyclohexanone, 2-ethyl-	27.108	Cyclopentane, 1-methyl-3-(2-methylpropyl)-
31.668	Phenol, 2-ethyl-	30.163	Phenol, 2-methyl-	27.108	Cyclohexane, 1-methyl-3-(1-methylethyl)-
37.252	4-Decene, 3-methyl-, (E)-	31.9	Phenol, 2-ethyl-	27.355	Cyclohexane, 1,2-dimethyl-, cis-
37.5	Octanoic Acid	37.58	Octanoic Acid	28.435	Phenol, 2-methyl-
39.274	C11	39.271	C11	32.037	Phenol, 2-ethyl-
40.192	Benzene, cyclohexyl-	40.16	Benzene, cyclohexyl-	33.252	Nonane, 3,7-dimethyl-
42.579	Cyclopentane, 1,2-dimethyl-3-(1-methylethyl)-	42.575	Cyclopentane, 1,2-dimethyl-3-(1-methylethyl)-	37.993	Octanoic Acid
46.59	Benzene, 1-cyclohexyl-3-methyl-	43.685	Benzene, (2,4-dimethylcyclopentyl)-	39.32	C11
52.065	Dodecane, 3-methyl-	46.588	Benzene, 1-cyclohexyl-3-methyl-	42.607	Cyclopentane, 1,2-dimethyl-3-(1-methylethyl)-
54.78	Bicyclo[8.2.0]dodecan-11-one, 12-chloro-	50.965	[1,1'-Bicyclohexyl]-2-one	46.708	Benzene, 1-cyclohexyl-3-methyl-
58.723	Hexadecane	51.793	[1,1'-Bicyclohexyl]-2-one	52.049	Dodecane, 3-methyl-
60.048	Phenol, 2-cyclohexyl-4-methyl-	52.07	Dodecane, 3-methyl-	54.768	Bicyclo[8.2.0]dodecan-11-one, 12-chloro-
63.599	Oxalic acid, isobutyl hexadecyl ester	54.787	Bicyclo[8.2.0]dodecan-11-one, 12-chloro-	60.047	Phenol, 2-cyclohexyl-4-methyl-
68.062	Phenol, 4-(phenylmethyl)-	57.06	Phenol, 2-cyclohexyl-	63.542	Oxalic acid, isobutyl hexadecyl ester
		62.652	Benzene, 1-cyclohexyl-2-methoxy-	68.063	4-Methyl-2-phenylphenol
		63.507	Benzene, 1-cyclohexyl-2-methoxy-	92.202	Nonane, 3-methyl-5-propyl-

Table 86 Continued

Trial #1 Pd/C		Trial #2 Pd/C		Trial #3 Pd/C	
Retention Time	**Compound Name**	**Retention Time**	**Compound Name**	**Retention Time**	**Compound Name**
		63.62	Oxalic acid, isobutyl hexadecyl ester		
		77.1	Pentadecanoic acid		

B6. GCMS Chromatograms and Spectrum Process Data for Shvo's Catalyst Hydrogenation Experiments

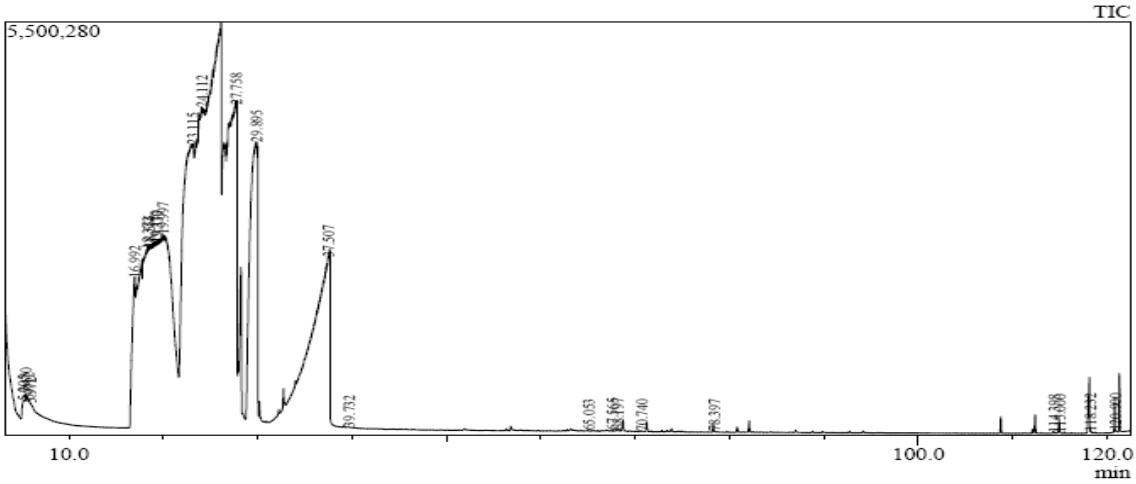

Figure 134. Trial #1 Hydrogenated Product Chromatogram and Spectrum Process Data Using Shvo's Catalyst.

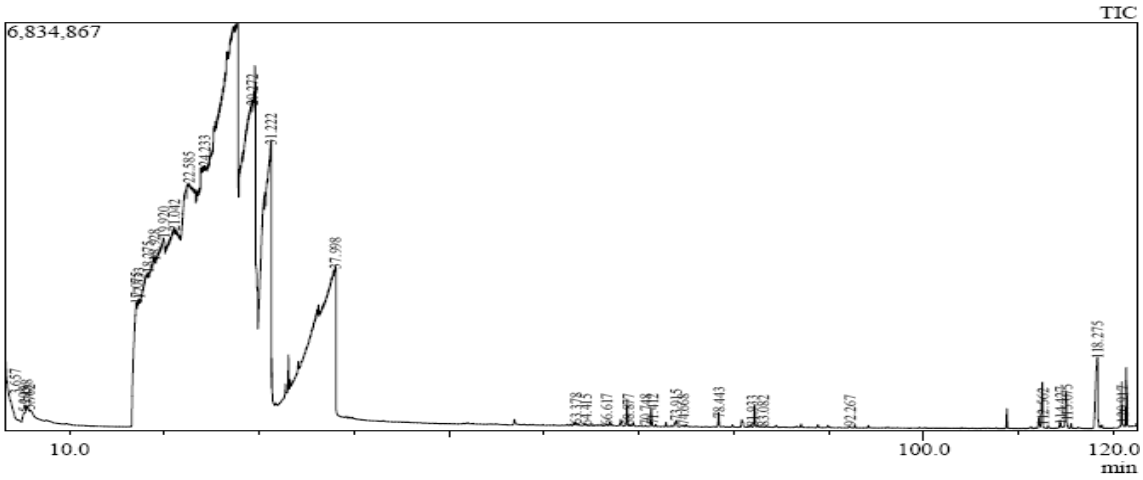

Figure 135. Trial #2 Hydrogenated Product Chromatogram and Spectrum Process Data Using Shvo's Catalyst.

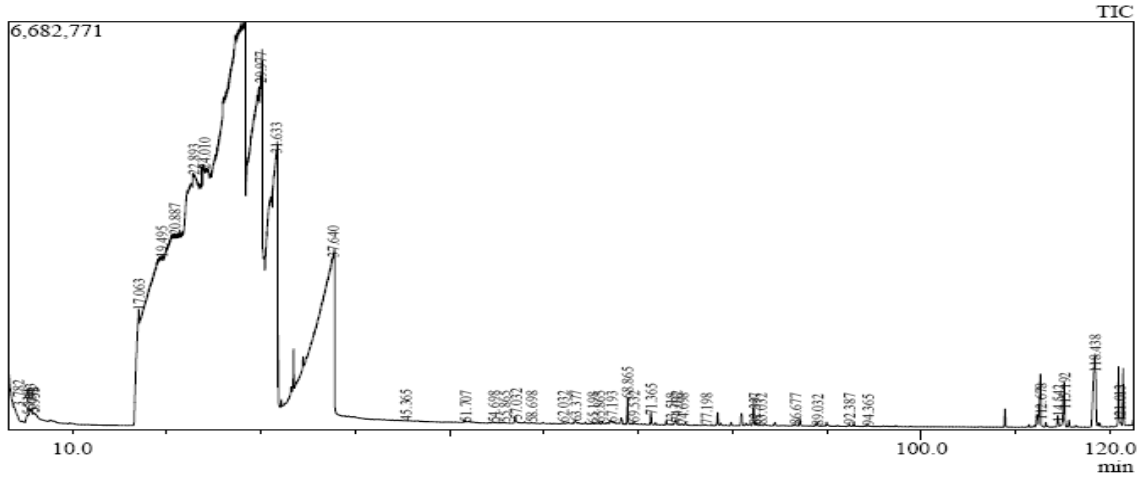

Figure 136. Trial #3 Hydrogenated Product Chromatogram and Spectrum Process Data Using Shvo's Catalyst.

Table 87. Spectrum Process Table For Shvo's Catalyst Hydrogenations

Trial #1 Shvo's Catalyst		Trial #2 Shvo's Catalyst		Trial #3 Shvo's Catalyst	
Retention Time	**Compound Name**	**Retention Time**	**Compound Name**	**Retention Time**	**Compound Name**
5.205	Methylene Chloride	3.657	Cyclohexene	5.318	Methylene Chloride
5.47	Toluene	5.295	Methylene Chloride	17.063	Phenol
16.992	Phenol	17.075	Phenol	19.495	Carbamic acid, phenyl ester
19.997	Phenol	17.333	Phenol	20.887	Phenol
23.115	Phenol, 2-methyl-	18.275	Phenol	24.01	Phenol, 2-methyl-
27.758	Phenol, 3-methyl-	18.928	Phenol	29.977	Phenol, 2-methyl-
29.895	Phenol, 2-ethyl-	19.92	Phenol	31.633	Phenol, 2-ethyl-
37.33	4-Decene, 3-methyl-, (E)-	21.042	Phenol	37.434	4-Decene, 3-methyl-, (E)-
37.507	Octanoic Acid	22.585	Phenol, 2-methyl-	37.64	Octanoic Acid
39.128	C11	24.233	Phenol, 2-methyl-	39.252	C11
51.943	Undecane, 2,10-dimethyl-	29.272	Phenol, 2-methyl-	52.08	Undecane, 2,10-dimethyl-
57.848	Tridecane, 6-methyl-	31.222	Phenol, 2-ethyl-	52.07	Dodecane, 3-methyl-
63.451	Oxalic acid, isobutyl hexadecyl ester	32.879	1-Pentanol, 4-methyl-2-propyl-	57.958	Tridecane, 6-methyl-
		32.879	Nonane, 3,7-dimethyl-	63.584	Oxalic acid, isobutyl hexadecyl ester
		37.221	4-Decene, 3-methyl-, (E)-		
		37.998	Octanoic Acid		
		51.977	Undecane, 2,10-dimethyl-		
		57.881	Tridecane, 6-methyl-		
		63.475	Oxalic acid, isobutyl hexadecyl ester		

VITA

Name: April Lovelady

Address: 201 Scoates Hall; MS 2117
College Station, TX 77843

Email Address: april.lovelady@gmail.com
a-lovelady@tamu.edu

Education: B.S., Biological Systems Engineering, Texas A&M University, 2002
M.S., Biological and Agricultural Engineering, Texas A&M University, 2005
Ph.D., Biological and Agricultural Engineering, Texas A&M University, 2012